Climate-driven mangrove dieback in the Gulf of Carpentaria, Australia: using stable isotopes as a tool to assess and monitor ecosystem changes

Author

Harada, Yota

Published

2020-04-01

Thesis Type

Thesis (PhD Doctorate)

School

School of Environment and Sc

DOI

10.25904/1912/2363

Climate-driven mangrove dieback in the Gulf of Carpentaria, Australia: using stable isotopes as a tool to assess and monitor ecosystem changes

Yota Harada *BSc* (*Hons*)

Australian Rivers Institute
School of Environment and Science
Griffith University

Submitted in fulfilment of the requirements of the degree of
Doctor of Philosophy
October 2019

Abstract

Extreme climatic events can trigger sudden but often long-lasting and irreversible changes in ecosystems by causing mortality of foundation (habitat-forming) species. The magnitude and frequency of such events are likely to increase due to human-induced climate change, but the dynamics of such extreme biological events remain poorly understood, with only a limited number of case studies reported in the past. In many cases, assessing the impact of rare, extreme biological events can be challenging because these events can be unexpected and sudden, often making pre-event sampling not achievable. In late 2015 to early 2016, an extensive area of mangrove forest along ~ 1,000 km of coastline in the Gulf of Carpentaria, Australia, experienced severe dieback as a result of a climatic extreme event that included extreme temperatures, drought conditions and lower than average sea levels.

My research aimed to address a knowledge gap in the effects of extreme climatic events on intertidal coastal ecosystems by assessing the ecological impacts of mass mortality of mangrove trees on the intertidal ecosystem. This aim was achieved through the use of a comparative experiment of an impacted forest and an adjacent unimpacted forest using traditional ecological survey techniques combined with conventional bulk stable isotope analyses and a more novel compound-specific isotope analysis of amino acids. My research also offers significant insights into the use of the more novel compound-specific isotope analysis of amino acids to complement the conventional bulk stable isotope analysis in mangrove ecosystem trophic analyses.

Firstly, I used a combination of traditional ecological survey techniques and bulk stable isotope analysis of carbon (C) and nitrogen (N) to measure the effects of mangrove forest mortality on benthic faunal communities, with a focus on functional aspects of food web dynamics. I tested if changes in benthic faunal assemblages would be evident due to mangrove mortality, and if food web structure was impacted by the mangrove mortality and alternations in available food resources. I found that in the forest that experienced tree mortality, there were fewer crabs that relied on mangrove litter as a food source but more crabs that fed on the microphytobenthos. As the microphytobenthos was largely unaffected by the die-back event, they provided a buffer to the food-web responses. The infauna, e.g. burrowing crabs, was also largely unaffected by the mortality effect. However, overall, the

habitat value for mangrove ecosystem services could be decreased due to lower physical habitat complexity following tree losses.

Secondly, the initial dieback and recovery of the impacted mangrove ecosystem were evaluated using a combination of bulk stable C, N and S isotopes and a more novel amino acid compound-specific isotope method. I tested if tree mortality changed the overall circulation of C, N and S elements, and if this change would be reflected in $\delta^{13}C$, $\delta^{15}N$ and $\delta^{34}S$ values of mangrove ecosystem components such as mangrove plants, soil and associated animals. I also tested if/how these isotopic compositions change over time with the recovery of mangrove vegetation. Stable isotope analyses confirmed significant changes to the circulation of C, N and S elements following tree mortality. Recovery of the mangrove vegetation was evident from increased numbers of mangrove seedlings and saplings in the impacted forest over the two-year survey, but recovery of CNS cycling was not evident even after 30 months, suggesting a long-lasting effect of the mortality event.

Finally, the use of bulk stable CNS isotopes and more novel compound-specific stable C and N isotopes of amino acids were compared to evaluate which isotopic compositions are more conservative tracers of mangrove organic matter and suited for analyses of mangrove food webs. I tested if stable isotopic compositions in essential amino acids that cannot be synthesised by animals would be more conservative in food web links between consumers and mangrove organic matter. Isotopic compositions in essential amino acids effectively separated mangrove organic matter from the microphytobenthos and helped to trace mangrove organic matter in a mangrove food web. These more sophisticated tracing techniques complemented traditional bulk stable isotope analyses by providing improved resolving power in mangrove trophic analyses.

The outcome of this research will be an important contribution to the emerging global body of case studies that show significant ecological impacts driven by extreme climatic events, and how changes in habitat forming species result in significant impacts on ecosystem community dynamics as well as biogeochemical processes including C, N and S cycling. My research also provides a framework for combining the use of conventional and novel stable isotope measurements with traditional ecological survey techniques in reporting difficult to measure impacts of extreme biological events. The results of this research may also be used

for planning and future-proofing coastal wetlands from future impacts of climatic extreme events, and support wetland conservation and restoration efforts.

Statement of originality

This work has not previously been submitted for a degree or diploma in any university. To the best of my knowledge and belief, the thesis contains no material previously published or written by another person except where due reference is made in the thesis itself.

(Signed)_____

Yota Harada

Acknowledgements

Supervisors, colleagues, friends and family helped with the completion of this thesis. I thank Professors Joe Lee, Brian Fry and Rod Connolly for their supervision and scientific insights. I thank Associate Professor Damien Maher (Southern Cross University) and his colleagues for their scientific guidance, collaboration and support during field work. I particularly thank James Sippo for his assistance and support. I thank colleagues from the Connolly lab and the Global Wetlands Project, particularly Ryan Pearson, Dale Bryan-Brown, Kristin Jinks and Tom Rayner for their constructive comments during lab meetings, and Matthew Hayes for help reviewing this thesis. I also thank colleagues from Joe Lee's lab, particularly Majid Bakhtiyari and Shafagh Kamal for their support. Field work was assisted by Adam Bourke, Gloria Reithmaier, Luke Jeffrey, Kylie Maguire, Dylan Brown, Steven Conrad, Ashly McMahon, Ceylena Holloway, Mitch Call, Alice Gauthey, Geoff Balland and Julia Kalla. I thank staff and colleagues at the Australian Rivers Institute and School of Environment and Science at Griffith University. I thank Rad Bak and Vanessa Fry for their help with stable isotope analyses. I also thank Brian Paterson for examining the PhD confirmation. This work was funded by an Australian Postgraduate Award / an Australian Government RTP Stipend Scholarship and the Holsworth Wildlife Research Endowment – Equity Trustees Charitable Foundation & the Ecological Society of Australia.

Acknowledgement of co-authored papers

Included in this thesis is one published manuscript (Chapter 2), one preprint manuscript (Chapter 3) and one to be submitted (Chapter 4). My contribution to each co-authored paper is outlined at the front of the relevant chapter. The bibliographic details for these papers are:

Harada Y, Fry B, Lee SY, Maher DT, Sippo JZ, Connolly RM (2019) Stable isotopes indicate ecosystem restructuring following climate-driven mangrove dieback. Limnology and Oceanography.

Harada Y, Connolly RM, Fry B, Maher DT, Sippo JZ, Jeffrey LC, Bourke AJ, Lee SY (2020) Stable isotopes track the ecological and biogeochemical legacy of mangrove forest dieback in the Gulf of Carpentaria, Australia. Biogeosciences discussions.

Harada Y, Fry B, Connolly RM, Lee SY (in preparation) Combined analysis of bulk stable CNS isotopes and compound-specific stable CN isotopes of amino acids in analysing mangrove food webs.

Appropriate acknowledgements of those who contributed to the research but did not qualify as authors are included in each paper.

(Signed) _____ (Date) 27/10/2018
Yota Harada

(Countersigned) _____ (Date) 27/10/2018
Supervisor: Rod M. Connolly

Related publications and presentations

Peer reviewed publications

Harada Y, Fry B, Lee SY, Maher DT, Sippo JZ, Connolly RM (2020) Stable isotopes indicate ecosystem restructuring following climate-driven mangrove dieback. Limnology and Oceanography.

Conference presentations based on this thesis

Harada Y, Fry B, Lee SY, Maher DT, Sippo JZ, Connolly RM. Stable isotopes indicate ecosystem restructuring following climate-driven mangrove dieback. IsoEcol, the 11th International Conference on the Applications of Stable Isotope Techniques to Ecological Studies, Viña del Mar, Chile, 2018.

Harada Y, Fry B, Lee SY, Maher DT, Sippo JZ, Connolly RM. Stable isotopes indicate ecosystem restructuring following climate-driven mangrove dieback. Ecological Society of Australia Annual Conference, Brisbane, Australia 2018.

Harada Y, Fry B, Lee SY, Maher DT, Sippo JZ, Connolly RM. Stable isotopes indicate ecosystem restructuring following climate-driven mangrove dieback. Australian Rivers Institute Annual Higher Degree Research Symposium, Griffith University, Brisbane, Australia, 2017

Harada Y, Fry B, Lee SY, Maher DT, Sippo JZ, Connolly RM. Stable isotopes indicate ecosystem restructuring following climate-driven mangrove dieback. Australian Mangrove and Saltmarsh Network Conference, Hobart, Tasmania, 2017.

Table of contents

List of tables

List of Figures

Chapter 1 - Introduction

Extreme climatic events including droughts and heatwaves negatively impact Earth's natural ecosystems (Harris et al. 2018). Such events can trigger sudden but often long-lasting and irreversible changes in ecosystems by causing mortality of foundation species that have key roles in structing communities, for example, habitat-forming corals (Hughes et al. 2017) and canopy-forming mangroves (Duke et al. 2017), seagrasses (Thomson et al. 2015), saltmarshes (Silliman et al. 2005) and kelp (Wernberg et al. 2016). Even brief disturbances, such as heatwaves lasting only a few weeks, can cause long-lasting impacts. For example, a heat-stress mass bleaching event of the Australian Great Barrier Reef, which resulted in more than 90% of the reef being impacted by bleaching, was caused by a relatively short marine heatwave (Hughes et al. 2017). These changes undermine biodiversity and reduce the capacity for ecosystem services provided by these ecosystems. Global heating has increased the magnitude and frequency of extreme climatic events (Coumou & Rahmstorf 2012, Stott 2016). In October 2018, the United Nations prescribed urgent action to limit warming to 1.5 °C and prevent the loss of ecosystems and their functions due to extreme climatic events (IPCC 2018). However, case studies of extreme biological events are limited, and the dynamics of ecosystem responses to extreme climatic events remain poorly understood.

In recent decades, our understanding of extreme climatic events in the changing climate has improved (Coumou & Rahmstorf 2012, Stott 2016), however, our understanding of the impact of extreme climatic events on biological systems, and their resulting extreme biological events, remains poorly addressed (Harris et al. 2018, Parmesan et al. 2013, Ummenhofer & Meehl 2017). Reporting rare, extreme biological events can be challenging because these events can be sudden and unpredictable, and often pre- and post-event comparisons cannot be achieved. Extreme climatic events not only cause mortality of habitat-forming species but also change associated faunal communities. For example, droughts and heatwaves can lead to changes in benthic communities of intertidal habitats (MacKay et al. 2010, Pillay and Perissinotto 2008, Pillay and Perissinotto 2009, Verdelhos et al. 2014, Veríssimo et al. 2013). In some cases, investigations of such events may involve long-term ecosystem analyses to detect underlying the biological mechanisms that drive changes (Dolbeth et al. 2007, Pollack et al. 2011).

Stable isotopes, with their ability to track changes and processes over time, provide ecologists with a quantitative tool to trace details of element cycling in the environment (Fry 2006). As elements circulate in the biosphere, stable isotopic compositions of biogenic substances can change in predictable ways (Peterson & Fry 1987, Wada et al. 1991). Traditional methods to evaluate structural and functional responses of ecosystems mainly focus on species composition, but these field assessments can be time consuming and expensive, and may not provide enough quantitative information about system functioning. Stable isotope analysis of ecosystem components is a powerful way of evaluating functional aspects of element cycling and the health of ecosystems, e.g. integrity of the food web. Over the past few decades, stable isotope analyses of total organic matter ("bulk") have become more common due to the relative ease and low cost of sample preparation and analysis (Fry 2006). However, compound-specific isotope analysis is progressively employed as a tool to complement bulk isotope analysis. For example, stable isotopic compositions of individual amino acids have been combined with the bulk analyses to measure details of organic matter cycling for food web analyses (Potapov et al. 2019). While patterns of C isotopic composition in individual amino acids ("fingerprint") help to estimate resource utilisations (Larsen et al. 2009, Larsen et al. 2013), N isotopic composition in amino acids such as phenylalanine, glutamic acid and methionine have been utilized to measure trophic levels of organisms in food web analyses (Chikaraishi et al. 2009, Ohkouchi et al. 2017, Ishikawa et al. 2018).

Mangrove forests are highly productive and support the livelihoods of millions of people, protect coastal communities, improve water quality and underpin global fisheries (Lee et al. 2014). In 2015-16, the world's largest recorded mangrove dieback occurred in the Gulf of Carpentaria, Australia. High temperatures combined with low sea levels that coincided with a strong El Niño resulted in the death of mangrove forests along ~1,000 km of coastline (Duke et al. 2017). At the same time, there were also other mangrove dieback events reported in Exmouth, Western Australia (Lovelock et al. 2017) and Kakadu National Park, Northern Territory, Australia (Asbridge et al. 2019). Mortality of mangrove trees can lead to shifts in biological communities due to alterations in primary productivity and associated changes in nutrient cycling, as well as disturbances from physical modifications of habitat structure provided by these foundation species (Kristensen et al. 2008, Lee et al. 2014, Alongi 2015).

Stable isotopes have been broadly used in investigations of mangrove ecosystems to investigate food web interactions (Lee 2000, Fry & Smith 2002, Fry & Ewel 2003,

Demopoulos et al. 2007, Bouillon et al. 2008, Mazumder & Saintilan 2010, Bui & Lee 2014, Abrantes et al. 2015), physiology of mangrove plants (Lin & Sternberg 1992a, Lin & Sternberg 1992b, McKee et al. 2002, Hayes et al. 2019), C cycling (Maher et al. 2013, Kelleway et al. 2018), N cycling (Fry et al. 2000, Fry & Cormier 2011) and S cycling (Fry et al. 1982, Okada & Sasaki 1995, 1998). While many of these investigations focused on the use of bulk stable isotope analysis of C and N and, to a lesser extent, S, the use of more novel compound-specific stable isotope methods of individual amino acids is fairly limited in mangrove ecosystem studies (Smallwood et al. 2003, Larsen et al. 2012, Bui & Lee 2015). While various stable isotopic measurements can help to trace organic matter cycling, it remains largely untested which stable isotope tracers are more conservative for tracing mangrove organic matter and, therefore, more suited for investigations of mangrove food webs. Testing isotopic fidelity in food web links between consumers and organic matter is particularly important for increasing our understanding of mangrove food webs that involve mixed food resources and complex detrital food web interactions (Fry & Ewel 2003). How novel compound-specific isotope measurements in amino acids complement traditional bulk stable isotope analysis is largely unexplored in mangrove food web analyses.

My research aimed to address a knowledge gap on the effects of extreme climatic events on intertidal coastal ecosystems by assessing the ecological impacts of the 2015-16 Gulf of Carpentaria mangrove dieback. I achieve this by using a comparative experiment of an impacted mangrove ecosystem and an adjacent unimpacted ecosystem and utilise traditional ecological survey techniques, combined with conventional bulk stable isotope analyses and a more novel compound-specific isotope analysis of amino acids (Fig. 1.1). My research also provides new insights into the use of novel compound-specific isotope analysis of amino acids to complement conventional bulk stable isotope analysis in mangrove ecosystem analyses. The outcome of this project will make a significant contribution to the emerging global body of studies that indicate ecosystem impacts driven by extreme climatic events. Examples of such extreme biological events include drought-associated saltmarsh die-off (Silliman et al. 2005), coral reef bleaching (Hughes et al. 2017), kelp forest die-off (Wernberg et al. 2016), and dieback of seagrass meadows (Thomson et al. 2015) that were associated with marine heatwaves. This research also provides a framework for combining the use of stable isotopes and traditional ecological survey techniques in reporting difficult to measure impacts of extreme biological events. The results of this research may also be used to develop a novel index for evaluating mangrove ecosystem condition and health, and help

measure future impacts of climatic extreme events, thereby improve wetland conservation and restoration efforts.

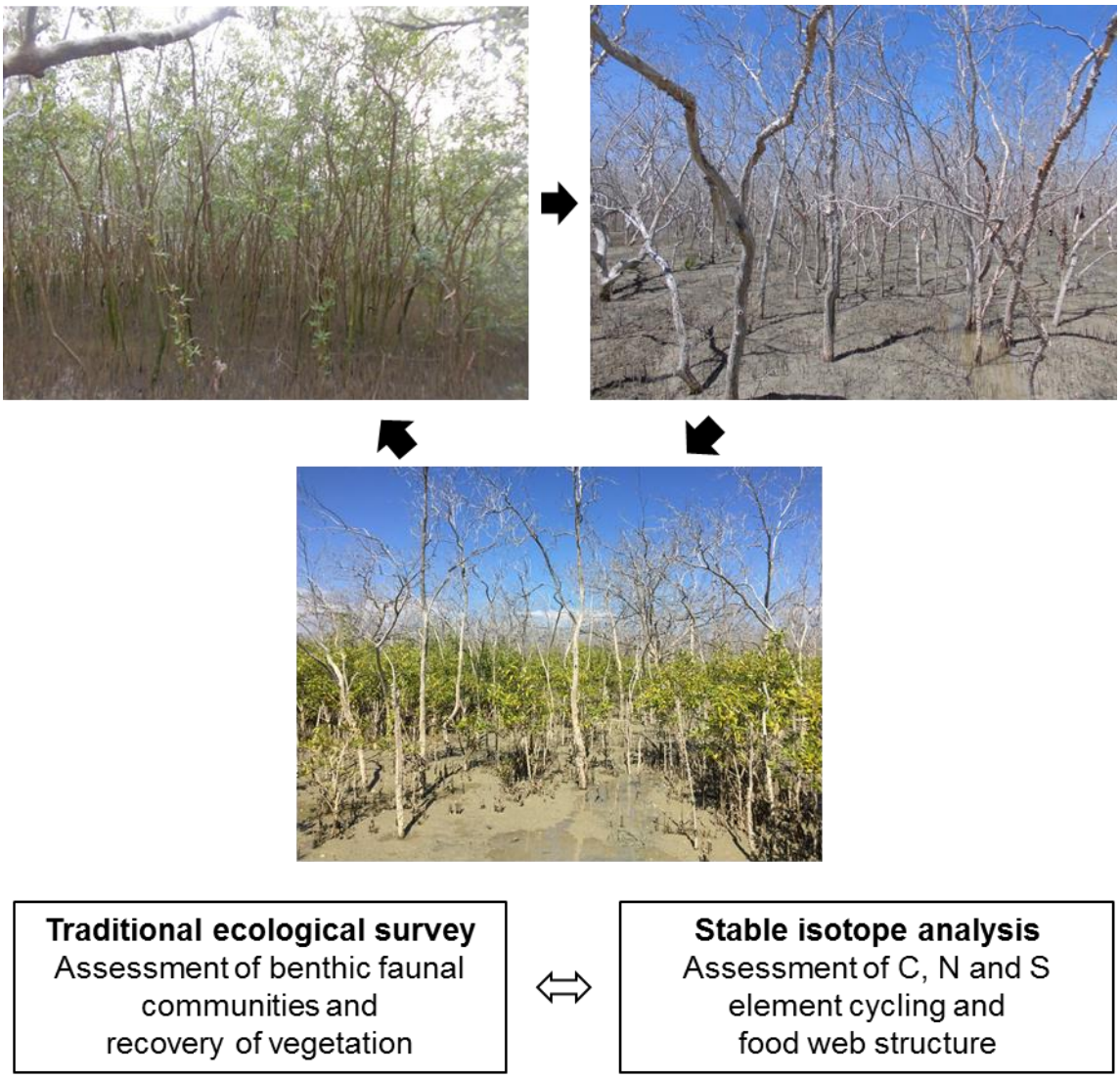

Fig. 1.1. A conceptual diagram of a stable isotope tracer experiment in the Gulf of Carpentaria, Australia. Traditional ecological survey techniques were combined with stable isotope analysis to assess the initial dieback as well as recovery of the mangrove ecosystem over time.

The focus of my research is to examine the impacts of extreme climatic events and associated mangrove forest mortality on benthic faunal communities and element (C, N, S) cycling, with a focus on the functional aspects of food web dynamics in the Gulf of Carpentaria, Australia. I tested the hypotheses that changes in benthic faunal assemblages would be evident due to mangrove mortality and food web structure would change as a result of changes in faunal

assemblages and the availability of food resources (chapter 2). I also hypothesised that tree mortality changed the cycling of C, N and S, and these biogeochemical changes would be reflected in the $\delta^{13}C$, $\delta^{15}N$ and $\delta^{34}S$ values of mangrove ecosystem components such as mangrove plants, soil and associated animals. I also tested how these isotopic indicators change over time with the recovery of mangrove vegetation (chapter 3). In chapter 4, I also tested how novel compound-specific isotope measurements of amino acids complement traditional bulk stable isotope analysis in mangrove food web analyses. I hypothesised that stable isotopic compositions in essential amino acids that cannot be synthesised by animals would be more conservative in food web links between consumers and mangrove organic matter.

References

Abrantes KG, Johnston R, Connolly RM, Sheaves M (2015) Importance of Mangrove Carbon for Aquatic Food Webs in Wet–Dry Tropical Estuaries. Estuaries Coasts 38:383-399

Alongi DM (2015) The Impact of Climate Change on Mangrove Forests. Curr Clim Change Rep 1:30-39

Asbridge EF, Bartolo R, Finlayson CM, Lucas RM, Rogers K, Woodroffe CD (2019) Assessing the distribution and drivers of mangrove dieback in Kakadu National Park, northern Australia. Estuar Coast Shelf Sci 228:106353

Bouillon S, Connolly RM, Lee SY (2008) Organic matter exchange and cycling in mangrove ecosystems: Recent insights from stable isotope studies. J Sea Res 59:44-58

Bui THH, Lee SY (2014) Does 'You Are What You Eat' Apply to Mangrove Grapsid Crabs? PLOS ONE 9:e89074

Bui THH, Lee SY (2015) Potential contributions of gut microbiota to the nutrition of the detritivorous sesarmid crab Parasesarma erythodactyla. Mar Biol 162:1969-1981

Chikaraishi Y, Ogawa NO, Kashiyama Y, Takano Y, Suga H, Tomitani A, Miyashita H, Kitazato H, Ohkouchi N (2009) Determination of aquatic food-web structure based on compound-specific nitrogen isotopic composition of amino acids. Limnol Oceanogr Methods 7:740-750

Coumou D, Rahmstorf S (2012) A decade of weather extremes. Nat Clim Change 2:491-496

Demopoulos AW, Fry B, Smith CR (2007) Food web structure in exotic and native mangroves: a Hawaii–Puerto Rico comparison. Oecol 153:675-686

Dolbeth M, Cardoso PG, Ferreira SM, Verdelhos T, Raffaelli D, Pardal MA (2007) Anthropogenic and natural disturbance effects on a macrobenthic estuarine community over a 10-year period. Mar Poll Bull 54:576-585

Duke NC, Kovacs JM, Griffiths AD, Preece L, Hill DJE, van Oosterzee P, Mackenzie J, Morning HS, Burrows D (2017) Large-scale dieback of mangroves in Australia's Gulf of Carpentaria: a severe ecosystem response, coincidental with an unusually extreme weather event. Mar Freshwater Res 68:1816-1829

Fry B (2006) Stable Isotope Ecology. Springer-Verlag New York

Fry B, Bern AL, Ross MS, Meeder JF (2000) $\delta^{15}N$ studies of nitrogen use by the red mangrove, Rhizophora mangle L. in South Florida. Estuar Coast Shelf Sci 50:291-296

Fry B, Cormier N (2011) Chemical ecology of red mangroves, Rhizophora mangle, in the Hawaiian Islands1. Pac Sci 65:219-235

Fry B, Ewel K (2003) Using stable isotopes in mangrove fisheries research - a review and outlook. Isot Environ Healt S 39:191-196

Fry B, Scalan RS, Winters JK, Parker PL (1982) Sulphur uptake by salt grasses, mangroves, and seagrasses in anaerobic sediments. Geochim Cosmochim Acta 46:1121-1124

Fry B, Smith TJ (2002) Stable isotope studies of red mangroves and filter feeders from the Shark River estuary, Florida. Bull Mar Sci 70:871-890

Harris RMB, Beaumont LJ, Vance TR, Tozer CR, Remenyi TA, Perkins-Kirkpatrick SE, Mitchell PJ, Nicotra AB, McGregor S, Andrew NR, Letnic M, Kearney MR, Wernberg T, Hutley LB, Chambers LE, Fletcher MS, Keatley MR, Woodward CA, Williamson G, Duke NC, Bowman DMJS (2018) Biological responses to the press and pulse of climate trends and extreme events. Nat Clim Change 8:579-587

Hayes MA, Jesse A, Welti N, Tabet B, Lockington D, Lovelock CE (2019) Groundwater enhances above-ground growth in mangroves. J Ecol 107:1120-1128

Hughes TP, Kerry JT, Álvarez-Noriega M, Álvarez-Romero JG, Anderson KD, Baird AH, Babcock RC, Beger M, Bellwood DR, Berkelmans R, Bridge TC, Butler IR, Byrne M, Cantin NE, Comeau S, Connolly SR, Cumming GS, Dalton SJ, Diaz-Pulido G, Eakin CM, Figueira WF, Gilmour JP, Harrison HB, Heron SF, Hoey AS, Hobbs J-

PA, Hoogenboom MO, Kennedy EV, Kuo C, Lough JM, Lowe RJ, Liu G, McCulloch MT, Malcolm HA, McWilliam MJ, Pandolfi JM, Pears RJ, Pratchett MS, Schoepf V, Simpson T, Skirving WJ, Sommer B, Torda G, Wachenfeld DR, Willis BL, Wilson SK (2017) Global warming and recurrent mass bleaching of corals. Nature 543:373-337

IPCC (2018) Global warming of 1.5°C. An IPCC Special Report on the impacts of global warming of 1.5°C above pre-industrial levels and related global greenhouse gas emission pathways, in the context of strengthening the global response to the threat of climate change, sustainable development, and efforts to eradicate poverty. Geneva, Switzerland:World Meteorological Organization

Ishikawa NF, Chikaraishi Y, Takano Y, Sasaki Y, Takizawa Y, Tsuchiya M, Tayasu I, Nagata T, Ohkouchi N (2018) A new analytical method for determination of the nitrogen isotopic composition of methionine: Its application to aquatic ecosystems with mixed resources. Limnol Oceanogr Methods 16:607-620

Kelleway JJ, Mazumder D, Baldock JA, Saintilan N (2018) Carbon isotope fractionation in the mangrove Avicennia marina has implications for food web and blue carbon research. Estuar Coastal Shelf Sci 205:68-74

Kristensen E, Bouillon S, Dittmar T, Marchand C (2008) Organic carbon dynamics in mangrove ecosystems: A review. Aquat Bot 89:201-219

Larsen T, Taylor DL, Leigh MB, O'Brien DM (2009) Stable isotope fingerprinting: a novel method for identifying plant, fungal, or bacterial origins of amino acids. Ecology 90:3526-3535

Larsen T, Ventura M, Andersen N, O'Brien DM, Piatkowski U, McCarthy MD (2013) Tracing Carbon Sources through Aquatic and Terrestrial Food Webs Using Amino Acid Stable Isotope Fingerprinting. PLoS ONE 8:e73441

Larsen T, Wooller MJ, Fogel ML, O'Brien DM (2012) Can amino acid carbon isotope ratios distinguish primary producers in a mangrove ecosystem? Rapid Commun Mass Spectrom 26:1541-1548

Lee SY (2000) Carbon dynamics of Deep Bay, eastern Pearl River estuary, China. II: Trophic relationship based on carbon-and nitrogen-stable isotopes. Mar Ecol Prog Ser 205:1-10

Lee SY, Primavera JH, Dahdouh-Guebas F, McKee K, Bosire JO, Cannicci S, Diele K, Fromard F, Koedam N, Marchand C, Mendelssohn I, Mukherjee N, Record S (2014) Ecological role and services of tropical mangrove ecosystems: a reassessment. Glob Ecol Biogeogr 23:726-743

Lin G, Sternberg L (1992a) Differences in morphology, carbon isotope ratios, and photosynthesis between scrub and fringe mangroves in Florida, USA. Aquat Bot 42:303-313

Lin G, Sternberg L (1992b) Effect of growth form, salinity, nutrient and sulfide on photosynthesis, carbon isotope discrimination and growth of red mangrove (Rhizophora mangle L.). Funct Plant Biol 19:509-517

Lovelock CE, Feller IC, Reef R, Hickey S, Ball MC (2017) Mangrove dieback during fluctuating sea levels. Sci Rep 7:1680

MacKay F, Cyrus D, Russell K-L (2010) Macrobenthic invertebrate responses to prolonged drought in South Africa's largest estuarine lake complex. Estuar Coast Shelf Sci 86:553-567

Maher DT, Santos IR, Golsby-Smith L, Gleeson J, Eyre BD (2013) Groundwater-derived dissolved inorganic and organic carbon exports from a mangrove tidal creek: The missing mangrove carbon sink? Limnol Oceanogr 58:475-488

Mazumder D, Saintilan N (2010) Mangrove Leaves are Not an Important Source of Dietary Carbon and Nitrogen for Crabs in Temperate Australian Mangroves. Wetlands 30:375-380
McKee KL, Feller IC, Popp M, Wanek W (2002) Mangrove isotopic ($\delta^{15}N$ and $\delta^{13}C$) fractionation across a nitrogen vs. phosphorus limitation gradient. Ecology 83:1065-1075
Ohkouchi N, Chikaraishi Y, Close HG, Fry B, Larsen T, Madigan DJ, McCarthy MD, McMahon KW, Nagata T, Naito YI, Ogawa NO, Popp BN, Steffan S, Takano Y, Tayasu I, Wyatt ASJ, Yamaguchi YT, Yokoyama Y (2017) Advances in the application of amino acid nitrogen isotopic analysis in ecological and biogeochemical studies. Org Geochem 113:150-174
Okada N, Sasaki A (1995) Characteristics of Sulfur Uptake by Mangroves: an Isotopic Study. Tropics 4:201-210
Okada N, Sasaki A (1998) Sulfur isotopic composition of mangroves. Isot Environ Healt S 34:61-65
Parmesan C, Burrows MT, Duarte CM, Poloczanska ES, Richardson AJ, Schoeman DS, Singer MC (2013) Beyond climate change attribution in conservation and ecological research. Ecol Lett 16:58-71
Peterson BJ, Fry B (1987) Stable Isotopes in Ecosystem Studies. Annu Rev Ecol Syst 18:293-320
Pillay D, Perissinotto R (2008) The benthic macrofauna of the St. Lucia Estuary during the 2005 drought year. Estuar Coast Shelf Sci 77:35-46
Pillay D, Perissinotto R (2009) Community structure of epibenthic meiofauna in the St. Lucia Estuarine Lake (South Africa) during a drought phase. Estuar Coast Shelf Sci 81:94-104
Pollack JB, Palmer TA, Montagna PA (2011) Long-term trends in the response of benthic macrofauna to climate variability in the Lavaca-Colorado Estuary, Texas. Mar Ecol Progr Ser 436:67-80
Potapov AM, Tiunov AV, Scheu S, Larsen T, Pollierer MM (2019) Combining bulk and amino acid stable isotope analyses to quantify trophic level and basal resources of detritivores: a case study on earthworms. Oecol 189:447-460
Silliman BR, van de Koppel J, Bertness MD, Stanton LE, Mendelssohn IA (2005) Drought, Snails, and Large-Scale Die-Off of Southern U.S. Salt Marshes. Science 310:1803-1806
Smallwood BJ, Wooller MJ, Jacobson ME, Fogel ML (2003) Isotopic and molecular distributions of biochemicals from fresh and buried Rhizophora mangle leaves. Geochem Trans 4:38
Stott P (2016) How climate change affects extreme weather events. Science 352:1517-1518
Thomson JA, Burkholder DA, Heithaus MR, Fourqurean JW, Fraser MW, Statton J, Kendrick GA (2015) Extreme temperatures, foundation species, and abrupt ecosystem change: an example from an iconic seagrass ecosystem. Glob Change Biol 21:1463-1474
Ummenhofer CC, Meehl GA (2017) Extreme weather and climate events with ecological relevance: a review. Philos. Trans. Royal Soc. B 372:20160135
Verdelhos T, Cardoso P, Dolbeth M, Pardal M (2014) Recovery trends of Scrobicularia plana populations after restoration measures, affected by extreme climate events. Mar Environ Res 98:39-48
Veríssimo H, Lane M, Patrício J, Gamito S, Marques JC (2013) Trends in water quality and subtidal benthic communities in a temperate estuary: Is the response to restoration

efforts hidden by climate variability and the Estuarine Quality Paradox? Ecol Indic 24:56-67
Wada E, Mizutani H, Minagawa M (1991) The use of stable isotopes for food web analysis. Crit Rev Food Sci Nutr 30:361-371
Wernberg T, Bennett S, Babcock RC, de Bettignies T, Cure K, Depczynski M, Dufois F, Fromont J, Fulton CJ, Hovey RK, Harvey ES, Holmes TH, Kendrick GA, Radford B, Santana-Garcon J, Saunders BJ, Smale DA, Thomsen MS, Tuckett CA, Tuya F, Vanderklift MA, Wilson S (2016) Climate-driven regime shift of a temperate marine ecosystem. Science 353:169-172

Chapter 2

Stable isotopes indicate ecosystem restructuring following climate-driven mangrove dieback

This chapter is a published paper. The bibliographical details of the co-authored paper, including all authors are:

Harada Y, Fry B, Lee SY, Maher DT, Sippo JZ, Connolly RM (2019) Stable isotopes indicate ecosystem restructuring following climate-driven mangrove dieback. Limnology and Oceanography.

Author Contributions
The study was conceptualized by all authors. Writing was led by YH and contributed to by all. Field surveys were executed by DTM, JZS and YH. Data compilation and analysis was coordinated by YH and contributed to by all.

(Signed) _____

Corresponding (1st) author: Yota Harada

(Countersigned) _____

Supervisor (and co-author): Rod M. Connolly

Abstract

Extreme climatic events can trigger sudden but often long-lasting impacts in ecosystems by causing near to complete mortality of foundation (habitat-forming) species. The magnitude and frequency of such events is expected to rise due to anthropogenic climate change, but the impact that such events have on many foundation species and the ecosystems that they support remains poorly understood. In many cases, manipulative experimentation is extremely challenging and rarely feasible at a large scale. In late 2015 to early 2016, an extensive area of mangrove forest along ~ 1,000 km of coastline in the Gulf of Carpentaria, Australia, experienced severe dieback, an event associated with climatic extremes. To assess the effect this dieback event had on the mangrove ecosystem, we assessed benthic faunal assemblages and food web structure using stable carbon and nitrogen isotopes in a comparative experiment of impacted forest and adjacent unimpacted forest. Eighteen months after the dieback, the forest that suffered dieback contained significantly fewer crabs that rely on mangrove litter food source but more crabs that rely on microphytobenthos food source than the unimpacted forest. However, the infaunal biomass was largely unaffected by the mortality effect. This is most likely because microphytobenthos was largely unaffected and consequently, this buffered the food-web responses. However, overall, the habitat value for mangrove ecosystem services most likely decreased due to lower physical habitat complexity following tree mortality. Longer-term monitoring could lead to better understanding of biological effects of this extreme event and underlying biological mechanisms that drive changes and recovery.

Introduction

Extreme climatic events including droughts, floods, and heatwaves have a major role in structuring ecological communities via reduction or elimination of foundation species (e.g. canopy-forming plants, reef-building corals) (Silliman et al. 2005; Stuart-Smith et al. 2018; Thomson et al. 2015; Wernberg et al. 2016). The occurrence of these events is anticipated to rise due to climate change (Coumou and Rahmstorf 2012; Stott 2016). However, biological effects of such extreme events remain poorly understood and case studies are limited (Harris et al. 2018). During 2015-16, extreme climatic conditions including high temperatures, dry conditions, and El Niño–Southern Oscillation-induced low sea level triggered a severe unprecedented mass mortality of mangroves along ~1,000 km of coastline in tropical Australia (Duke et al. 2017; Lovelock et al. 2017), the largest known mangrove dieback event from natural causes (Sippo et al. 2018). This coincided with the heat-stressed mass bleaching event of the Australian Great Barrier Reef (Hughes et al. 2017). How the extreme climate-driven loss of mangroves that provide the foundation for habitats and support core ecological processes, can change ecosystem structure remains unclear. It is expected that mangrove tree losses will lead to changes in biological communities due to changes in primary production and associated shifts in nutrients cycling, and to disturbances from physical modifications of habitat structure provided by the mangrove foundation species (Alongi 2015; Kristensen 2008; Lee et al. 2014).

Understanding of individual extreme weather events in human-induced climate change has advanced in the recent decades (Coumou and Rahmstorf 2012; Stott 2016), however, a similar understanding of extreme biological events is limited (Harris et al. 2018; Parmesan et al. 2013; Ummenhofer and Meehl 2017). Climate-driven environmental stresses as well as extreme events such as droughts and heatwaves can change benthic communities of estuarine habitats (Dolbeth et al. 2007; MacKay et al. 2010; Pillay and Perissinotto 2008; Pillay and Perissinotto 2009; Pollack et al. 2011; Verdelhos et al. 2014; Veríssimo et al. 2013). In some cases, investigations of such biological responses to climate-driven environmental stresses and detecting underlying biological mechanisms that drive such responses involve long-term monitoring (Dolbeth et al. 2007; Pollack et al. 2011). The initiation of monitoring after an extreme biological event is therefore essential to interpret these extreme biological events and to anticipate such events in the future (Altwegg et al. 2017). In most cases, ‘before and after’ monitoring is not achievable, however, experimental studies with spatial and temporal controls, for example comparisons with areas that did not experience the extreme event might

produce biological data that can help to identify the mechanisms driving a response. This might also establish casual relationships, possibly detecting other important, non-climatic drivers (Altwegg et al. 2017; Bailey and van de Pol 2016; Verdelhos et al. 2014; Verissimo et al.2013).

Stable isotope tracer data that provide biogeochemical source and process information over time help ecosystem analyses, because as elements circulate in the biosphere, stable isotopic compositions can change in predictable ways (Peterson & Fry 1987). Stable isotopes have been widely used in investigations of C and N cycling in mangrove ecosystems (Adame et al. 2018) and mangrove food webs (Fry & Smith 2002, Bouillon et al. 2008). Mangrove faunal communities including infauna that live within the sediment and epifauna that live at the sediment-water interface or on solid substrata generally constitute much of the benthic food web and perform important functions in coastal habitats (Bouillon et al. 2002, Demopoulos et al. 2007). For example, they serve as food for animals at higher trophic levels and stimulate detrital decomposition (Sheaves & Molony 2000, Lee 2008). Disturbances such as losses of mangrove trees can change organic matter inputs and degradation of sediment organic matter (Adame et al. 2018; Atwood et al. 2017) and consequently change overall sediment conditions with consequences to benthic faunal assemblages (Sweetman et al. 2010, Bernardino et al. 2018). However, detailed knowledge of such trophic interactions in mangrove ecosystems is lacking. Therefore, to assess the effects of climate-driven loss of mangroves on mangrove food webs, a careful evaluation of food web structure, including food resource utilization, is needed. In such isotope investigations, it is typically assumed that consumer isotope values resemble those of food resources, with a trophic shift of +0 to 1‰ for $\delta^{13}C$ and +2 to 3‰ for $\delta^{15}N$ (McCutchan et al. 2003; Vander Zanden and Rasmussen 2001).

The study aims to identify changes in ecosystem structure following this climate-driven mangrove dieback. We combined field survey and stable isotope data at impacted mangrove forest and adjacent unimpacted forest (Fig. 2.1a,b). We hypothesized that (A) changes in benthic faunal assemblages between unimpacted and impacted forests would be evident due to mangrove mortality; and (B) food web structure would be noticeably different between unimpacted and impacted forests as a result of changes in assemblages and on food sources.

Materials and Methods

2015-16 mangrove dieback in the Gulf of Carpentaria, Australia

In late 2015 to early 2016, large areas of mangrove vegetation along ~ 1,000 km of coastline in the Gulf of Carpentaria experienced severe dieback (Duke et al. 2017; Sippo et al. 2018). This led to the complete to near death of mangrove trees. There were coincidental mangrove mortality events that occurred in Exmouth, Western Australia (Lovelock et al. 2017) and Kakadu National Park, Northern Territory (Asbridge et al. 2019). At the time, this region in the Gulf of Carpentaria had not experienced any other significant coincidental disturbances e.g. cyclones and pollution, and was most likely a pristine mangrove forest (Duke et al. 2017). Mangroves in the Gulf region experience harsh environmental conditions such as seasonal aridity, high variability in air and sea surface temperatures and salinity. Due to these conditions, the extent of mangroves is limited in the Gulf region (Asbridge et al. 2016; Duke et al. 2017). The climate in this region is wet-dry tropical with highly seasonal rainfall driven by the Australian monsoon. This tropical arid region experiences drought annually for 6 to 8 months with the majority of rainfall occurring between December and March, and receives mean annual precipitation ranging from approximately 600 to 900 mm (Bureau of Meteorology, see www.bom.gov.au). The cause of the Gulf mangrove dieback is most likely due to a weak monsoon (i.e. drier summer-wet season in 2015-16) combined with unusual climate/weather events at the time including high air and surface sea water temperatures, and El Niño–Southern Oscillation induced low sea-level. These factors most likely resulted in hypersalinization of mangrove sediments and caused adequate hydric, thermal and radiant stresses (Duke et al. 2017; Lovelock et al. 2017). The details of causality are documented by Duke et al. (2017) (see their Figure 12 for the meteorological data showing key climatic drivers) and Harris et al. (2018) (see their Supplementary Material, S1.52).

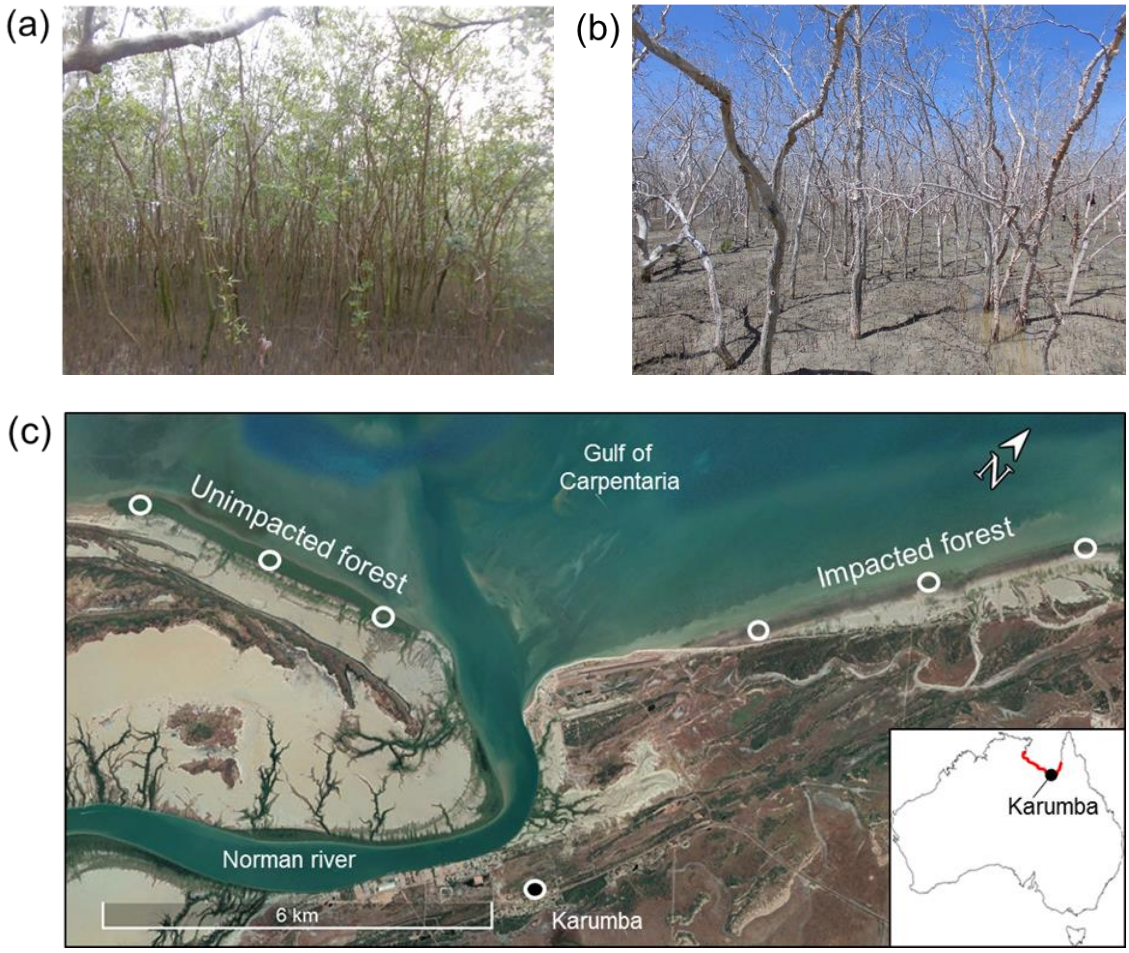

Fig. 2.1. Comparative experiment of unimpacted (a) and impacted (b) mangrove forests. (c) Study location at Karumba in the Gulf of Carpentaria, Queensland, Australia (-17.435572S, 140.844766E). An aerial image/map shows the mangrove vegetation loss and the extent of mangrove loss along the coastline (shown in red). There are three sampling areas within the unimpacted forest and three within the impacted forest (shown as white circles). Two sites within each area were independently sampled.

Experimental design

The main study aim was to assess the effect of climate–driven mangrove tree mortality on mangrove ecosystem structure with particular focus on benthic faunal assemblages and food-web structure. Controlled experimentation as well as 'before and after' comparisons were not easily achievable. For these reasons, we undertook a comparative experiment of an impacted forest vs. an unimpacted forest. This comparative study was carried out at Karumba in the Gulf of Carpentaria, Queensland, Australia (Fig. 2.1c). A major field campaign was conducted in August 2017 in the winter dry-season, 18 months after the dieback event. A forest that had suffered dieback, as well as an adjoining unimpacted forest, provide the settings for a comparative experiment (Fig. 2.1a,b). *Avicennia marina* was the dominant

mangrove species. In this experiment, three areas (2 to 2.5 km apart) within the unimpacted forest and three within the impacted forest were surveyed (Fig. 2.1c). At each area, two independent sites (> 50 m apart) were sampled, one site about 20 m from the forest edge (seaward) and one about 70 m from the forest edge (seaward) to cover the general variability across the intertidal zone and ensure that the physical-oceanographic conditions between the two forests were as similar as possible. Tree density data from Jeffrey et al. (2019) shows the likely similarity in forest structure across the two locations and indicates that the two forests were similar prior to the dieback.

Field survey and sampling

The field surveys were carried out during low tide when the forest ground was exposed. At each sampling site, we conducted sampling using quadrats of sizes 4 m^2 (n=3) and 1 m^2 (n=3), to quantify the populations of common benthic epifauna (ind. m^{-2}). The location of quadrats were randomly chosen at each sampling site and at least 3 m away from each other. In total, n=36 quadrats (6 quadrats × 6 sampling sites) were obtained for each forest. We combined data from 4 m^2 and 1 m^2 quadrats because the smaller quadrat underestimated low abundant species. Individuals were counted visually throughout the quadrats, and each observation lasted 10 to 15 min to ensure that burrowing crabs recover from the initial disturbance (a modified method from Nobbs and McGuinness 1999; Skov and Hartnoll 2001; Skov et al. 2002). Although every care was taken to avoid double-counting individuals, this visual estimation method may have overestimated epifaunal densities by over counting individuals and/or underestimated the densities by under counting those that remained belowground e.g. burrowing crabs and very small individuals that are difficult to observe (Skov et al. 2002). Ten species were identified and sorted into five groups based their feeding modes, namely, algae-feeder (crab) = *Tubuca signata*, *Uca flammula* (Kon et al. 2010; Tue et al. 2012), detritivore (crab) = *Paracleistostoma wardi* (Jones and Clayton 1983), grazer (gastropod) = *Telescopium telescopium*, *Terebralia sulcata* (Pape et al. 2008), leaf-feeder (crab) = *Parasesarma molluccensis*, *Episesarma* sp. (Harada and Lee 2016; Kristensen et al. 2017), omnivore (crab) = *Metopograpsus frontalis* (Poon et al. 2010). Populations (ind. m^{-2}) of the five benthic epifaunal groups were estimated for each forest.

Pneumatophores, crab holes and leaves on the forest floor were quantified using smaller quadrats (size 0.25 m^2, n=15 to 25 per site). In total, n=161 for the unimpacted forest and n=173 for the impacted were obtained to estimate densities (ind. m^{-2}) of pneumatophores,

crab holes and leaves for each forest. In this process, photographs were taken, and counts were made later in the laboratory. To quantify biomass of benthic infauna, sediment core samples (n=3) were collected independently (>10 m apart) at each site using a soil corer (15 cm in diameter and 20 cm in depth) following the method modified from Alfaro (2006). The sediment core samples were immediately wet-sieved using a 0.5 mm sieve onsite. For each sample, the residue retained on the sieve was transferred into sealed plastic containers and preserved in 70% ethanol. The preserved animals mainly consisting of burrowing crabs and some clams and worms in the ethanol solution were separated under a binocular microscope and later weighted (wet g) in a laboratory. In total, n=18 cores (n=3 × 6 sampling sites) were obtained from each forest to estimate infaunal biomass (g/m^2) of each forest. One additional sediment core sample (5 cm in diameter and 20 cm in depth) was collected at each site (total n=6 each forest) for analyzing total carbon (TO), total organic carbon (TOC), total nitrogen (TN), stable isotope values ($\delta^{13}C$ and $\delta^{15}N$) and particle sizes. Particle sizes were analyzed using a particle size analyzer (Malvern Mastersizer Hydro). At each sampling site, pH and salinity were measured from a water sample obtained by digging bores to the depth of water table (total n=6 each forest). The top 0.5 cm surface sediment (200ml) was also collected at each site (total n=6 each forest) for TO, TOC, TN, $\delta^{13}C$ and $\delta^{15}N$ measurements. 150 ml of each 0.5 cm surface sediment sample was used to extract microphytobenthos (MPB) as described below. Extracted MPB samples were also analyzed for $\delta^{13}C$ and $\delta^{15}N$ values. The Chl a content of the surface sediment samples was also measured to assess the abundance of MPB. Chl a was extracted using 90% aqueous acetone in darkness for 24 hours. Chl a concentration was measured following the spectrophotometric method (Parsons 2013). In this process, three measurements were made for each sample and the mean of three measurements was determined for each sample for data analysis. 5 g of sediment was used for each measurement.

Stable isotope analysis

To compare stable carbon and nitrogen isotopic compositions of primary producers including mangrove (*A. marina*) and MPB as well as invertebrate consumers from the above-mentioned five feeding groups between unimpacted and impacted forests, samples were gathered from each forest. Each forest consists of three sampling areas (2 to 2.5 km apart) as shown in Fig. 3c. At each sampling area, samples were collected between 20 to 70m from the forest edge (seaward). Samples were collected by hand and were frozen immediately after the collection. All stable isotope samples were stored separately in sealed plastic containers at -20°C until

analysis. In total, 15 mangrove leaves, 6 MPB samples and > 141 individual invertebrates from the unimpacted forest and 12 mangrove leaves, 6 MPB samples and > 102 individual invertebrates for the impacted forest were collected and analyzed as described below. Senescent yellow leaves were picked from mangroves (*A. marina*). Leaves samples were washed thoroughly, rinsed with distilled water and the main vein was removed. Three leaves from the same sampling area were composited for each isotope measurement.

MPB was extracted from the top 0.5 cm soil samples by density gradient centrifugation in colloidal silica (Bui and Lee 2014; Hamilton et al. 2005). The soil was suspended in distilled water and then filtered through a 63 µm sieve to remove larger particles. The filtrate was centrifuged at 4,400 rpm for five min, and the supernatant was discarded. Pellets were resuspended with 40 mL of 30% Ludox colloidal silica (Sigma) and centrifuged again at 4,400 rpm for five minutes. The top layer containing algal cells (mostly diatom and filamentous cyanobacteria), confirmed by microscopic examination, was collected and centrifuged again with distilled water to remove silica. The MPB samples were dried and collected in tin capsules for analysis.

For fauna stable isotope analysis, muscle tissues were used. Several individuals (2 to 10) of the same species from the same sampling area were pooled to efficiently obtain the mean isotope values (Fry 2006). Each sediment sample of < 0.5 cm surface sediment (n=6 per forest) and 0.5 -20 cm deep sediment (n=6 per forest) as described above were mixed, dried and homogenised before stable isotope analysis. For sediment $\delta^{13}C$ measurements, samples were acidified with 1N HCl to remove inorganic fraction. All samples were dried at 60°C, powdered, homogenized and collected in tin capsules for stable isotope analysis. Stable isotope analyses of $\delta^{13}C$ and $\delta^{15}N$ were carried out on an elemental analyzer (Europa EA-GSL) coupled to an isotope ratio mass spectrometer (Sercon 20-22, SERCON, UK) at Griffith University, Brisbane, Australia. Vienna PeeDee Belemnite (VPDB) and atmospheric air (AIR) were used as standards for C, and N, respectively. Stable isotope values are reported in δ-notation (‰), i.e. $\delta^{13}C$ or $\delta^{15}N = (R_{sample}/R_{standard} - 1) \times 1000$, where R is respectively $^{13}C/^{12}C$ or $^{15}N/^{14}N$. The elemental compositions, i.e. % C and % N, of samples were also provided.

Data analysis

All statistical analyses were undertaken in R version 3.4.3 with RStudio interface version 1.1.414. Differences among group means were tested with ANOVA. Before performing ANOVA, the assumptions of homogeneity of variance and normality were checked using Levene's and Shapiro-Wilk's tests, respectively. When the ANOVA assumptions were violated, the data were log transformed and ensured that the assumptions were met before performing the ANOVAs. For the sediment TC, TOC, TN, $\delta^{13}C$ and $\delta^{15}N$ data, when the ANOVA test was significant, a post hoc Turkey test was performed to check which specific groups differed (< 0.5 cm surface sediment and 0.5 -20 cm deep sediment). A generalized linear model with Poisson distribution was performed for count data. PERMANOVA was performed to compare epifaunal compositions (i.e. abundance of the five feeding groups, ind. m^{-2}) between the two forests and to test whether the compositions between the two forests differ in spread or position in a multivariate space. In this analysis, square-root transformation was applied to minimize influence of the most abundant groups, then the Bray-Curtis index was used as the distance metric. Permutation test of multivariate homogeneity of dispersions was performed to check whether dispersions around the centroids are similar between the two forests. All statistical tests used a significance criterion of 0.05.

Results

Population densities (ind. m^{-2}) of the five epifaunal feeding groups across unimpacted and impacted forests are shown in Table 2.1. The forest that suffered dieback contained fewer leaf-feeding crabs but more algae-feeding crabs than the unimpacted forest (mean, SE and GLM statistics provided in Table 2.1). However, populations of other dominant faunal groups including omnivores (crab), detritivores (crab) and grazers (gastropod) did not differ significantly (Table 2.1). Epifaunal species composition (%) for each forest (Fig. 2.2a) indicates that the impacted forest is dominated by the algae-feeding crabs. PERMANOVA indicated that the two forests differed in the assemblages of five epifaunal feeding groups (df = 1, $r^2 = 0.29$, F = 27.22, p = 0.001), but the data dispersions did not differ significantly (df = 1, F = 1.95, P = 0.15; Fig. S2.1). There was also no significant difference in the total infaunal biomass, i.e. mostly burrowing crabs (Fig. 2.2b and Table 2.1). Consistent with this, the densities of crab burrows (burrows. m^{-2}) did not differ significantly between the impacted (mean = 64.3, SE = 2.0) and the unimpacted forest (mean = 65.2, SE = 2.3) (Table 2.1). In terms of trophic resource availabilities, leaf litter abundance (leaves. m^{-2}) significantly differed, with fewer leaves on the ground in the impacted (mean = 3.8, SE = 1.3) than the

unimpacted forest (mean = 76.1, SE = 11.7) (Table 2.1). The leaves in the impacted forest probably arrived as subsidies from adjacent healthy areas, or minor patches of regrowth. Microphytobenthos (MPB) density estimated by soil chlorophyll content (μg g^{-1}) did not differ significantly between the impacted (mean = 8.4, SE = 0.9) and the unimpacted (mean = 6.7, SE = 1.1) forests (Table 2.1). However, forest floor habitat structure differed between the two forests, with significantly fewer pneumatophores in the impacted (mean = 4.4, SE = 0.6 ind. m^{-2}) than the unimpacted (mean = 184.5, SE = 8.1) forests (Table 2.1).

Table 2.1. Summary of values (mean, SE) of ecological components from each forest.

	Forest				ANOVA/GLM
	Unimpacted		Impacted		
	Mean (SE)	n	Mean (SE)	n	DF, F, p
Algae-feeder (crab) (ind. m^{-2})*	3.5 (0.7)	36	10.9 (1.2)	36	1, -1.1, <0.001
Detritivore (crab) (ind. m^{-2})*	0.9 (0.2)	36	0.7 (0.4)	36	1, 0.28, 0.30
Grazer (gastropod) (ind. m^{-2})*	0.8 (0.1)	36	0.8 (0.2)	36	1, -0.08, 0.78
Leaf-feeder (crab) (ind. m^{-2})*	1.6 (0.2)	36	0.2 (0.04)	36	1, 2.2, <0.001
Omnivore (crab) (ind. m^{-2})*	0.8 (0.1)	36	0.5 (0.1)	36	1, 0.47, 0.11
Crab burrows (burrows. m^{-2})	65.2 (2.3)	161	64.3 (2.0)	173	1, -0.014, 0.272
Pneumatophore (pneumatophores. m^{-2})	184.5 (8.1)	161	4.4 (0.6)	173	1, -3.74, <0.001
Leaf litter (leaves m^{-2})	76.1 (11.7)	161	3.8 (1.3)	173	1, 2.91, <0.001
Infaunal biomass (wet g m^{-2})	63.3 (21.8)	18	87.7 (43.7)	18	1, 0.03, 0.86
Surface <0.5 cm sediment TC (%)	2.37 (0.44)	6	2.18 (0.16)	6	1, 0.01, 0.92
Surface <0.5 cm sediment TOC (%)	2.15 (0.61)	6	1.37 (0.29)	6	1, 1.34, 0.28
Surface <0.5 cm sediment N (%)	0.15 (0.03)	6	0.11 (0.02)	6	1, 1.43, 0.26
0.5-20 cm sediment TC (%)	2.10 (0.20)	6	2.51 (0.45)	6	1, 0.52, 0.49
0.5-20 cm sediment TOC (%)	1.72 (0.27)	6	1.56 (0.29)	6	1, 0.27, 0.61
0.5-20 cm sediment N (%)	0.12 (0.01)	6	0.08 (0.01)	6	1, 7.80, 0.02
Soil Chl a (μg soil g^{-1})	6.7 (1.1)	6	8.4 (0.9)	6	1, 2.07, 0.18
Mean particle size (μm)	17.3 (5.4)	6	26.8 (3.3)	6	1, 4.27, 0.07
% clay (<2 μm)	13.7 (1.5)	6	10.4 (0.4)	6	-
% silt (2 – 50 μm)	60.5 (3.4)	6	57.8 (1.8)	6	-
% sand (50 to 2000 μm)	25.8 (4.6)	6	31.8 (2.2)	6	-
Salinity	58.6 (6.9)	6	56.8 (4.5)	6	1, 0.05, 0.83
pH	6.9 (0.1)	6	6.9 (0.1)	6	1, 0.01, 0.94
Tree density (tree m^{-2})	0.18 (0.03)	3	0.18 (0.04)	3	1, 0.04, 0.99

*algae-feeder (crab) = *Tubuca signata*, *Uca flammula*, detritivore (crab) = *Paracleistostoma wardi*, grazer (gastropod) = *Telescopium telescopium*, *Terebralia sulcata*, leaf-feeder (crab) = *Parasesarma molluccensis*, *Episesarma* sp., omnivore (crab) = *Metopograpsus frontalis*

-Tree density (tree m^{-2}) is taken from Jeffrey et al. 2019 (their Table 1). The value reported here is an average of three intertidal zones (upper, middle and lower).

-Infaunal biomass is > 0.5cm size fraction

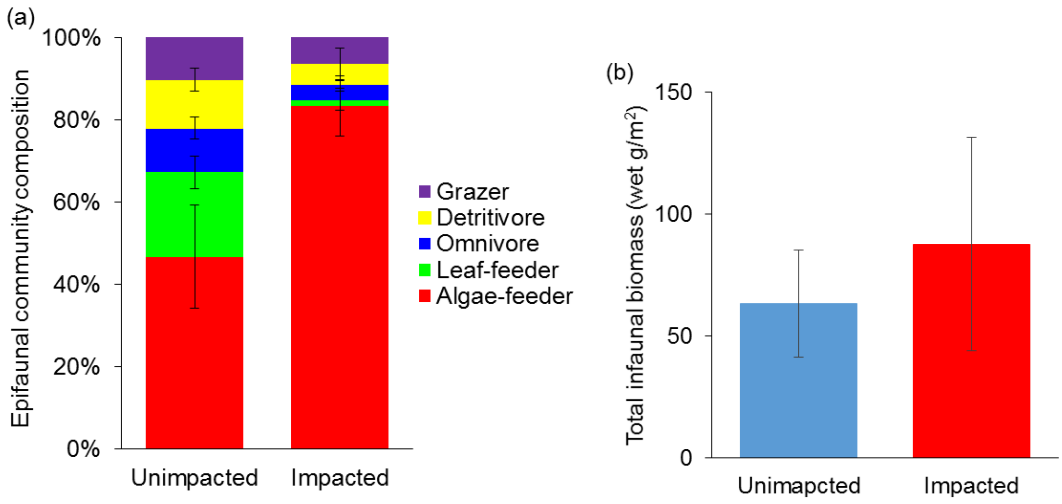

Fig. 2.2. Observed differences in benthic faunal community between unimpacted and impacted mangrove forests. (a) Proportions of dominant epifaunal feeding groups (% mean, SE): Algae-feeder (crab) = *Tubuca signata, Uca flammula*. Detritivore (crab) = *Paracleistostoma wardi*. Grazer (gastropod) = *Telescopium telescopium, Terebralia sulcata*. Leaf-feeder (crab) = *Parasesarma molluccensis, Episesarma* sp., Omnivore (crab) = *Metopograpsus frontalis*. (b) Total > 0.5 cm size fraction infaunal biomass estimated from coring (mean, SE, n=18 per treatment).

TC, TOC and TN measurements (%) of the two types of sediment (i.e. surface < 0.5 cm and 0.5 – 20 cm deep) across two forests are provided in Table 2.1 with the mean values and ANOVA statistics. For the surface sediment samples, TC, TOC and TN (%) measurements did not significantly differ between the two forests. For the 0.5 – 20 cm deep sediment, TC and TOC (%) did not differ between the forests, but TN (%) differed, being significantly lower in the impacted forest. $\delta^{13}C$ and $\delta^{15}N$ values of sediment samples are provided in Table 2.2 and shown in Fig 2.3ab with their C and N elemental compositions (TOC and TN %) (Fig 2.3cd). While the $\delta^{13}C$ and $\delta^{15}N$ values in the 0.5 – 20 cm deep sediment samples did not differ significantly between the two forests, the $\delta^{13}C$ and $\delta^{15}N$ values for the surface sediment samples were significantly higher in the impacted forest (Table 2.2). The surface sediment $\delta^{13}C$ and $\delta^{15}N$ values in the impacted forest were significantly higher than all the other groups including those for the 0.5 – 20 cm deep samples from both forests (Post hoc Turkey test, $P < 0.05$) (Fig. 2.3a,b). Overall, sediment $\delta^{13}C$ values ranged from -26.3 to -23.8‰ for the unimpacted forest and -25.3 to -21.2‰ for the impacted forest. Sediment $\delta^{15}N$ values ranged from 0.9 to 2.8‰ for the unimpacted forest and 1.3 to 3.7‰ for the impacted forest. Mean particle size (μm) of 0.5 – 20 cm deep sediment did not differ between the two forests with

silt (2 - 50μm) being the main component (Table 2.1). Salinity and pH did not differ between the two forests (Table 2.1).

Table 2.2. C and N isotope values (mean, SE) of primary producers, sediment and consumers collected from unimpacted and impacted forests.

Type/Taxon		Forest						ANOVA (DF, F, P)	
		Unimpacted			Impacted				
		$\delta^{13}C$ (SE), ‰	$\delta^{15}N$ (SE), ‰	n, pooled	$\delta^{13}C$ (SE), ‰	$\delta^{15}N$ (SE), ‰	n, pooled	$\delta^{13}C$	$\delta^{15}N$
Primary producers									
Mangrove	*Avicennia marina*	-28.0 (0.8)	3.8, (0.4)	5 (3)	-25.9 (0.2)	3.3 (0.5)	4 (3)	1, 5.13, 0.06	1, 0.57, 0.48
MPB		-25.3 (0.3)	2.5, (0.3)	6 (1)	-20.7, (0.4)	3.1 (0.2)	6 (1)	1, 85.1 <0.001	1, 3.00, 0.11
Sediment									
Surface <0.5cm		-24.7 (0.4)	2.0 (0.2)	6 (1)	-22.4 (0.4)	2.8 (0.2)	6 (1)	1, 19.1, 0.001	1, 6.57, 0.03
0.5-20cm		-24.8 (0.3)	1.7 (0.2)	6 (1)	-24.5 (0.2)	1.7 (0.1)	6 (1)	1, 0.63, 0.45	1, 0.01, 0.98
Consumers									
Algae-feeder, crab	*Tubuca signata*	-17.9 (0.7)	6.0, (0.4)	4 (3)	-15.3 (0.6)	7.6 (0.6)	4 (3)	1, 8.42, 0.03	1, 5.23, 0.06
	Uca flammula	-20.9	4.6	1 (1)	-14.4 (0.1)	4.3 (0.5)	2 (1)	-	-
Omnivore, crab	*Metopograpsus frontails*	-20.0 (0.4)	7.7, (0.9)	2 (2)	-15.9 (0.6)	9.9 (0.7)	4 (3-4)	1, 18.72, 0.01	1, 3.60, 0.13
Detritivore, crab	*Paracleistostoma wardi*	-21.9 (0.5)	6.0, (0.3)	4 (2)	-17.1 (0.8)	8.7 (0.6)	3 (3-5)	1, 26.93 0.004	1, 18.26 0.008
Leaf-feeder, crab	*Parasesarma molluccensis*	-21.5 (0.4)	7.9, (0.3)	8 (5)	-18.5 (0.2)	9.3 (0.6)	4 (1)	1,22.52 <0.001	1, 7.25 0.02
	Episesarma	-22.6	8.0	1 (1)	-	-	-	-	-
Grazer, gastropod	*Telescopium telescopium*	-19.1 (1.3)	6.4, 0.1	3 (4-5)	-17.4 (0.7)	6.9 (0.1)	4 (4-5)	1, 1.52, 0.27	1, 10.59, 0.02
	Terebralia sulcata	-20.3 (1.3)	5.6 (0.3)	4 (2-3)	-16.9 (0.3)	6.5 (0.1)	3 (2)	1, 3.03, 0.14	1, 8.55, 0.03
Filter-feeder, bivalve	Mussel	-20.9 (0.1)	6.8, (0.1)	3 (5-10)	-21.7 (0.1)	6.8 (0.1)	3 (3)	1, 18.48, 0.01	1, 0.07, 0.81
	Oyster *Crassostrea*	-20.0 (0.2)	7.7 (0.2)	4 (10)	-19.9 (0.5)	7.9, (0.3)	4 (10)	1, 0.05, 0.83	1, 0.52, 0.50

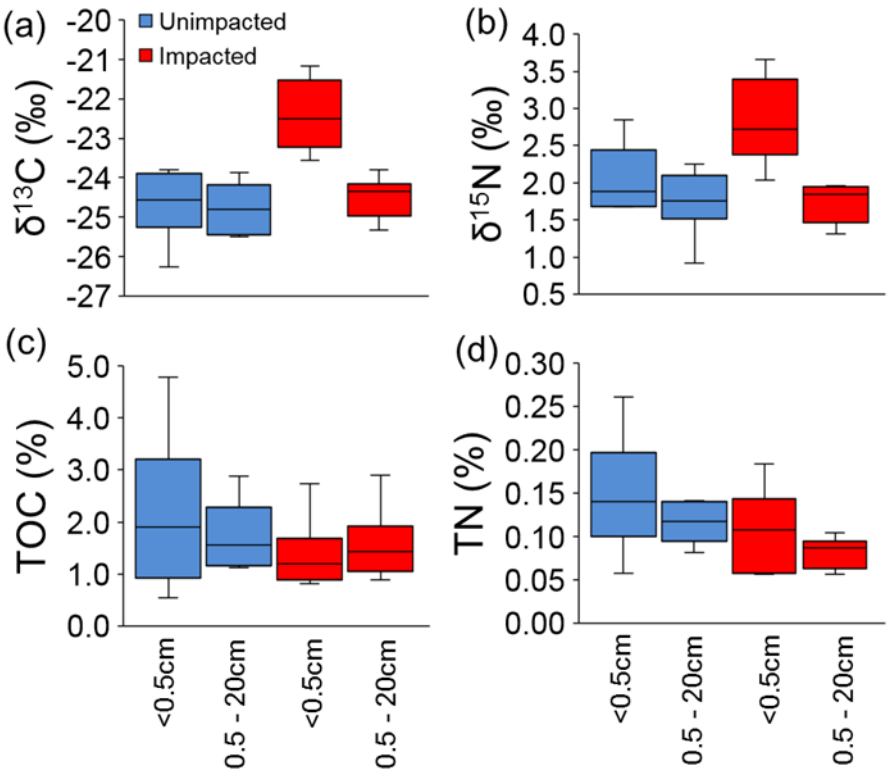

Fig. 2.3. $\delta^{13}C$, $\delta^{15}N$, TOC and TN measurements from surface < 0.5 cm sediment and 0.5 – 20 cm deep sediment in unimpacted and impacted mangrove forests. Box plots present the median, 68% credible interval and 95% credible interval. n=6 per treatment. See Table 2.1, Table 2.2 and the text for mean, SE values and ANOVA statistics.

$\delta^{13}C$ and $\delta^{15}N$ values of primary producers including mangrove leaves of *A. marina* and MPB as well as epifaunal consumers from different feeding groups are reported in Table 2.2 with the mean, SE values and ANOVA statistics and shown in Fig. 2.4. Mangrove leaf $\delta^{13}C$ and $\delta^{15}N$ values did not differ between the two forests. The leaf $\delta^{13}C$ values ranged from -28.4 to -25.6‰ for the unimpacted forest and -26.4 to -25.6 in the impacted forest. The leaf $\delta^{15}N$ values ranged from 2.4 to 4.7‰ for the unimpacted forest and 2.1 to 4.3‰ in the impacted forest. MPB $\delta^{13}C$ values were significantly higher in the impacted forest than the unimpacted forest, but the $\delta^{15}N$ values did not differ significantly. Overall, MPB $\delta^{13}C$ values ranged from -26.5 to -24.7‰ for the unimpacted forest and -22.0 to -18.9‰ in the impacted forest and MPB $\delta^{15}N$ values ranged from 1.5 to 3.5‰ for the unimpacted forest and 2.4 to 3.9‰ in the impacted forest. Overall, consumer $\delta^{13}C$ values ranged from -23.4 to -16.7‰ in the unimpacted forest with lower values (-23.4 to -21.5‰) associated with the leaf-feeders and higher values (-16.7 to -20.9‰) associated with the algae-feeders. Overall, the impacted forest had a relatively higher $\delta^{13}C$ range of -20.1 to -14.4‰. Consumer $\delta^{15}N$ values ranged from 4.6 to 8.7‰ in the unimpacted forest. Compared to this, the impacted forest had a

relatively higher range of 3.7 to 11.2‰. $\delta^{13}C$ and $\delta^{15}N$ measurements of the individual consumer samples were shown in Fig S2.2. The individual epifaunal species and the feeding groups showed substantial differences in the $\delta^{13}C$ and $\delta^{15}N$ values between the two forests, except for filter-feeders (bivalve) more reliant on water column resources (Table. 2.2 and Fig. 2.4). The patterns of isotope difference between the two forests were fairly consistent across all the faunal groups, also mirroring those of the surface sediment and MPB (Fig. 2.4).

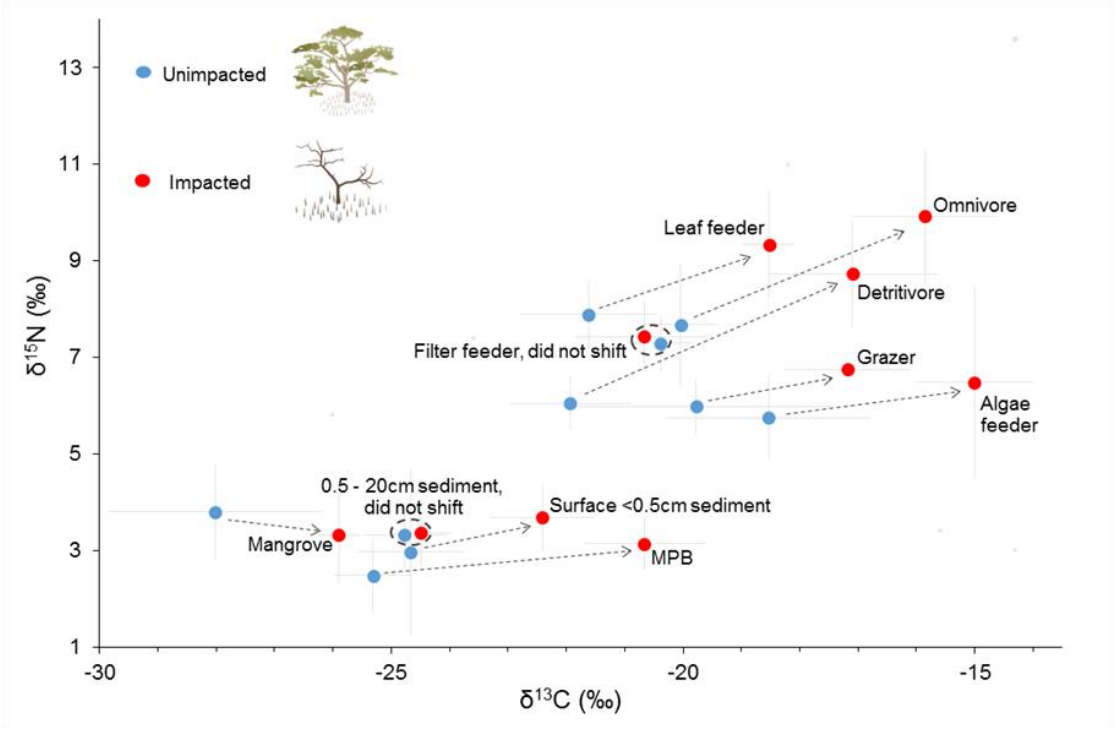

Fig. 2.4. Patterns of $\delta^{13}C$ and $\delta^{15}N$ values (mean, SD) of dominant epifaunal groups and trophic resources across unimpacted and impacted mangrove forests. Patterns of isotope differences between the two forests shown as arrows were similar between all the faunal groups and correspond to shifts of surface <0.5 cm sediment and MPB samples. 0.5 – 20 cm deep sediment samples and filter-feeder samples (mussels and oysters) did not show large shifts. See Table 2.2 for taxonomic details, mean values and ANOVA statistics.

Discussion

Overall, results from our study that compared between the impacted and unimpacted forests suggest that the climate-driven mangrove mortality has most likely changed the epifaunal species composition, i.e. increased population densities of algae-feeders (*Tubuca* and *Uca*) and decreased population densities of leaf-feeders (Sesarmidae). However, it did not have a significant effect on the total infaunal biomass, i.e., mostly burrowing crabs and some clams and worms. Consistent with this, the densities of crab burrows did not differ significantly between the impacted and unimpacted forest. Overall, such findings generally suggested that

epifauna, as well as infauna in the impacted forest (mostly burrowing crabs and gastropods), are fairly abundant, regardless of the mangrove loss. In most cases, epifaunal as well as infaunal communities in mangrove ecosystems are controlled by various factors including tidal regime, sediment (grain size, pH), trophic resource availability, habitat complexity and predation (Lee 2008; Nagelkerken et al. 2008). One explanation for our results is that MPB, an important food source in many mangrove ecosystems (Larsen et al. 2012; Mazumder and Saintilan 2010; Oakes et al. 2010) was largely unaffected and consequently, this buffered the food web responses, maintaining overall abundance/biomass of mangrove fauna. In many cases, disturbances such as loss of mangrove trees can change abiotic factors including light intensity and temperature (Granek and Ruttenberg 2008) as well as organic matter inputs and sediment conditions with consequences to benthic assemblages (Sweetman et al. 2010, Bernardino et al. 2018). In some cases, after clearing of mangroves, MPB biomass can increase due to changes in abiotic factors such as light intensity and temperature (Granek and Ruttenberg 2008). In our case, MPB (sediment Chl a) did not differ between the two forests, but it may be possible that feeding ground for MPB may have increased in the impacted forest where there are now relatively less canopy cover and pneumatophores with more open cleared spaces (i.e. more space for foraging MPB).

While the effects of the climate-driven mangrove mortality and those of other deforestation events may differ, consistent with our case, similar patterns in faunal communities have been observed in mangrove ecosystems that experienced deforestation. For example, while benthic faunal assemblages changed after clearing of mangroves, the total abundance and biomass did not respond to the mangrove removal effect (Bernardino et al. 2018) or they even increased (Alfaro 2010). Similar to our case, in cleared areas of mangrove forest (due to typhoon), relative abundances of algae-feeding crabs (i.e. fiddler crabs, *Tubuca* and *Uca*) increased whereas leaf feeding crabs (Sesarmidae, typical forest species) were less abundant in the cleared gaps than in the forest (Diele et al. 2013). The increased relative abundance of *Tubuca* and *Uca* spp. in the cleared gaps may relate to improved availability of MPB, its main food source (Kon et al. 2007). In general, these algae-feeder crabs (*Tubuca* and *Uca*) may also prefer more open areas than closed forests due to enhanced visibility that facilitates their visual communication through claw waving for mating and antagonistic interactions (Crane 2015; Nobbs 2003). In contrast, the leaf-feeding crabs (Sesarmidae) are generally associated more with mangrove trees and prefer sheltered areas of mangrove forests (Diele et

al. 2013; Lee 2008). The dominance of algae-feeder crabs in our impacted site is shown in Fig. S2.3.

In many cases, organic matter within mangrove sediment decreases following mangrove forest loss (Otero et al. 2017, Adame et al. 2018). In our study site, TOC and N (%) did not differ statistically between the two forests except for 0.5 – 20 cm deep sediment N, but those mean values were consistently lower in the impacted forest, most likely suggesting some degradation of sediment organic matter and lower mangrove organic matter input with the low leaf litter availability. Overall, stable C and N isotope values from sediment, MPB and consumers were generally higher in the impacted forest, suggesting that the impacted ecosystem had relatively lower mangrove carbon fixation input that generally shows lower $\delta^{13}C$ values near -27‰ (Bouillon et al. 2008). The higher $\delta^{15}N$ values may be associated with lower N fixation input, generally near 0‰ (Fogel et al. 2008) as well as degradation of organic matter that can enrich available N with ^{15}N (Adame and Fry 2016; Natelhoffer and Fry 1988). The $\delta^{13}C$ and $\delta^{15}N$ values in the 0.5 to 20 cm deep sediment did not differ significantly between the two forests. Although, bioturbation can transport surface organic matter to the range of > 0.5 cm deep sediment, one explanation for such consistency in 0.5 to 20 cm sediment $\delta^{13}C$ and $\delta^{15}N$ values between the two forests can be that the C and N cycle of the two forests were fairly consistent previously. Furthermore, distinctively high surface (<0.5 cm) sediment $\delta^{13}C$ and $\delta^{15}N$ values in the impacted forest compared to those of other sediment including those of 0.5 to 20 cm deep sediment, as well as those of the unimpacted forest, suggest that there was a probable effect of recent mangrove mortality on the surface sediment compositions. This may be because the surface sediment layer (surface <0.5 cm) can be more likely to be oxidised than the 0.5 – 20 cm deep sediment layers. Similar to our case, increase in sediment $\delta^{13}C$ and $\delta^{15}N$ values were observed in mangrove forests in Malaysia that experienced deforestation (Adame et al. 2018), an effect likely due to decomposition of organic matter (Adame and Fry 2016; Natelhoffer and Fry 1988) as well as lower mangrove C input following mangrove losses.

There were also substantial differences in epifaunal $\delta^{13}C$ and $\delta^{15}N$ values among the two forests, with those from the impacted forest generally having higher $\delta^{13}C$ and $\delta^{15}N$ values, fairly consistent with the differences observed in sediment and MPB $\delta^{13}C$ and $\delta^{15}N$ values. The individual epifaunal groups show substantial isotope differences except for filter-feeders (bivalve) more reliant on water column resources such as phytoplankton that may be

unaffected by the mangrove mortality. However, MPB $\delta^{13}C$ values largely differed between the forests. This may reflect differences in respiratory inputs from mangrove organic matter (Maher et al. 2013). Mangrove leaf $\delta^{13}C$ values did not significantly differ between the forests, but showed substantial variability with the impacted forest having relatively higher values. Such C isotope pattern may be due to reduced stomatal conductance that causes lower internal carbon dioxide concentrations and lower carbon isotope fractionation (Farquhar et al. 1989; Lin & Sternberg 1992a; Lin & Sternberg 1992b).

Overall, there were high variabilities in $\delta^{13}C$ values of trophic resources (mangrove and MPB) that limit the interpretation of our epifaunal consumer isotope dataset. However, a simpler explanation for the large difference in epifaunal $\delta^{13}C$ values between the two forests is that the impacted food web had a lower mangrove C input but substantial inputs from MPB and phytoplankton. Similar to our case, increases in mangrove fauna $\delta^{13}C$ and $\delta^{15}N$ values were observed in mangrove ecosystems in eastern Brazil that experienced deforestation, suggesting a shift of the nutrient sources with more food web reliance on marine carbon sources after clearing of mangroves (Bernardino et al. 2018). In a more quantitative sense, overall primary producer (mangrove and MPB) $\delta^{13}C$ values ranged from -30.5 to -24.7‰ in the unimpacted forest and -26.4 to -18.9‰ in the impacted forest, whereas epifaunal consumer $\delta^{13}C$ values ranged from -23.4 to -16.7‰ in the unimpacted and -20.1 to -14.4‰ in the impacted forest. So that there were substantial isotope mismatches between the end-member food resources and consumers suggesting that our characterization of end-members were generally weak. However, in many cases, such isotope mismatches can occur and characterisation of end-members in mangrove detrital food web interactions is often not easily achieved (Bui and Lee 2014). Due to these reasons, we could not confidently conduct stable isotope mixing analysis using our current isotope dataset with typical assumptions that consumer isotope values resemble those of food resources, with a trophic shift of +0–1‰ for $\delta^{13}C$ and +2–3‰ for $\delta^{15}N$ (McCutchan et al. 2003; Vander Zanden and Rasmussen 2001). Additional tracers such as $\delta^{34}S$ (Fry and Smith 2002) as well as $\delta^{13}C$ of individual amino acids (Larsen et al. 2012) may be needed to resolve such isotope mixing problems. However, in a more qualitative sense, the algae-feeder that displayed the mean $\delta^{13}C$ value of -15.5 ‰ (SE 0.6), was the dominant feeding group in the impacted forest with the population contributing to 83% (SE 13) of the community total (Fig. 2.2a). Therefore, it is likely that the epifaunal community in the impacted forest is largely supported by MPB than mangrove detritus food resources that generally show $\delta^{13}C$ values of near -27‰.

In many cases, more nutritious MPB as well as phytoplankton contribute substantially to mangrove food webs, with consumers generally showing lower importance of low quality mangrove leaf litter in their diet (Larsen et al. 2012; Mazumder and Saintilan 2010; Oakes et al. 2010). Consistent with this, in our study, the mangrove epifauna as well as infauna were fairly abundant in the impacted forest and they did not greatly respond to the reduced mangrove leaf litter food availability following the mangrove mortality. This is probably because nutritious trophic resources such as MPB and phytoplankton were largely unaffected and such food resources were probably highly available in this fringe and narrow mangrove ecosystem adjacent to an extensive mudflat habitat. It is also possible that this ecosystem in the Gulf region (tropical-arid Australia) with probable low tree density relative to forests of similar latitudes (Sanders et al. 2016, Jeffrey et al. 2019) formerly had a high food web reliance on MPB. This is partially evident from our isotope data that the patterns of isotope difference in most epifaunal groups between the two forests corresponded to those of MPB. Furthermore, it may be possible that such large difference in epifaunal $\delta^{13}C$ values between the two forests was largely driven by the difference in MPB food values, rather than differences in nutritional reliance on food resources (e.g. mangrove vs. MPB). Although, the overall isotope difference (i.e. high $\delta^{13}C$ values in the impacted forest) is most likely related to the mangrove mortality effect (e.g. low leaf litter and low mangrove respiratory inputs), our current data could not confirm the changes in the nutritional dependency on food resources (mangrove vs. MPB) and could not eliminate the possibility that there is high importance of MPB in the unimpacted forest. More detailed isotope investigations are required to elucidate whether nutritional dependency of consumers on food resources have changed due to the mangrove mortality. In such isotope investigations, stable carbon isotopic compositions in essential amino acids (e.g., Larsen et al. 2012) may be useful.

It is most likely that this mangrove dieback will impact the provision of key ecosystem services including food and habitat provision, carbon sequestration and coastal protection. While this study did not characterize meiofaunal fractions as well as larvae that could be affected by mangrove mortality, given that benthic macrofaunal fractions were fairly abundant after the mangrove mortality, trophic contribution by the mangrove ecosystem to adjoining coastal communities (e.g. fish that forage in mangrove forests during high tide) might be sustained. However, animals that rely more on mangroves for habitat structure (e.g. juvenile nekton) might suffer from physical habitat modifications (e.g. reduced shade and habitat complexity). Changes in fish assemblage and decreases in fish abundance, especially

smaller schooling species were observed in mangrove ecosystems that experienced mangrove losses, an effect likely due to reduced habitat complexity (Shinnaka et al. 2007; Taylor et al. 2007). Our study also captured substantial changes in C and N dynamics including decomposition and loss of mangrove organic matter. A recent study shows rapid losses of sediment C and N stocks after clearing of mangroves (Adame et al. 2018), suggesting that losses of the C and N stocks (including underground roots) following the mangrove mortality are expected with changes to carbon outwelling to the coastal ocean (Sippo et al. 2019). The loss of pneumatophore root structure suggests reduced sediment stability leading to a higher risk of erosion. Considering that there is a large amount of dead mangrove materials slowly decaying in the forest, and the recovery of mangrove vegetation to the original state probably takes decades (Adame et al. 2018), the full impact of the 2015-16 mangrove dieback needs to be further monitored.

We faced limitations and challenges in this investigation of an extreme biological event and these also apply to single-event studies elsewhere. Firstly, 'before and after' comparisons are rarely possible and experimentation is extremely difficult, therefore investigations largely rely on spatial comparisons (e.g. impacted vs unimpacted) (Altwegg et al. 2017; Harris et al. 2018). Secondly, extreme events are rare, so that inference from such single-event studies cannot be simply made under the typical statistical paradigm that depends on replication and control (Altwegg et al. 2017). The inference of our observational data from this experimental study largely relies on an assumption that the unimpacted and impacted forests were comparable and similar before the dieback event. The experimental and control conditions in our study were determined by nature, so we cannot rule out natural variability as an explanation for some of our observational data. However, some of the trends we detected seem to be driven by mangrove mortality, and are consistent with observations from mangrove ecosystems that experienced deforestation (i.e. mangrove removal) and with the general ecology of mangrove faunal communities (Lee 2008). Long-term monitoring would support the interpretation of this extreme event and multi-annual observational data could help to understand how the mangrove ecosystem may recover from this climate-driven disturbance and underlying biological mechanisms. Experimental studies, e.g. Adame et al. (2018) that used a chronosequence of mangrove forests in Matang Mangrove Forest Reserve in Malaysia to test the effect of mangrove clearing and recovery would help to compare and validate observational data from such single-event study. Initiation of monitoring after an

extreme biological event is an important contribution to our understanding of biological effects of extreme climatic events.

Acknowledgments

We acknowledge support from: YH – Holsworth Wildlife Research Endowment – Equity Trustees Charitable Foundation & the Ecological Society of Australia; DTM - Australian Research Council (DE1500100581, DP180101285); RMC – Global Wetlands Project. We thank R. Bak (Griffith University) for stable isotope analysis, and A. Bourke for field assistance.

References

Adame, M., and B. Fry. 2016. Source and stability of soil carbon in mangrove and freshwater wetlands of the Mexican Pacific coast. Wetl. Ecol. Manage. **24:** 129-137.

Adame, M. and others 2018. Loss and recovery of carbon and nitrogen after mangrove clearing. Ocean Coast Manage. **161:** 117-126.

Alfaro, A. C. 2006. Benthic macro-invertebrate community composition within a mangrove/seagrass estuary in northern New Zealand. Estuar. Coast. Shelf Sci. **66:** 97-110.

---. 2010. Effects of mangrove removal on benthic communities and sediment characteristics at Mangawhai Harbour, northern New Zealand. ICES J. Mar. Sci. **67:** 1087-1104.

Alongi, D. M. 2015. The Impact of Climate Change on Mangrove Forests. Curr. Clim. Change Rep. **1:** 30-39.

Altwegg, R., V. Visser, L. D. Bailey, and B. Erni. 2017. Learning from single extreme events. Philos. Trans. R. Soc. B **372:** 20160141.

Asbridge, E., R. Lucas, C. Ticehurst, and P. Bunting. 2016. Mangrove response to environmental change in Australia's Gulf of Carpentaria. Ecol. Evol. **6:** 3523-3539.

Asbridge, E. F., R. Bartolo, C. M. Finlayson, R. M. Lucas, K. Rogers, and C. D. Woodroffe. 2019. Assessing the distribution and drivers of mangrove dieback in Kakadu National Park, northern Australia. Estuar. Coast. Shelf Sci. **228**: 106353.

Atwood, T. B. and others 2017. Global patterns in mangrove soil carbon stocks and losses. Nat. Clim. Change **7**: 523.

Bailey, L. D., and M. van de Pol. 2016. Tackling extremes: challenges for ecological and evolutionary research on extreme climatic events. J. Animal Ecol. **85:** 85-96.

Bernardino, A. F., L. E. D. O. Gomes, H. L. Hadlich, R. Andrades, and L. B. Correa. 2018. Mangrove clearing impacts on macrofaunal assemblages and benthic food webs in a tropical estuary. Mar. Pollut. Bull. **126:** 228-235.

Bouillon, S., N. Koedam, A. Raman, and F. Dehairs. 2002. Primary producers sustaining macro-invertebrate communities in intertidal mangrove forests. Oecologia **130**: 441-448.

Bouillon, S., R. M. Connolly, and S. Y. Lee. 2008. Organic matter exchange and cycling in mangrove ecosystems: Recent insights from stable isotope studies. J. Sea Res. **59:** 44-58.

Bui, T. H. H., and S. Y. Lee. 2014. Does 'You Are What You Eat' Apply to Mangrove Grapsid Crabs? PLoS One **9:** e89074.

Coumou, D., and S. Rahmstorf. 2012. A decade of weather extremes. Nat. Clim. Change **2:** 491-496.

Crane, J. 2015. Fiddler crabs of the world: Ocypodidae: genus *Uca*. Princeton University Press.

Demopoulos, A. W., B. Fry, and C. R. Smith. 2007. Food web structure in exotic and native mangroves: a Hawaii - Puerto Rico comparison. Oecologia **153**: 675-686.

Diele, K. and others 2013. Impact of typhoon disturbance on the diversity of key ecosystem engineers in a monoculture mangrove forest plantation, Can Gio Biosphere Reserve, Vietnam. Glob. Planet. Change **110:** 236-248.

Dolbeth, M., P. G. Cardoso, S. M. Ferreira, T. Verdelhos, D. Raffaelli, and M. A. Pardal. 2007. Anthropogenic and natural disturbance effects on a macrobenthic estuarine community over a 10-year period. Mar. Pollut. Bull. **54**: 576-585.

Duke, N. C. and others 2017. Large-scale dieback of mangroves in Australia's Gulf of Carpentaria: a severe ecosystem response, coincidental with an unusually extreme weather event. Mar. Freshwater Res. **68:** 1816-1829.

Farquhar, G. D., J. R. Ehleringer, and K. T. Hubick. 1989. Carbon isotope discrimination and photosynthesis. Annu. Rev. Plant Biol. **40**: 503-537.
Fogel, M. and others 2008. Unusually negative nitrogen isotopic compositions ($\delta^{15}N$) of mangroves and lichens in an oligotrophic, microbially-influenced ecosystem. Biogeosci. **5**: 937-969.
Fry, B. 2006. Stable Isotope Ecology. Springer-Verlag New York.
Fry, B., and T. J. Smith. 2002. Stable isotope studies of red mangroves and filter feeders from the Shark River estuary, Florida. Bull. Mar. Sci. **70**: 871-890.
Granek, E., and B. I. Ruttenberg. 2008. Changes in biotic and abiotic processes following mangrove clearing. Estuar. Coast. Shelf Sci. **80:** 555-562.
Hamilton, S. K., S. J. Sippel, and S. E. Bunn. 2005. Separation of algae from detritus for stable isotope or ecological stoichiometry studies using density fractionation in colloidal silica. Limnol. Oceanogr.: Methods **3:** 149-157.
Harada, Y., and S. Y. Lee. 2016. Foraging behavior of the mangrove sesarmid crab Neosarmatium trispinosum enhances food intake and nutrient retention in a low-quality food environment. Estuar. Coast. Shelf Sci. **174:** 41-48.
Harris, R. M. B. and others 2018. Biological responses to the press and pulse of climate trends and extreme events. Nat. Clim. Change **8:** 579-587.
Hughes, T. P. and others 2017. Global warming and recurrent mass bleaching of corals. Nature **543:** 373-377.
Jeffrey, L. C. and others 2019. Are methane emissions from mangrove stems a cryptic carbon loss pathway? Insights from a catastrophic forest mortality. New Phytol **224**: 146-154.
Jones, D., and D. Clayton. 1983. The systematics and ecology of crabs belonging to the genera Cleistostoma De Haan and Paracleistostoma De Man on Kuwait mudflats. Crustaceana **45:** 183-199.
Kon, K., H. Kurokura, and K. Hayashizaki. 2007. Role of microhabitats in food webs of benthic communities in a mangrove forest. Mar. Ecol. Prog. Ser. **340:** 55-62.
Kon, K., H. Kurokura, and P. Tongnunui. 2010. Effects of the physical structure of mangrove vegetation on a benthic faunal community. J. Exp. Mar. Biol. Ecol. **383:** 171-180.
Kristensen, E. 2008. Mangrove crabs as ecosystem engineers; with emphasis on sediment processes. J. Sea Res. **59:** 30-43.
Kristensen, E., S. Y. Lee, P. Mangion, C. O. Quintana, and T. Valdemarsen. 2017. Trophic discrimination of stable isotopes and potential food source partitioning by leaf-eating crabs in mangrove environments. Limnol. Oceanogr. **62:** 2097-2112.
Larsen, T., M. J. Wooller, M. L. Fogel, and D. M. O'Brien. 2012. Can amino acid carbon isotope ratios distinguish primary producers in a mangrove ecosystem? Rapid Commun. Mass Spectrom. **26:** 1541-1548.
Lee, S. Y. 2008. Mangrove macrobenthos: Assemblages, services, and linkages. J. Sea Res. **59:** 16-29.
Lee, S. Y. and others 2014. Ecological role and services of tropical mangrove ecosystems: a reassessment. Glob. Ecol. Biogeogr. **23:** 726-743.
Lin, G., and Sternberg, L.S.L. 1992a. Differences in morphology, carbon isotope ratios, and photosynthesis between scrub and fringe mangroves in Florida, USA. Aquat. Bot. **42**: 303-313.
Lin, G., and Sternberg, L.S.L. 1992b. Effect of growth form, salinity, nutrient and sulfide on photosynthesis, carbon isotope discrimination and growth of red mangrove (Rhizophora mangle L.). Funct. Plant Biol. **19**: 509-517.
Lovelock, C. E., I. C. Feller, R. Reef, S. Hickey, and M. C. Ball. 2017. Mangrove dieback during fluctuating sea levels. Sci. Rep. **7:** 1680.

MacKay, F., D. Cyrus, and K.-L. Russell. 2010. Macrobenthic invertebrate responses to prolonged drought in South Africa's largest estuarine lake complex. Estuar. Coast. Shelf Sci. **86**: 553-567.

Maher, D. T. and others 2013. Novel Use of Cavity Ring-down Spectroscopy to Investigate Aquatic Carbon Cycling from Microbial to Ecosystem Scales. Environ. Sci. Technol. **47:** 12938-12945.

Mazumder, D., and N. Saintilan. 2010. Mangrove leaves are not an important source of dietary carbon and nitrogen for crabs in temperate Australian mangroves. Wetlands **30:** 375-380.

McCutchan, J. H., W. M. Lewis Jr, C. Kendall, and C. C. McGrath. 2003. Variation in trophic shift for stable isotope ratios of carbon, nitrogen, and sulfur. Oikos **102**: 378-390.

Nagelkerken, I. and others 2008. The habitat function of mangroves for terrestrial and marine fauna: A review. Aquat. Bot. **89:** 155-185.

Natelhoffer, K. J., and B. Fry. 1988. Controls on Natural Nitrogen-15 and Carbon-13 Abundances in Forest Soil Organic Matter. Soil Sci. Soc. Am. J. **52:** 1633-1640.

Nobbs, M. 2003. Effects of vegetation differ among three species of fiddler crabs (*Uca* spp.). J. Exp. Mar. Biol. Ecol. **284:** 41-50.

Nobbs, M., and K. A. McGuinness. 1999. Developing methods for quantifying the apparent abundance of fiddler crabs (Ocypodidae: *Uca*) in mangrove habitats. Aust. J. Ecol. **24:** 43-49.

Oakes, J. M., R. M. Connolly, and A. T. Revill. 2010. Isotope enrichment in mangrove forests separates microphytobenthos and detritus as carbon sources for animals. Limnol. Oceanogr. **55:** 393-402.

Otero, X. L. and others 2017. High fragility of the soil organic C pools in mangrove forests. Mar. Poll. Bull. **119**: 460-464.

Pape, E., A. Muthumbi, C. P. Kamanu, and A. Vanreusel. 2008. Size-dependent distribution and feeding habits of Terebralia palustris in mangrove habitats of Gazi Bay, Kenya. Estuar. Coast. Shelf Sci. **76:** 797-808.

Parmesan, C. and others 2013. Beyond climate change attribution in conservation and ecological research. Ecol. Lett. **16:** 58-71.

Parsons, T. R. 2013. A manual of chemical & biological methods for seawater analysis. Elsevier.

Peterson, B. J., and B. Fry. 1987. Stable Isotopes in Ecosystem Studies. Annu Rev Ecol Syst **18**: 293-320.

Pillay, D., and R. Perissinotto. 2008. The benthic macrofauna of the St. Lucia Estuary during the 2005 drought year. Estuar. Coast. Shelf Sci. **77**: 35-46.

---. 2009. Community structure of epibenthic meiofauna in the St. Lucia Estuarine Lake (South Africa) during a drought phase. Estuar. Coast. Shelf Sci. **81**: 94-104.

Poon, D. Y. N., B. K. K. Chan, and G. A. Williams. 2010. Spatial and temporal variation in diets of the crabs Metopograpsus frontalis (Grapsidae) and Perisesarma bidens (Sesarmidae): implications for mangrove food webs. Hydrobiologia **638:** 29-40.

Pollack, J. B., T. A. Palmer, and P. A. Montagna. 2011. Long-term trends in the response of benthic macrofauna to climate variability in the Lavaca-Colorado Estuary, Texas. Mar. Ecol. Prog. Ser. **436**: 67-80.

Sanders, C. J. and others 2016. Are global mangrove carbon stocks driven by rainfall? J. Geophys. Res.: Biogeosci. **121:** 2600-2609.

Sheaves, M., and B. Molony. 2000. Short-circuit in the mangrove food chain. Mar. Ecol. Prog. Ser. **199**: 97-109.

Shinnaka, T., M. Sano, K. Ikejima, P. Tongnunui, M. Horinouchi, and H. Kurokura. 2007. Effects of mangrove deforestation on fish assemblage at Pak Phanang Bay, southern Thailand. Fish. Sci. **73:** 862-870.

Silliman, B. R., J. van de Koppel, M. D. Bertness, L. E. Stanton, and I. A. Mendelssohn. 2005. Drought, Snails, and Large-Scale Die-Off of Southern U.S. Salt Marshes. Science **310:** 1803-1806.

Sippo, J. Z., C. E. Lovelock, I. R. Santos, C. J. Sanders, and D. T. Maher. 2018. Mangrove mortality in a changing climate: An overview. Estuar. Coast. Shelf Sci. **215:** 241-249.

Sippo, J. Z. and others 2019. Carbon outwelling across the shelf following a massive mangrove dieback in Australia: Insights from radium isotopes. Geochim. Cosmochim. Acta **253:** 142-158.

Skov, M., and R. Hartnoll. 2001. Comparative suitability of binocular observation, burrow counting and excavation for the quantification of the mangrove fiddler crab *Uca annulipes* (H. Milne Edwards). Hydrobiologia **449:** 201-212.

Skov, M., M. Vannini, J. Shunula, R. Hartnoll, and S. Cannicci. 2002. Quantifying the density of mangrove crabs: Ocypodidae and Grapsidae. Mar. Biol. **141:** 725-732.

Stott, P. 2016. How climate change affects extreme weather events. Science **352:** 1517-1518.

Stuart-Smith, R. D., C. J. Brown, D. M. Ceccarelli, and G. J. Edgar. 2018. Ecosystem restructuring along the Great Barrier Reef following mass coral bleaching. Nature **560:** 92-96.

Sweetman, A. and others 2010. Impacts of exotic mangrove forests and mangrove deforestation on carbon remineralization and ecosystem functioning in marine sediments. Biogeosci. **7**: 2129-2145.

Taylor, D. S., E. A. Reyier, W. P. Davis, and C. C. McIvor. 2007. Mangrove removal in the belize cays: effects on mangrove-associated fish assemblages in the intertidal and subtidal. Bull. Mar. Sci. **80:** 879-890.

Thomson, J. A. and others 2015. Extreme temperatures, foundation species, and abrupt ecosystem change: an example from an iconic seagrass ecosystem. Glob. Change Biol. **21:** 1463-1474.

Tue, N. T., H. Hamaoka, A. Sogabe, T. D. Quy, M. T. Nhuan, and K. Omori. 2012. Food sources of macro-invertebrates in an important mangrove ecosystem of Vietnam determined by dual stable isotope signatures. J. Sea Res. **72:** 14-21.

Ummenhofer, C. C., and G. A. Meehl. 2017. Extreme weather and climate events with ecological relevance: a review. Philos. Trans. Royal Soc. B **372:** 20160135.

Vander Zanden, M. J., and J. B. Rasmussen, J.B. 2001. Variation in $\delta^{15}N$ and $\delta^{13}C$ trophic fractionation: Implications for aquatic food web studies. Limnol. Oceanogr. **46**: 2061-2066.

Verdelhos, T., P. Cardoso, M. Dolbeth, and M. Pardal. 2014. Recovery trends of Scrobicularia plana populations after restoration measures, affected by extreme climate events. Mar. Environ. Res. **98**: 39-48.

Veríssimo, H., M. Lane, J. Patrício, S. Gamito, and J. C. Marques. 2013. Trends in water quality and subtidal benthic communities in a temperate estuary: Is the response to restoration efforts hidden by climate variability and the Estuarine Quality Paradox? Ecol. Indic. **24**: 56-67.

Wernberg, T. and others 2016. Climate-driven regime shift of a temperate marine ecosystem. Science **353:** 169-172.

Chapter 3

Stable isotopes track the ecological and biogeochemical legacy of mangrove forest dieback in the Gulf of Carpentaria, Australia

This chapter is a preprint paper. The bibliographical details of the co-authored paper, including all authors are:

Harada Y, Connolly RM, Fry B, Maher DT, Sippo JZ, Jeffrey LC, Bourke AJ, Lee SY (2020) Stable isotopes track the ecological and biogeochemical legacy of mangrove forest dieback in the Gulf of Carpentaria, Australia. Biogeosciences discussions.

Author Contributions
The study was conceptualized by all authors. Writing was led by YH and contributed to by all. Field surveys were executed by DTM, JZS, LCJ, AJB and YH. Data compilation and analysis was coordinated by YH and contributed to by all.

(Signed) _____

Corresponding (1st) author: Yota Harada

(Countersigned) _____

Supervisor (and co-author): Rod M. Connolly

Abstract

A combination of elemental and stable isotopic measurements was used to assess and monitor C, N and S cycling of a mangrove ecosystem that suffered mass dieback of trees in the Gulf of Carpentaria, Australia in 2015-16, a rare event attributed to climatic extremes. Mangroves, sediment and invertebrate animals collected over a two-year period from 2016 to 2018, six to 30 months after the event, were analysed for CNS elemental and isotopic compositions (including compound-specific isotope analysis of amino acids). Samples collected from the impacted ecosystem were generally enriched in ^{13}C, ^{15}N and ^{34}S relative to those from an adjacent unimpacted reference ecosystem, suggesting lower mangrove carbon fixation, lower nitrogen fixation and lower sulfate reduction in the impacted ecosystem. Invertebrates representing the feeding types of grazing, leaf feeding, and algae feeding were more ^{13}C enriched at the impacts site, by ~ 1 – 2‰ and these differences did not change over the 2-year survey. Compound specific amino acid isotope analysis indicated widespread ^{13}C enrichment across all amino acids and all groups sampled (except filter feeders) within the impacted site. Mangrove seedling and sapling populations increased substantially over the two years in the impacted forest, suggesting recovery of the mangrove vegetation. Recovery of CNS cycling, however, was not evident even after 30 months, suggesting a biogeochemical legacy of the mortality event. Continued monitoring of the post-dieback forest would help to predict the long-term trajectory of ecosystem recovery. In such long-term monitoring programs, bulk stable isotope analysis that can track biogeochemical changes over time can help to detect underlying biological mechanisms that drive changes and recovery of the mangrove ecosystem. To gain further insight, compound-specific stable C isotope analysis of amino acids, as used in this study, can help unravel feeding dependencies in mangrove food webs and their response to disturbances.

Introduction

Stable isotope tracer data that provide biogeochemical source and process information over time, help environmental assessment and monitoring. As elements circulate in the biosphere, stable isotopic compositions of ^{13}C, ^{15}N and ^{34}S change in predictable ways due to mixing and fractionation, giving insights into sources and cycling of these elements (Peterson & Fry 1987). Stable isotopes have been widely used in mangrove ecosystem studies to better understand food web interactions (Fry & Smith 2002, Bouillon et al. 2008, Larsen et al. 2012, Bui & Lee 2014, Abrantes et al. 2015), mangrove nutrient uptake (McKee et al. 2002), mangrove water use (Santini et al. 2015, Hayes et al. 2019), cycling of C (Maher et al. 2013a; Maher et al. 2017), N (Fry et al. 2000, Fry & Cormier 2011) and S (Fry et al. 1982, Okada & Sasaki 1998), and greenhouse gas emissions (Maher et al. 2013b).

In late 2015 to early 2016, an extensive area (>7000 ha) of mangrove forest along ~1,000 km of coastline in the Gulf of Carpentaria, Australia, experienced severe dieback, an event associated with climatic extremes (Duke et al. 2017). Mangroves show characteristics of pioneer species (Tomlinson 2016) and large-scale disturbances have likely played an important role in their evolution. However, the processes, rates and patterns of recovery from disturbances are still largely unknown. In most cases, recovery of mangroves primarily relies on the recruitment of seedlings (Smith et al. 1994). Disturbances in mangrove forests not only affect recruitment, but can also change the cycling of carbon, nitrogen and sulfur. Loss of mangrove trees and root structures can change organic matter inputs, sediment oxygenation and degradation of sediment organic matter. These changes alter overall sediment conditions, with consequences for benthic assemblages (Sweetman et al. 2010, Bernardino et al. 2018, Harada et al. 2019 (chapter 2)), sediment C and N stocks (Adame et al. 2018), microbial assemblages, and associated nutrient processes e.g. nitrogen fixation and sulfate reduction (Sjöling et al. 2005).

Traditional methods to evaluate structure and functioning of ecosystems include measures of species composition but these field assessments can be time-consuming and expensive, and may not provide enough quantitative information about system functioning (e.g. Kling et al.1992). Stable isotope analysis of ecosystem components is a powerful way of quantitatively evaluating functional aspects of element cycling and the health of ecosystems (e.g. integrity of the food web; Fry 2006). Stable isotope analyses of total organic matter (‘‘bulk’’) have become widespread due to the relative ease and low cost of sample

preparation and analysis (Fry 2006; Wada et al. 1991). Compound specific isotope analysis is increasingly employed as a complementary tool to bulk stable isotope analyses. For instance, while bulk stable isotopes of C, N and S provide an overview of food webs (Fry & Smith 2002), compound-specific isotopic compositions in amino acids help measure details of organic matter cycling (Ishikawa et al. 2018; Larsen et al. 2013; Ohkouchi et al. 2017)

We investigated changes in C, N and S element cycling associated with the Gulf of Carpentaria mangrove forest dieback (Duke et al. 2017), using a combination of traditional ecological techniques and novel stable isotope analytical methods. We hypothesised that the mortality of mangrove foundation species has changed the overall circulation of C, N and S elements and these biogeochemical changes would most likely be reflected in $\delta^{13}C$, $\delta^{15}N$ and $\delta^{34}S$ values of mangrove ecosystem components such as mangrove plants, sediment and associated animals. We also tested the hypothesis that these isotopic compositions changed over time with the recovery of mangrove vegetation. $\delta^{13}C$, $\delta^{15}N$ and $\delta^{34}S$ values were measured for samples including mangroves, sediment and invertebrates collected in a comparative setting of impacted mangrove forest site and an adjoining unaffected reference forest site in the Gulf of Carpentaria, Australia.

Methods

Study site

Over 7,000 ha of mangroves along ~ 1,000 km of the Gulf of Carpentaria coastline in Australia experienced mass mortality during the summer in 2015-16, (Duke et al. 2017), the most extensive known mangrove forest dieback from natural causes (Sippo et al. 2018). At the same time, there were coincidental mangrove mass mortality events in Exmouth, Western Australia (Lovelock et al. 2017) and Kakadu National Park, Northern territory (Asbridge et al. 2019). The climate in the Gulf region is wet-dry tropical with mean annual precipitation ranging from approximately 600 to 900 mm. Dry conditions prevail for six to eight months and most rainfall occurs between December and March (Bureau of Meteorology, see www.bom.gov.au). The climatic conditions limit the extent of mangroves in the region (Asbridge et al. 2016). The dieback was most likely linked to a weak monsoon (low rainfall), combined with high vapor pressure deficit, and El Niño–Southern Oscillation-induced low sea-levels (Duke et al. 2017, Lovelock et al. 2017, Harris et al. 2018). These conditions most likely resulted in hypersalinization and caused accumulative hydric, thermal and radiant stresses (Duke et al. 2017, Lovelock et al. 2017, Harris et al. 2018). The event led to the

widespread death of mangrove trees in the region providing a unique opportunity to test tree mortality effects on biogeochemical and ecological functioning of mangroves and capture recovery patterns.

Fieldwork was conducted over a two-year period from August 2016 to August 2018 in the winter dry-seasons in Karumba, Gulf of Carpentaria, Australia (Fig. 3.1A). A forest that had suffered dieback (impacted) on the east of Norman River outlet and an adjoining unaffected forest (unimpacted) on the west, provided the setting for comparisons. Some local factors (e.g. river influence) presumably kept mangroves from dying back at the unimpacted site. These local factors might also explain striking observations at particular times at the unimpacted site, such as changes in seedling density. *Avicennia marina* was the dominant mangrove species. In order to assess differences between the two forests (impacted vs unimpacted) as well as to capture trends from low to high intertidal zones and to ensure that the physical-oceanographic conditions between the two forests were as similar as possible, three sampling transects (2 to 2.5km apart) were set for each forest with the length of each transect being approximately 200m (Fig. 3.1B, C). Due to logistical constraints and the presence of crocodiles, fieldwork was restricted to daytime, low tide and dry seasons.

Samples

Over a two-year period from August 2016 to August 2018 in the winter dry-seasons, four common mangrove faunal groups with different feeding modes were collected from each forest including a leaf-eating crab (*Parasesarma* or *Episesarma*), an algae-eating crab (*Tubuca signata*), a grazer gastropod (*Telescopium telescopium*) and a filter-feeding bivalve (*Crassostrea sp,* an oyster). For each group, 3 to 5 individuals at each of the sampling transects (n=3) within the forest were collected and muscle tissues were pooled for analysis.

In 2018, we further divided each transect into five zones (50m apart), namely forest edge (landward), high, mid, low and forest edge (seaward). Fully developed green leaves of *A. marina* were collected from at about 1 to 1.5m height from 3 to 5 individual trees (1 to 3 leaves per tree) at each zone, stored in plastic containers, then composited. In the impacted site, regrowth was occurring in some trees, and leaves were collected from this regrowth. Leaf samples were washed thoroughly, rinsed with distilled water and the main vein was removed. Additionally, wood samples (n=2) were collected from each forest. Two to 3 measurements were made for each wood sample then measurements were averaged. Wood

samples were generally very low in S, so wood $\delta^{34}S$ value was determined for only one sample that had sufficient S for analysis.

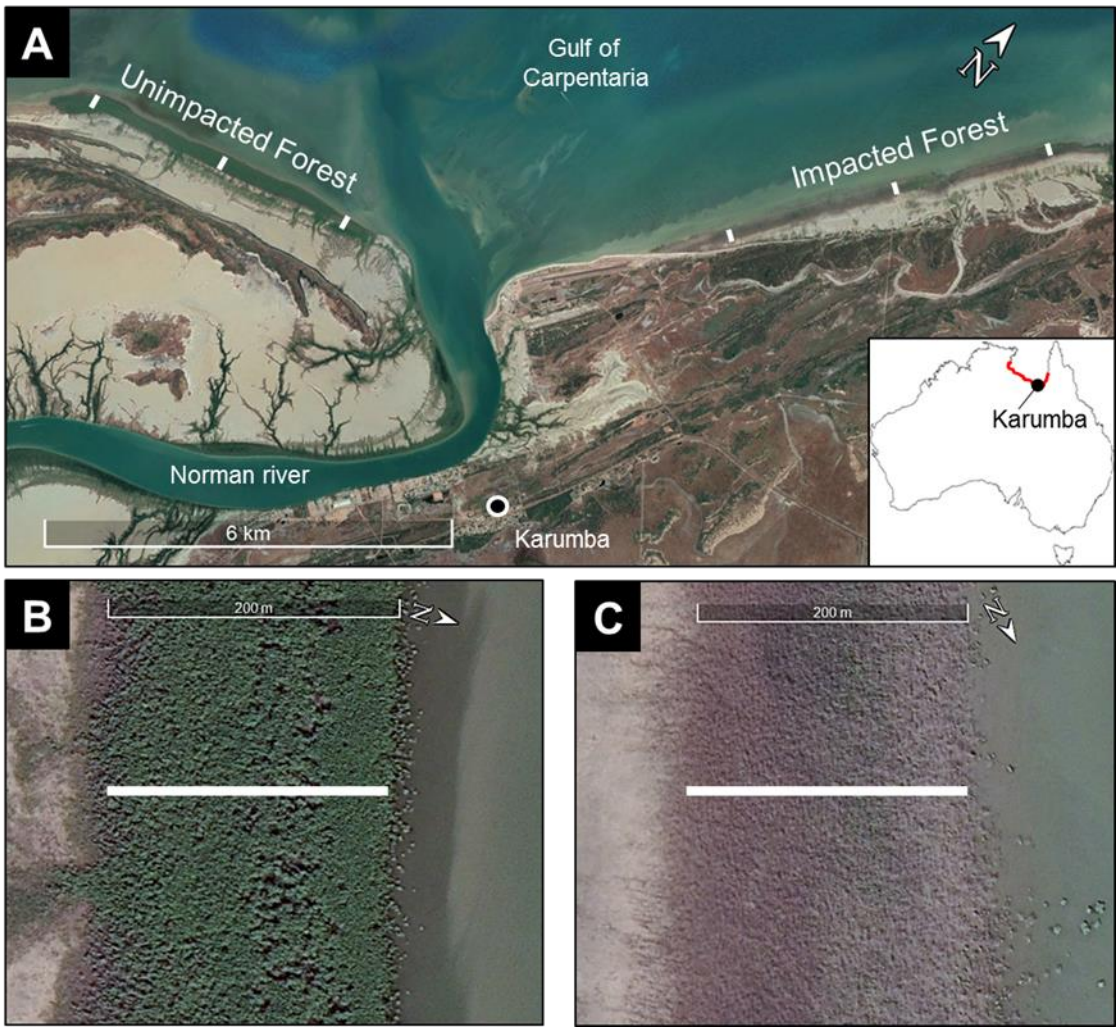

Fig. 3.1. The study location at Karumba in the Gulf of Carpentaria, Queensland, Australia (-17.435572S, 140.844766E). (A) Three sampling transects within the unimpacted reference site and three within the impacted site (shown as a white line). (B, C) Representative transects from the unimpacted (B) and impacted (C) sites. Each transect was approximately 200m. Samples were collected along each transect from higher to lower intertidal zones.

In 2018, surface (<0.5 cm) sediment was collected along the intertidal zones of each transect from the forest edge (landward) to forest edge (seaward) and also in the adjacent mudflat. Additionally, in each forest, 0.5 to 20cm sediment samples (n=6) were collected using a core sampler, 5 cm in diameter and 20 cm deep. For $\delta^{13}C$ measurements, the sediment samples were acidified with 1M HCl to remove the inorganic fraction. Microphytobenthos (MPB) samples (n=6) were separated from surface sediment collected at each forest. The separation was done by density gradient centrifugation in Ludox colloidal silica (Sigma) as described in

Bui and Lee (2014). The MPB extraction was followed by microscopic examination to confirm that samples mostly contained green cells (i.e. diatoms and filamentous cyanobacteria). Additionally, surface sediment samples were also collected from offshore (approx. 1km) using a grab sampler and from the adjacent saltpan (approx. 200m from the forest). Water samples (n=3) were also collected from offshore and filtered through glass fiber filters (Whatman GFF) to sample particulate organic matter (POM).

To estimate mangrove seedling/sapling densities (ind. m^{-2}) from each forest and their changes over the two-year period (2016 to 2018), seedling/saplings were counted with 50 × 50 cm quadrats. In this process, photographs were taken in the field (n=80 to 175 per forest for each year) and then counts of seedlings and samplings were made later in the laboratory. The seedlings/samplings were mostly *A.marina* but also include some *Aegiceras corniculatum*.

Stable isotope analysis

All samples were stored separately in sealed plastic containers at -20°C until analysis, then dried at 60°C, powdered, homogenized and put in tin capsules for stable isotope analysis. $\delta^{13}C$, $\delta^{15}N$ and $\delta^{34}S$ measurements were carried out on an elemental analyzer (Europa EA-GSL) coupled to an isotope ratio mass spectrometer (Sercon 20-22, SERCON, UK) at Griffith University, Brisbane, Australia. Isotope values are reported relative to Vienna Pee Dee Belemnite (PDB), atmospheric N_2 (AIR), and Vienna Canyon Diablo Troilite (VCDT) for C, N and S, respectively. Harada et al. (2019, chapter 2), reported $\delta^{13}C$ and $\delta^{15}N$ values for some of the samples collected in 2017 from the same study location.

The samples collected in 2017 from each forest including the mangrove leaf (n=2), MPB (n=1), algae feeder (n=3), leaf feeder (n=2 to 3), grazer (n=3), filter feeder (n=2) were measured for carbon isotopic composition of individual amino acids ($\delta^{13}C_{AA}$). For this compound-specific stable isotope analysis, 8 mg (for animal tissues) or 30 mg (for plant tissues) of sample materials were transferred to borosilicate vials with heat and acid-resistant caps. They were then flushed with N_2 gas, sealed and hydrolysed in 0.5mL (animal tissues) or 2mL (plant tissues) of 6M HCl at 150°C for 70 minutes, then dried in a heating block at 60°C under a stream of N_2 gas. The dried samples were derivatised by methoxycarbonylation as described by Walsh et al. 2014. AA derivatives were separated by a Trace GC Ultra gas chromatograph (Thermo Scientific) using a DB-23 column, Agilent, 30m × 0.25mm, 0.25µm film at the stable isotope facility at the University of California (Davis, CA, USA). The GC

was interfaced with a Delta V Plus isotope ratio mass spectrometer via a GC IsoLink (Thermo Scientific). L-Norleucine was used as an internal standard and to calculate provisional values.

Pure AAs mixtures with calibrated $\delta^{13}C$ were co-measured. One mixture was used for final calibration and others were for the scale normalisation standard and the primary quality assurance standard (unused in corrections). Two working standards were co-measured as secondary quality assurance materials. Exogenous carbon was accounted by the method mentioned by Docherty et al. (2001). Following these processes, $\delta^{13}C$ values were determined for 10 AAs (Gly, glycine; Asx, aspartic acid/asparagine; Pro, proline; Glx, glutamic acid/Glutamine; Ala, alanine; Lys, lysine; Ile, isoleucine; Leu, leucine; Phe, phenylalanine; and Val, valine). Met, methionine; His, Histidine; and Hyp, Hydroxyproline presented at or below the limit of quantitation (LOQ) for some samples. Since we were interested in $\delta^{13}C$ values of essential amino acids ($\delta^{13}C_{EAA}$), we only report $\delta^{13}C$ values of Lys, Ile, Leu. Phe and Val.

Data analysis

All statistical analyses were undertaken in R version 3.4.3 with RStudio interface version 1.1.414. Differences among group means were explored with ANOVA, but for the count data i.e. seedling/ sampling populations, generalized linear model (GLM) with Poisson distribution was used. Before performing ANOVA, the assumptions of homogeneity of variance and normality were tested using Levene's and Shapiro-Wilk's tests, respectively. To explore $\delta^{13}C$ patterns among five EAAs, $\delta^{13}C_{EAA}$ values were normalised to the respective sample means following the procedure of Larsen et al. (2009) as follows: $Norm(\delta_{EAA}) = \delta_{EAA} - \mu$, where μ represents the mean value of all five EAAs (Ile, Leu, Lys, Phe and Val) in the sample. PERMANOVA was performed to test if the pattern of $\delta^{13}C$ among five EAAs of samples differ between the forests. In this analysis, the normalized $\delta^{13}C_{EAA}$ dataset was used and the Euclidean distance was used as distance metric. Permutation test of multivariate homogeneity of dispersions was performed to check whether dispersions around the centroids are similar between the two forests. All statistical tests used a significance criterion of α=0.05.

Results

Mangroves

In 2016, approx. 6 months after the mangrove mortality event, at the impacted site, mangrove seedling and sapling populations were lower than the unimpacted site (GLM, df = 1, estimate 3.75, $p < 0.001$) but significantly increased throughout the two-year period from 2016 to 2018 (GLM, df = 2, estimate 0.01, $p < 0.001$; Fig. 3.2). C, N and S elemental compositions (%) of the dominant mangrove species, *A. marina* did not differ greatly between the two sites, but the isotopic compositions varied considerably (Table 3.1). The $\delta^{13}C$ values (mean ± SD) of green leaves harvested from *A. marina* trees, were significantly more ^{13}C-enriched in the impacted site (-25.8 ± 1.0‰) than the unimpacted site (-28.4 ± 1.5‰; ANOVA, $F_{1, 28} = 32.9$, $p < 0.001$; Fig. 3.3A, Table 3.1). The $\delta^{15}N$ values varied more in the impacted site (ranged from -0.9 to 6.7‰) than in the unimpacted site (ranged from 2.9 to 6.2‰; Fig. 3.3A). The $\delta^{34}S$ values were generally higher in the impacted site (13.5 ± 5.4‰, range 7.7 to 23.3‰) than the unimpacted site (12.6 ± 5.6‰, range 5.0 to 21.9‰). Leaf $\delta^{34}S$ values became more ^{34}S depleted from higher to lower intertidal zones in the impacted site (ANOVA, $F_{4, 10} = 5.56$, $p = 0.013$; Fig. 3.3B). This pattern was weaker in the unimpacted site, but leaf $\delta^{34}S$ values substantially varied across intertidal zones (ANOVA, $F_{4, 10} = 6.48$, $p = 0.007$; Fig. 3B). Leaf $\delta^{13}C$ and $\delta^{15}N$ values did not display such patterns along the intertidal zones. Leaf C, N and S (%) did not show any clear trends among two forests and along transects. Yellow leaves generally had a higher S content (~1.2%) than green leaves (0.5 to 0.7%) (Table 3.1). Wood samples generally had very low N and S contents, significantly lower than the leaves. However, wood samples from the impacted site had a relatively high S content (0.31 ± 0.37%) and had a $\delta^{34}S$ value of 16.6‰ (Table 3.1).

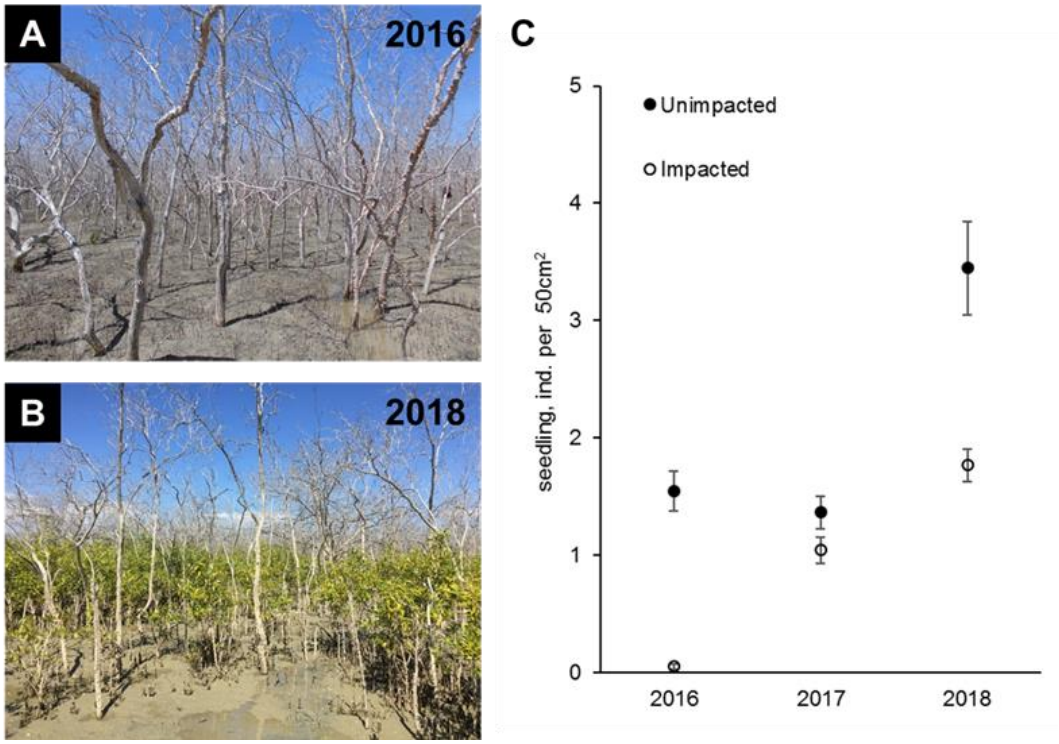

Fig. 3.2. Recovery of mangrove vegetation at the impacted site during a two-year period from 2016 to 2018 (A and B; approx. 6 and30 months, respectively after the mangrove dieback event). Seedling and sampling populations of mangrove species (mostly, *A. marina*) significantly increased in the impacted site (C).

Table 3.1. Elemental and isotopic compositions of the mangrove *A. marina* (mean, SD).

Tissue type	Forest	%C	%N	%S	$\delta^{13}C$, ‰	$\delta^{15}N$, ‰	$\delta^{34}S$, ‰	n
Green leaf	Unimpacted	39.3, 1.7	1.75, 0.37	0.54, 0.23	-28.4, 1.5	4.4, 0.8	12.6, 5.6	15
	Impacted	40.0, 1.6	1.82, 0.45	0.73, 0.14	-25.8, 1.0	4.3, 1.9	13.5, 5.4	15
Yellow leaf	Unimpacted	41.6, 2.2	0.67, 0.23	1.18, 0.47	-26.4, 1.3	6.5, 1.1	14.6, 7.7	3
	Impacted	41.9, 1.0	0.52, 0.05	1.18, 0.38	-26.2, 0.6	7.4, 0.2	12.5, 2.8	3
Wood	Unimpacted	42.6, 3.0	0.38, 0.27	0.04, 0.01	-24.8, 1.8	6.1, 2.0	-	2
	Impacted	39.9, 5.7	0.40, 0.16	0.31, 0.37	-24.9, 1.0	4.7, 1.0	16.6	2

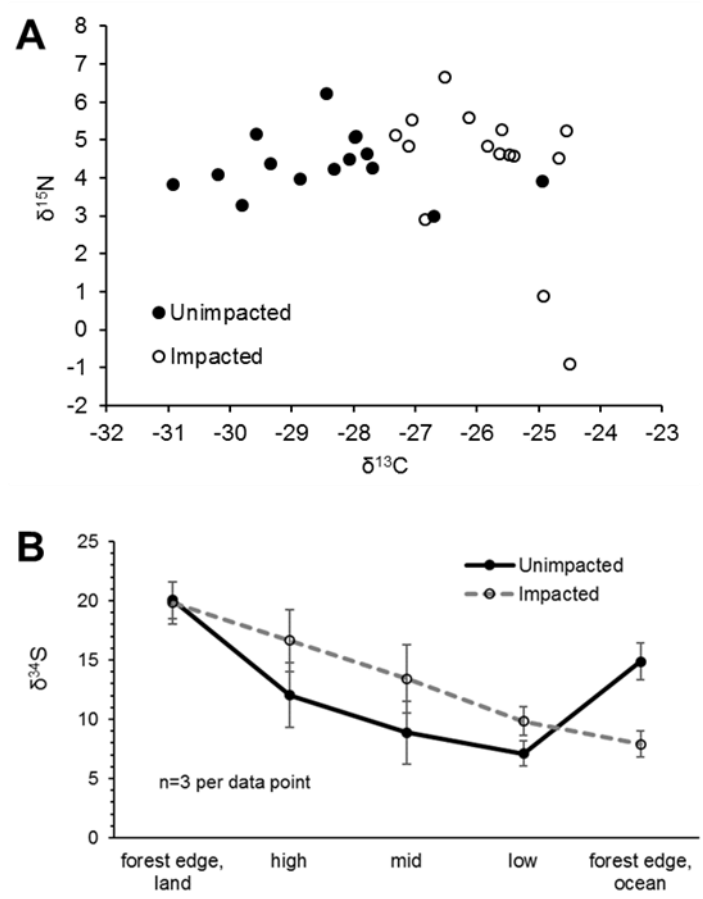

Fig. 3.3. CNS isotopic compositions of green leaves of *A. marina* from the unimpacted and impacted sites. All samples were collected in 2018, 30 months after the dieback. (A) Leaf $\delta^{13}C$ and $\delta^{15}N$ values. (B) Leaf $\delta^{34}S$ values across the intertidal zones. Error values are SE.

Sediment

For the surface (0 - 0.5cm) sediment, TOC (%) differed significantly between the two forests with the values (mean ± SD) of 2.02 ± 1.16% for the unimpacted site and 1.06 ± 0.37% for the impacted site (ANOVA $F_{1, 28} = 12.75$, P = 0.001), suggesting that the surface sediment from the impacted site contains ~48% lower TOC relative to those of the unimpacted site (Table 3.2). The pattern was consistent across the intertidal zones (Fig 3.4A). The surface sediment TN (%) was also significantly lower for the impacted site (0.09 ± 0.03) than the unimpacted site (0.15 ± 0.06%; ANOVA $F_{1, 28} = 9.32$, P = 0.005). TOC of mudflat (<0.5 cm) sediment collected adjacent to the two forests also differed significantly with those of impacted site being lower (0.58, 0.18%) than the unimpacted site (1.02, 0.08%; ANOVA $F_{1, 4} = 14.54$, P = 0.019). TN (%) of mudflat (<0.5 cm) sediment was also significantly lower for the impacted site (ANOVA $F_{1, 4} = 9.81$, P = 0.035). TOC (%) of 0.5 - 20cm sediment did not differ significantly between the two sites with the values of 1.83 ± 0.73% for the unimpacted

and 1.29 ± 0.55 % for the impacted site (ANOVA $F_{1, 10} = 2.07$, P = 0.181). TN (%) of 0.5 - 20cm sediment also did not differ significantly between the two sites with the values of 0.09 ± 0.03% for the unimpacted and 0.12 ± 0.04% for the impacted site (ANOVA $F_{1, 10} = 3.02$, P = 0.113).

$\delta^{13}C$ values of surface (< 0.5cm) sediment differed significantly between the two sites with those from the impacted site showing higher values (-21.8 ± 1.0‰) than the unimpacted site (-24.3 ± 1.2‰; ANOVA $F_{1, 28} = 22.48$, P < 0.001). This pattern was consistent across the intertidal zones with $\delta^{13}C$ values from the impacted site becoming similar to those from the adjacent mudflat (Fig. 3.4b). However, those of 0.5 to 20cm sediment did not differ significantly with the values of -24.4 ± 0.5‰ for the impacted site and -25.2 ± 0.9‰ for the unimpacted site (ANOVA $F_{1, 10} = 3.92$, P = 0.076). Surface (< 0.5cm) sediment collected in the adjacent mudflat did not display a significant difference in $\delta^{13}C$ values between the two sites with the values of -21.2 ± 0.9‰ for those collected adjacent to the unimpacted forest and -21.8 ± 0.8‰ for those collected adjacent to the impacted site (ANOVA $F_{1, 4} = 0.64$, P = 0.47). The $\delta^{13}C$ value of the surface sediment (-21.8 ± 1.0‰) in the impacted forest was similar to those collected in the mudflat (-21.2 ± 0.9‰) which were also similar to those collected from offshore (-21.8 ± 1.1‰). Those $\delta^{13}C$ values also matched with the $\delta^{13}C$ value of POM collected offshore (-21.5 ± 1.5‰). Surface (< 0.5cm) sediment collected from adjacent unvegetated saltpan areas also showed similar values (Table 3.2). MPB extracted from the surface <0.5cm sediment showed significantly different $\delta^{13}C$ values between the impacted site (-21.5 ± 1.3‰) and unimpacted site (-25.2 ± 1.0‰; ANOVA $F_{1, 10} = 28.53$, P < 0.001).

Table 3.2. Elemental and isotopic compositions of sediment (mean, SD).

	Forest/site	%TOC	%TN	$\delta^{13}C$, ‰	$\delta^{15}N$, ‰	n
Mangrove forest, 0 to 0.5cm	Unimpacted	2.02, 1.16	0.15, 0.06	-24.3, 1.2	2.0, 0.5*	15
	Impacted	1.06, 0.37	0.09, 0.03	-21.8, 1.0	2.8, 0.6*	15
Mangrove forest, 0.5 to 20cm	Unimpacted	1.83, 0.73	0.12, 0.04	-25.2, 0.9	1.7, 0.5*	6
	Impacted	1.29, 0.55	0.09, 0.03	-24.4, 0.5	1.7, 0.3*	6
Mudflat, 0 to 0.5cm	Unimpacted	1.02, 0.08	0.11, 0.01	-21.8, 0.8	-	3
	Impacted	0.58, 0.18	0.07, 0.02	-21.2, 0.9	-	3
Saltpan, 0 to 0.5cm	Unimpacted	1.87, 2.03	0.19, 0.24	-18.9, 1.7	-	4
	Impacted	0.83, 0.07	0.07, 0.01	-20.8, 0.7	-	4
Offshore, 0 to 0.5cm	1km offshore	0.70, 0.27	0.08, 0.03	-21.8, 1.1	-	5
POM	1km offshore	-	-	-21.1, 1.5	3.6, 2.1	3
MPB	Unimpacted	-	-	-25.2, 1.0	-	6
	Impacted	-	-	-21.5, 1.3	-	6

*$\delta^{15}N$ values were taken from Harada et al. (2019, chapter 2)

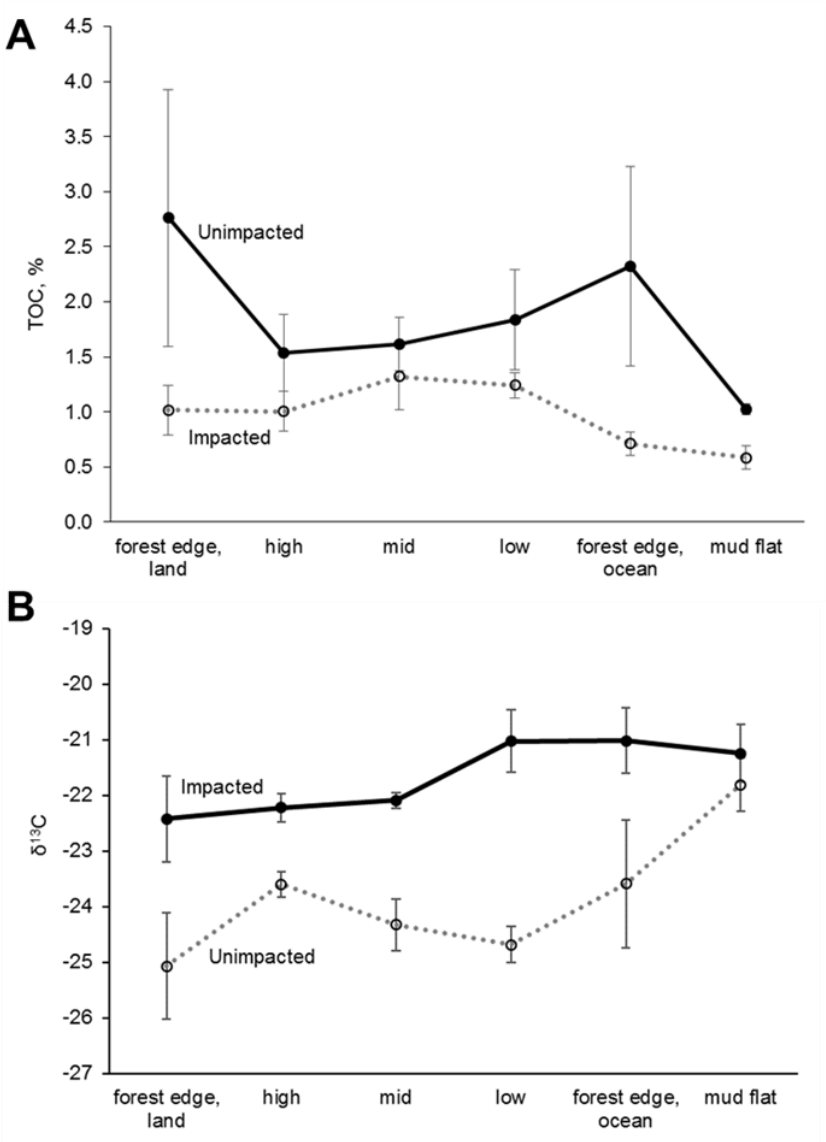

Fig. 3.4. C elemental and isotopic compositions of surface (< 0.5 cm) sediment along the unimpacted reference transects vs impacted transects (n=3 per data point). Error values are SE. (A) Sediment TOC, %. (B) Sediment $\delta^{13}C$ values, ‰.

Fauna

CNS isotopic compositions of mangrove faunal groups representing algivores, grazers and leaf feeders from the impacted site were consistently more enriched in ^{13}C, ^{15}N and ^{34}S than their counterparts from the impacted forest throughout the 2-year period between 2016 and 2018, but the filter feeder was largely unaffected (Fig. 3.5). Overall, $\delta^{13}C$ values of the four feeding groups range from -23 to -15‰ for the unimpacted site and -20 to 14‰ for the impacted site. The $\delta^{15}N$ values ranged from 5.5 to 9.1‰ for the unimpacted site with the fauna in the impacted site having a slightly higher range of 5.6 to 9.5‰. The $\delta^{34}S$ values

ranged from 8.2 to 16‰ for the unimpacted site and 13.4 to 21.7‰ for the impacted site. The effect of forest type was significant for $\delta^{13}C$, $\delta^{15}N$ and $\delta^{34}S$ values of the algae feeder and the grazer (ANOVA $p < 0.05$). The effect of forest type was also significant for $\delta^{13}C$ and $\delta^{34}S$ values of the leaf feeder (ANOVA $p < 0.05$), but was not significant for their $\delta^{15}N$ values (ANOVA $F_{1, 13} = 1.72$, $p = 0.212$). $\delta^{13}C$, $\delta^{15}N$ and $\delta^{34}S$ values of the filter feeder (oyster, *Crassostrea* sp.) that relies on water column organic matter showed relatively less differences among the forests (Fig. 3.5). The effect of forest type was not significant for the filter feeder $\delta^{13}C$ values (ANOVA $F_{1, 8} = 1.719$, $p = 0.212$), but was significant for the $\delta^{15}N$ and $\delta^{34}S$ values (ANOVA $p < 0.05$). Overall, $\delta^{13}C$, $\delta^{15}N$ and $\delta^{34}S$ values consistently differed between the impacted site and unimpacted site during a two-year period from 2016 to 2018. In 2018, leaf feeder $\delta^{13}C$ values, grazer $\delta^{34}S$ values and algae feeder $\delta^{34}S$ values significantly differed between the impacted and unimpacted sites (Turkey post hoc test, $P < 0.05$), so that this dataset does not support the recovery of fauna $\delta^{13}C$, $\delta^{15}N$ and $\delta^{34}S$ status after 30 months from the dieback event. However, $\delta^{15}N$ values that started showing matches between the two forests in 2018 may suggest faster recovery of $\delta^{15}N$ status to the background conditions (Fig. 3.5).

Compound-specific isotope analysis of amino acids

The samples collected in 2017 were further measured for carbon isotopic compositions in individual essential amino acids. $\delta^{13}C_{EAA}$ values corresponded to the bulk $\delta^{13}C$ values with the samples from the impacted site consistently showing higher values than those from the unimpacted forest. (Table 3.3 and Fig 3.6). The pattern of $\delta^{13}C$ among five EAAs (Lys, Ile, Val, Leu and Phe) for all the consumers did not differ between the two forest types ($p > 0.05$; Table 3.3), including the algae-feeder, leaf feeder, grazer and filter feeder. The $\delta^{13}C_{EAA}$ pattern of mangrove leaves did not differ between the forests, regardless of the substantial bulk isotope difference between the unimpacted (-26.7 ± 2.2) and impacted (-25.4 ± 0.1) (Table 3.3). This isotope pattern was fairly consistent for all of the four consumers as well as for the MPB samples (Fig. 3.6).

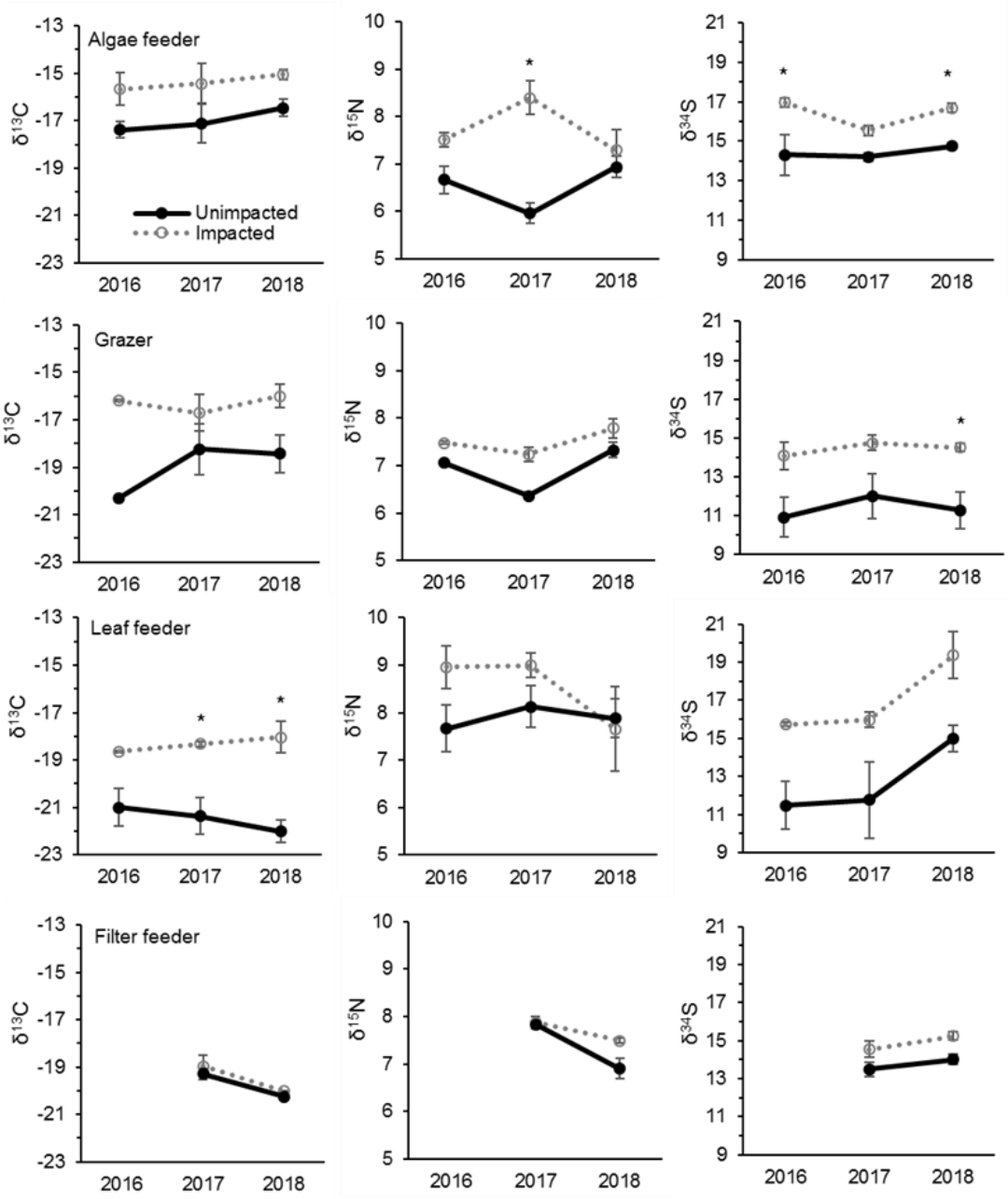

Fig. 3.5. Changes in CNS isotopic compositions of mangrove macrofaunal groups with four different feeding modes from 2016 to 2018 between the unimpacted reference and impacted mangrove forest sites. Error bars are SE (n=2 to 6 per data point). (*) indicates a significant difference in the year. Mean ± SE values and sample sizes are also provided in Table S3.1.

Table 3.3. Bulk $\delta^{13}C$ values and mean $\delta^{13}C$ values of five EAAs (‰).

Group	Taxa	Forest	Bulk $\delta^{13}C$ (‰)	SD	Mean $\delta^{13}C$ of five EAAs (‰)	SD	n	Permanova p value
Algal feeder	*Tubuca signata*	Unimpacted	-17.1	1.4	-21.9	1.5	3	0.90
		Impacted	-15.4	1.4	-20.5	1.8	3	
Leaf feeder	Sesarmidae	Unimpacted	-21.4	1.5	-25.3	1.6	3	0.40
		Impacted	-18.3	0.2	-23.9	0.1	2	
Grazer	*Telescopium telescopium*	Unimpacted	-18.2	1.9	-24.0	1.8	3	0.80
		Impacted	-16.7	1.3	-22.2	1.1	3	
Filter feeder	*Crassostrea* (oyster)	Unimpacted	-19.3	0.4	-22.8	0.2	2	0.33
		Impacted	-19.0	0.8	-22.9	0.3	2	
Mangrove	*Avicennia marina*	Unimpacted	-26.7	2.2	-28.8	0.6	2	0.67
		Impacted	-25.4	0.1	-27.0	0.3	2	
MPB		Unimpacted	-25.4	0.8	-27.4	-	1	-
		Impacted	-20.9	1.2	-20.7	-	1	

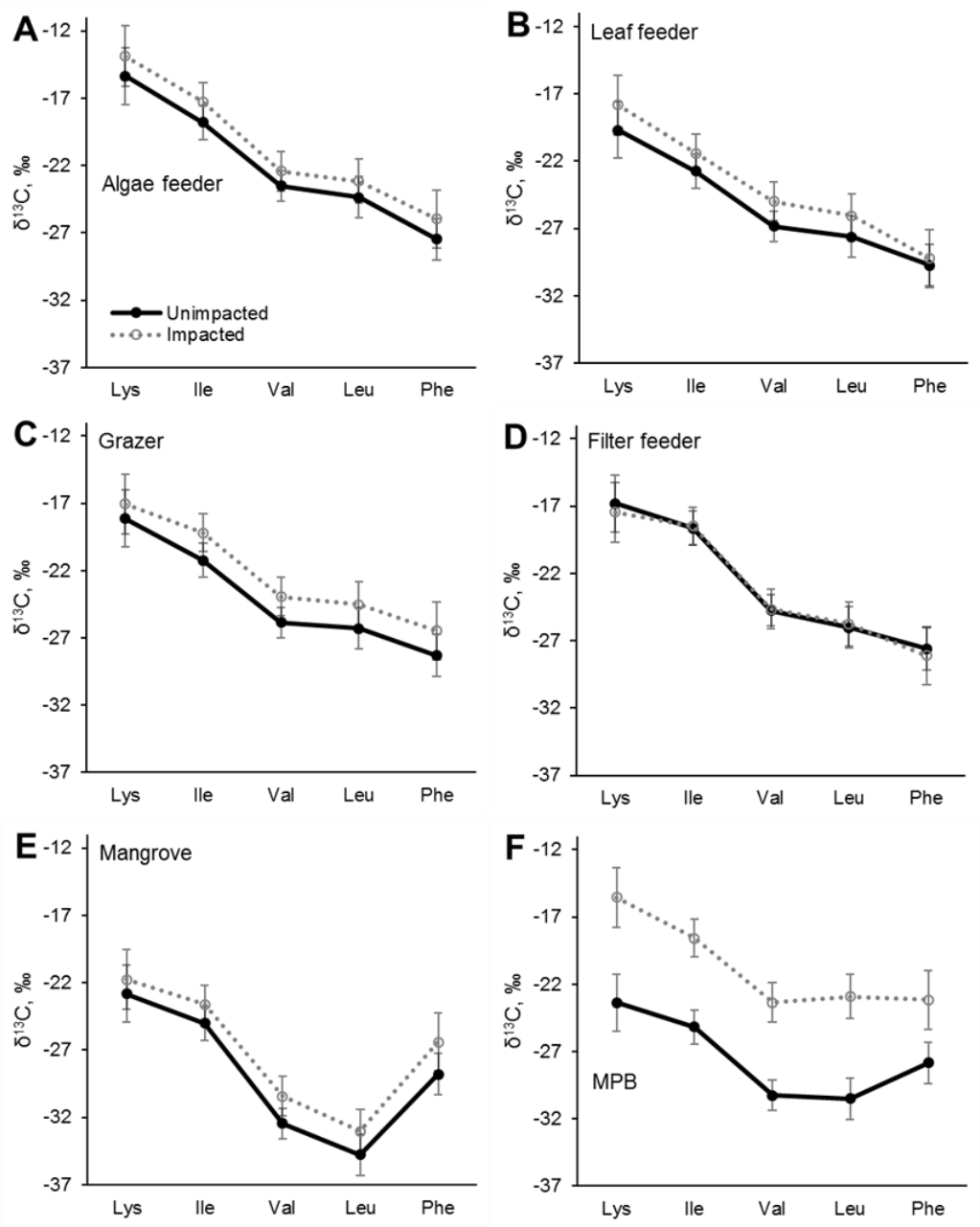

Fig. 3.6. C isotopic compositions in essential amino acids (EAAs) for four mangrove consumer groups and resources including mangrove leaves (*A.marina*) and MPB from the unimpacted and impacted mangrove sites. While there are clear offsets in individual $\delta^{13}C_{EAA}$ values between the two forests, normalized $\delta^{13}C_{EAA}$ fingerprint patterns as per Larsen (2009) did not differ. Error bars show SD.

Discussion

Mangroves

Recovery of mangrove forests from tree mortality events due to disturbances such as cyclones generally rely on recruitment of seedlings (Smith et al. 1994) so that degraded habitats with reduced seed production and delivery, e.g. by habitat fragmentation, may show slower recovery (Milbrandt et al. 2006). Establishment of seedlings may be prevented by persistent inundation due to a decreased sediment elevation (Asbridge et al. 2018). While mangroves cope with or recover from perturbations, the forest may display 'cryptic ecological degradation' in which mangrove associates or minor mangrove species dominate the forest of the true mangrove species without loss of spatial extent (Dahdouh-Guebas et al., 2005). Faunal assemblages are also known to display such cryptic degradation. For example, perturbations can alter or reduce ecosystem engineering activities of crabs such as burrowing and foraging that rework top sediment and benefit mangrove growth and ecosystem functioning (Bartolini et al., 2011). Mangroves are resilient ecosystems and may recover rapidly from natural disturbances such as cyclones (Sherman et al. 2001), but in some cases, recovery may take more than 10 years (Imbert et al. 2000) and degradations may be followed by rapid colonisations by non-mangrove herbaceous species (McKee et al. 2007, Rashid et al. 2009), e.g. succulent saltmarsh (Mbense et al. 2016). In our impacted mangrove forest, the density of mangrove seedling/samplings significantly increased throughout the period from 2016 to 2018, suggesting that recovery is starting to occur within two years after the dieback (Fig. 3.2).

The substantial difference in CNS isotopic compositions in *A. marina* between the two sites, suggested differences in the environmental conditions and biogeochemical processes that were possibly associated with the mangrove mortality effect. The leaf $\delta^{13}C$ values in the impacted forest were relatively enriched in ^{13}C. This C isotope pattern may be due to reduced stomatal conductance that causes lower internal carbon dioxide concentrations and lower carbon isotope fractionation (Farquhar et al. 1989, Lin & Sternberg 1992a, Lin & Sternberg 1992b). High leaf $\delta^{13}C$ values can also be associated with increased carboxylation efficiency associated with higher nutrients, .e.g. N in leaves (Cordell et al. 1999) and thicker leaves with higher internal resistance to carbon dioxide diffusion. Younger leaves can show higher $\delta^{13}C$ values than aged leaves due to ^{13}C enriched fractions (e.g. carbohydrates) transported from older autotrophic leaves to more heterotrophic young leaves (Werth et al. 2015). Leaves exposed to full sun can show higher $\delta^{13}C$ values than shaded leaves (Farquhar et al. 1989).

$\delta^{13}C$ values can vary among different plant tissues in *A. marina* (Kelleway et al. 2018). Leaf N (%) did not differ between the two forests, partially suggesting that the two sites having similar plant N availability. Previous studies show additions of nutrients such as N and/or P did not play a considerable role in mangrove leaf $\delta^{13}C$ variations (McKee et al. 2002), but salinity played an important role (Lin & Sternberg 1992b). Overall, higher leaf $\delta^{13}C$ values in the impacted forest likely suggest that there are chronic, particularly salinity, stresses associated with the dieback event that reduced stomatal conductance. Such environmental stresses may include hypersalinization of sediments and hydric, thermal and radiant stresses following mangrove losses (e.g. canopy loss).

Leaf $\delta^{15}N$ values varied more in the impacted (ranged from -0.9 to 6.7‰) than in the unimpacted forest (ranged from 2.9 to 6.2‰) (Fig. 3.3), but the means were similar (4.3 ± 1.9‰ for the impacted and 4.4 ± 0.8‰ for the unimpacted), suggesting that two sites have similar background $\delta^{15}N$ conditions. Generally, leaf $\delta^{15}N$ varies due to N sources, microbial processes that enrich or deplete ^{15}N in soil or water, and isotope fractionation during plant N uptake. Previous studies showed that in pristine mangrove forests, leaf $\delta^{15}N$ values range around -2‰ to 3‰ (Fry et al. 2000, Fry & Smith 2002, Smallwood et al. 2003). Such low $\delta^{15}N$ values may reflect long-term N fixation inputs (e.g. around 0‰) (Fogel et al. 2008) and marine nitrate inputs (Dore et al. 2002). Much higher $\delta^{15}N$ values (>10‰) may be associated with anthropogenic N inputs (Fry et al. 2000, Fry & Cormier 2011). Our sites showed a moderate level of $\delta^{15}N$ values (not low and not high with $\delta^{15}N$ values averaged around 4‰), suggesting that in addition to N fixation inputs and marine N inputs, there may be considerable microbial ^{15}N enrichment in dissolved inorganic nitrogen pools of ammonium and nitrate. The higher variability in leaf $\delta^{15}N$ in the impacted forest suggest higher variability in such processes affecting the $\delta^{15}N$ status of available N, for example environmental changes including changes to sediment conditions following the dieback affected microbial processes of N, whereas the unimpacted forest has more stable N processes and inputs. Isotope fractionation during plant N uptake may be an explanation for leaf $\delta^{15}N$ variability (Fry et al. 2000), but such fractionation is poorly known for mangroves. A study reported that additions of P nutrients increased N demand and decreased ^{15}N fractionation (McKee et al. 2002).

Leaf $\delta^{34}S$ values differed considerably between the two forests, with the impacted forest generally having higher values (13.5 ± 5.4‰, range 7.7 to 23.3‰) than the unimpacted forest (12.6 ± 5.6‰, range 5.0 to 21.9‰). Leaf $\delta^{34}S$ values showed trends along the transects, with the values decreasing from higher to lower intertidal zones (Fig. 3.3). Based on previous studies, mangrove leaf $\delta^{34}S$ values can vary between -20 to 20‰ (Fry et al. 1982, Okada & Sasaki 1995, 1998, Fry & Smith 2002). Higher $\delta^{34}S$ values are likely associated with seawater sulfate, which is ^{34}S enriched (i.e. 21‰) and due to a large isotope fractionation (up to 70‰) during sulfate reduction (Kaplan & Rittenberg 1964), lower $\delta^{34}S$ values are likely associated with sedimentary sulfide-S that is ^{34}S depleted, for example, -21‰ (Okada & Sasaki 1995). Leaf $\delta^{34}S$ values of around 14 to 18‰ suggest mangrove incorporations of seawater sulfate-S ($\delta^{34}S$, ~ 21‰), with only a small isotopic fractionation occurring through absorption and assimilation steps (Okada & Sasaki 1995). Plants generally show $\delta^{34}S$ values slightly lower than source sulfate-S by an average of -1.5‰ (Trust & Fry 1992). Low leaf $\delta^{34}S$ values, for instance, the lowest value of 5‰ found in the unimpacted site suggest that the most probable source of this ^{34}S-depleted S is sulfide oxidation, followed by mixing with seawater sulfate. Low $\delta^{34}S$ values in mangrove root vascular tissues may indicate assimilation/oxidation of sulfide, potentially to reduce their toxic sulfide exposure (Fry et al. 1982, Raven et al. 2019), with reported isotope effect of -5.2‰ for non-biological oxidation of sulfide (Fry et al. 1988) and a smaller +1-3 ‰ effect for anaerobic oxidation of sulfide by photosynthetic bacteria (Fry et al. 1984).

An explanation for our observed $\delta^{34}S$ pattern may be lower plant incorporation of sulfide-S in the impacted site and also in the higher intertidal zones where mangrove sediment is relatively more oxidised, and production of sulfide may be lower due to lower sulfate reduction. High wood $\delta^{34}S$ values (16.6‰) and S content (0.31%) in the impacted forest may suggest degradation of wood by fungi and/or bacteria that incorporate seawater sulfate-S and increase overall wood $\delta^{34}S$ values and S content. Such $\delta^{34}S$ patterns have been reported in mangroves (Fry & Smith 2002) and saltmarsh (Currin et al. 1995), where $\delta^{34}S$ values of fresh organic matter evolved during degradation steps and gradually increased and became closer to the $\delta^{34}S$ value of seawater sulfate-S (i.e. 21‰).

Sediment

In healthy mangrove forests, the fate of C fixed by primary producers include burial within the sediment, atmospheric emissions and outwelling to the ocean (Maher et al. 2018), but how mangrove losses alter such processes is poorly understood. In most cases, C within in mangrove sediment decreases following forest loss due to degradation with increased CO_2 emissions (Otero et al. 2017, Adame et al. 2018). Lower TOC (%) and higher sediment $\delta^{13}C$ values in the impacted forest (Table 3.2 and Fig. 3.4) are probably related to sediment C loss and lower mangrove C inputs (i.e. leaf litter) following the mangrove mortality event. Consistent with this, the sediment N (%) and $\delta^{15}N$ data showed a similar pattern. The surface sediment (0 - 0.5 cm) differed relatively more than the deeper (0.5 to 20 cm) fraction. One explanation for this is that the surface sediment fraction is generally more aerobic, and therefore remineralization of organic matter occurs more rapidly (Burdidge, 2011). Sediment $\delta^{13}C$ and ^{15}N values can increase during degradation of sediment organic matter (Natelhoffer & Fry 1988, Adame & Fry 2016). This isotope pattern has been reported following mangrove loss (Adame et al. 2018). Changes in sediment C and N may also be associated with root turnover. The MPB $\delta^{13}C$ values significantly differed, with those from the impacted being higher (-21.5 ± 1.3‰) than the unimpacted (-25.2 ± 1.0‰). The higher values probably indicate lower respiratory inputs of CO_2 from mangroves (Maher et al. 2013b). Our findings here are consistent with the finding of Sippo et al. (2019) that changes to oceanic carbon outwelling rates following mangrove loss are likely associated with a gradual loss of sediment carbon; similar to our finding of increased sediment $\delta^{13}C$ values in the impacted site, an isotope effect likely due to loss of sediment mangrove C.

Fauna

CNS isotopic compositions of consumers including an algae feeder, a grazer and a leaf feeder from the impacted site were consistently more enriched in ^{13}C, ^{15}N and ^{34}S. These differences did not change throughout the 2-year period between 2016 and 2018 (Fig. 5). Consistent with the findings from mangrove leaves, MPB and soil, these data suggested substantial changes in cycling of CNS associated with the mangrove mortality event. Overall, the consumer $\delta^{13}C$ values ranged from -22.9 to -15.2‰ for the unimpacted site, but at the impacted site, consumers were more ^{13}C-enriched (range of -20.0 to -14.0‰), likely due to the loss of ^{13}C-depleted mangrove organic matter. Consumer $\delta^{13}C$ values can change due to changes to available organic matter, altered feeding dependencies as well as changes to organic matter

$\delta^{13}C$ values; for example, MPB $\delta^{13}C$ values can change in response to organic matter respiratory inputs. The consumer $\delta^{13}C$ values and their ranges at our study site are fairly consistent with the reported mangrove consumer $\delta^{13}C$ values elsewhere (Lee 2000, Bouillon et al. 2002, Demopoulos et al. 2007). Lower consumer $\delta^{13}C$ values near -27‰ are generally associated with mangrove detritus, but in many cases, typical mangrove leaf-eating crab species (Sesarmidae) can be enriched by about +5‰ from the mangrove detritus (Bui & Lee 2014). Higher $\delta^{13}C$ values of consumers are generally tied to MPB with a typical isotope effect during assimilation, e.g. $< \sim 1$‰ estimated for small invertebrates (Vander Zanden & Rasmussen 2001, McCutchan et al. 2003). Our MPB endmember $\delta^{13}C$ values of -25.2‰ for the unimpacted site and -21.5‰ for the impacted site did not match with the consumer $\delta^{13}C$ values (around -15 to -14‰), suggesting our characterization of MPB endmember $\delta^{13}C$ values was incomplete. This is probably because MPB can vary substantially in mangrove ecosystems (Bouillon et al. 2008) and consumers may be preferentially assimilating more ^{13}C enriched fractions of MPB, for example, diatom and/or filamentous cyanobacteria that can range about -15 to -20‰ (Craig 1953, Fry & Wainright 1991). The leaf feeder that showed $\delta^{13}C$ values of about -21 to -18‰ was substantially enriched compared to mangrove leaves (-27 to -25‰), consistent with the finding of Bui and Lee (2014).

Due to difficulties obtaining representative endmembers, mixing analysis using sampled organic matter (mangrove leaf and MPB) was not possible in this study to assess feeding dependencies. Alternatively, the consumer data was used to infer endmembers, e.g. Riekenberg et al (2016). In the unimpacted site, using the lowest consumer as an endmember (-22.9‰) for mangrove C, and the highest consumer as an endmember (-15.2‰) for MPB C, a two-source mixing model analysis estimated respective contributions of 39% and 61% to the grazer (-18.2‰). Similarly, for the impacted site, a two-source mixing model analysis using the highest consumer (-20.0‰) and the lowest consumer (-14.0‰) estimated respective contributions of 45% mangrove C and 55% MPB C to the grazer (-16.7‰). These two mixing model analyses provided fairly consistent results, indicating that the feeding dependencies did not differ, but organic matter $\delta^{13}C$ values most likely differed between the two sites.

Consumer $\delta^{34}S$ values were generally higher in the impacted site (range 13.4 to 21.7‰) than in the unimpacted site (range 8.2 to 16‰) suggesting lower sulfate reduction with decreased

sulfide inputs at the impacted site. Fixation of sulfate by phytoplankton occurs with a small isotope effect, around 1 to 2‰ (Fry 2006), so that $\delta^{34}S$ values of phytoplankton from the coastal ocean should be close to the seawater sulfate-S value of 21‰. MPB generally have lower $\delta^{34}S$ values than phytoplankton, with reported average values near 10‰ for MPB in a mangrove ecosystem (Harada et al. unpublished, chapter 4), likely due to some use of sedimentary sulfide-S (depleted in ^{34}S). Our mangrove leaf $\delta^{34}S$ values averaged 13.5‰ for the impacted site and 12.6‰ for the unimpacted site, lower than the seawater sulfate-S. For these reasons, the unimpacted site that had lower consumer $\delta^{34}S$ values should be associated with sulfide inputs with some use of mangrove organic matter and MPB, whereas the impacted site that had higher consumer $\delta^{34}S$ values are associated more with seawater sulfate and indicated changes to the S cycling and use of S by plants as well as microbial intermediates in the food web.

The consumer $\delta^{15}N$ also indicate possible changes to N cycling with the consumer in the impacted site generally having higher values than those from in the unimpacted site. The higher $\delta^{15}N$ may be associated with degradation of organic matter, microbial ^{15}N enrichment in dissolved inorganic N such as ammonium and nitrate during degradation, and use such ^{15}N enriched N by microbial intermediates in the food web. The high ^{15}N may also indicate lower N fixation inputs that typically show low $\delta^{15}N$ values, round 0‰. While the $\delta^{13}C$ and $\delta^{34}S$ values consistently differed between the two forests during the two-year survey, the $\delta^{15}N$ values started showing matches between the two forests in 2018. This may suggest recovery of $\delta^{15}N$ status to the background conditions and recovery of N could be faster than C and N elements. This is probably because mangrove ecosystems are generally N limited, and circulation of N elements is faster than those of C and S elements.

Compound-specific isotope analysis of amino acids

It is considered that environmental resources such as vascular plants and microalgae have different $\delta^{13}C$ patterns ('fingerprint') in AAs due to differing biosynthesis of AAs (Larsen et al. 2009, Larsen et al. 2013). It is also reported that $\delta^{13}C$ patterns are largely unaffected by environmental conditions, for example $\delta^{13}C_{AA}$ patterns of the marine diatom *Thalassiosira weissflogii* did not respond to changing environmental conditions such as light, salinity, temperature and pH, despite substantial changes in bulk $\delta^{13}C$ values (Larsen et al. 2015). Similar isotope pattern was reported for seagrass *Posidonia oceanica* and the giant kelp

Macrocystis pyrifera that showed consistent $\delta^{13}C_{AA}$ patterns despite season and growth conditions (Larsen et al. 2013). The $\delta^{13}C_{AA}$ patterns in producers especially those of essential amino acids ($\delta^{13}C_{EAA}$) can reflect consumer tissues with little isotope effect since animals need to obtain EAAs from their diet and EAA fractions are thought to be directly assimilated (McMahon et al. 2010). These basic expectations were reasonably met in our $\delta^{13}C_{EAA}$ dataset that was normalized to means of five EAAs as per Larsen et al. (2009). Normalized $\delta^{13}C_{EAA}$ patterns of our producer samples including mangrove leaves (yellow leaves of *A. marina*) and MPB did not differ between the two sites despite differing environmental conditions and substantial differences in bulk $\delta^{13}C$ values (Table 3.3 and Fig 3.6). Furthermore, the consumer $\delta^{13}C_{EAA}$ patterns also did not differ between the two sites. (Fig. 3.6). These findings did not support changes to feeding dependency following mangrove loss but suggested that the overall differences in the consumer bulk $\delta^{13}C$ values were most likely driven due to differences in the resource organic matter $\delta^{13}C$ values e.g. changes to MPB $\delta^{13}C$ values that were likely associated with lower mangrove C fixation/respiratory inputs following the mangrove mortality. Furthermore, such findings indicate that the reported substantial change to the mangrove benthic faunal assemblage following the mangrove loss (Harada et al. 2019, chapter 2) was probably driven more by modification of physical habitat structure than changes in the use of food resources.

Conclusions

Reporting rare, extreme biological events can be challenging because in many cases they can be sudden and before vs. after comparisons often cannot be easily achieved. Our field investigation that compared an impacted system vs. an adjacent unimpacted reference system using traditional ecological techniques combined with stable isotopes measured the initial dieback and also recovery of the mangrove ecosystem alongside a nearby unimpacted site. Mangrove seedling and sapling populations that increased during the two-year period between 2016 to 2018 (18 to 30 months after the mortality event) in the impacted site, suggest recovery of the mangrove vegetation. This also suggests that the environmental conditions at the impacted site are still conducive for re-establishment of mangroves allowing recruitment of seedlings and development of regrowth. However, mangrove leaves collected in the impacted site in 2018 showed relatively higher $\delta^{13}C$ values that are probably associated with water stresses. Overall, our stable CNS isotope data supported the hypothesis that changes to biogeochemical processes occur following the mangrove mortality. These changes

include lower mangrove C fixation/respiration, lower N fixation and lower sulfate reduction. However, our isotope data did not support the second hypothesis that the isotopic compositions change over time with recovery of mangrove vegetation. Recovery of biogeochemical processes was not evident even after two years, suggesting an ongoing impact of the mortality event.

Considering that the environmental conditions at the site play an important role in facilitating recolonisation of mangroves, it could be conceptualised that the recovery of the mangrove forest could be driven by several key processes (Fig. 3.7): 1) The forest recovers with mangroves being able to recolonise at the site without future perturbations; 2) the forest recovers with future perturbations such as climatic events, for example, mangrove recolonisation is driven by events as such ENSO cycles; 3) the forest does not recover and is transformed into intertidal mudflats; and 4) the forest recovers partially at the site and in a reduced size and/or is recolonised by other plants such as saltmarshes, e.g., mangroves only recolonise in the lower intertidal zone. Each of these scenarios will have a distinct isotopic trajectory for C, N and S. Continued monitoring of the post-dieback forest would require to predict the long-term trajectory of ecosystem recovery and help understand how on-going climate change and extreme climatic events affect the recovery of mangroves and the environmental conditions that allow recolonisation of mangroves in the impacted region. In such a long-term investigation, stable isotope analysis can track changes in biogeochemical processes over time, helping ecosystem analyses and detect underlying biological mechanisms that drive changes and recovery.

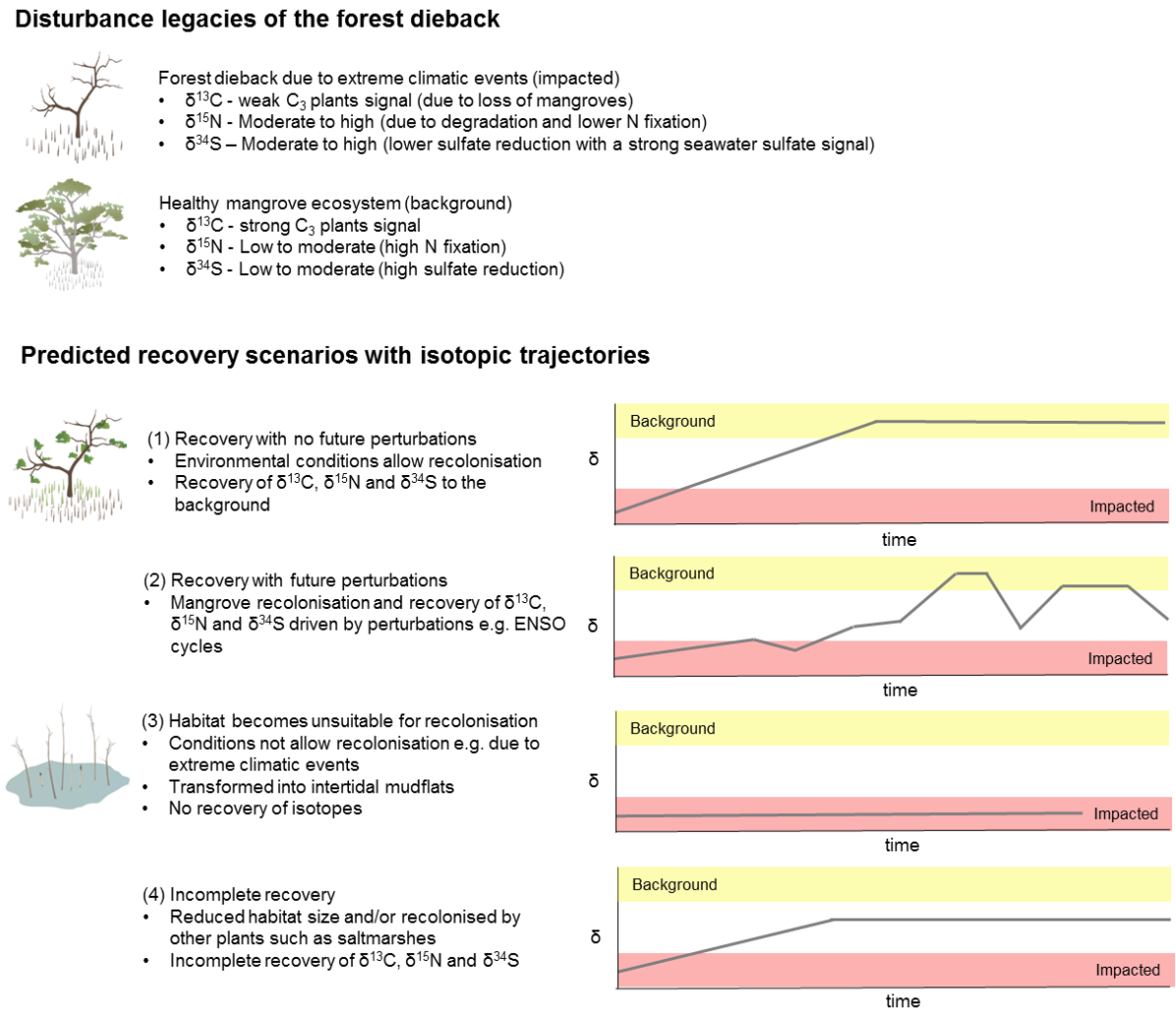

Fig. 3.7. A conceptual diagram showing the ecological and biogeochemical legacy of the mangrove forest dieback in the Gulf of Carpentaria and four predicted recovery scenarios of the mangrove ecosystem with isotopic trajectories.

References

Abrantes KG, Johnston R, Connolly RM, Sheaves M (2015) Importance of Mangrove Carbon for Aquatic Food Webs in Wet–Dry Tropical Estuaries. Estuaries Coasts 38:383-399

Adame M, Fry B (2016) Source and stability of soil carbon in mangrove and freshwater wetlands of the Mexican Pacific coast. Wetl Ecol Manag 24:129-137

Adame M, Zakaria R, Fry B, Chong V, Then Y, Brown C, Lee SY (2018) Loss and recovery of carbon and nitrogen after mangrove clearing. Ocean Coast Manag 161:117-126

Asbridge E, Lucas R, Rogers K, Accad A (2018) The extent of mangrove change and potential for recovery following severe Tropical Cyclone Yasi, Hinchinbrook Island, Queensland, Australia. Ecol Evo 8:10416-10434

Asbridge E, Lucas R, Ticehurst C, Bunting P (2016) Mangrove response to environmental change in Australia's Gulf of Carpentaria. Ecol Evo 6:3523-3539

Asbridge EF, Bartolo R, Finlayson CM, Lucas RM, Rogers K, Woodroffe CD (2019) Assessing the distribution and drivers of mangrove dieback in Kakadu National Park, northern Australia. Estuar Coast Shelf Sci 228:106353

Bartolini F, Cimo F, Fusi M, Dahdouh-Guebas F, Lopes GP, Cannicci S (2011) The effect of sewage discharge on the ecosystem engineering activities of two East African fiddler crab species: Consequences for mangrove ecosystem functioning. Mar Environ Res 71:53-61

Bernardino AF, Gomes LEDO, Hadlich HL, Andrades R, Correa LB (2018) Mangrove clearing impacts on macrofaunal assemblages and benthic food webs in a tropical estuary. Mar Poll Bull 126:228-235

Bouillon S, Koedam N, Raman A, Dehairs F (2002) Primary producers sustaining macro-invertebrate communities in intertidal mangrove forests. Oecol 130:441-448

Bouillon S, Connolly RM, Lee SY (2008) Organic matter exchange and cycling in mangrove ecosystems: Recent insights from stable isotope studies. J Sea Res 59:44-58

Bui THH, Lee SY (2014) Does 'You Are What You Eat' Apply to Mangrove Grapsid Crabs? PLOS ONE 9:e89074

Burdige D (2011) 5.09 Estuarine and coastal sediments–coupled biogeochemical cycling. Treatise on Estuarine and Coastal Science 5:279-308

Cordell S, Goldstein G, Meinzer F, Handley LJFE (1999) Allocation of nitrogen and carbon in leaves of Metrosideros polymorpha regulates carboxylation capacity and $\delta^{13}C$ along an altitudinal gradient. Funct Ecol 13:811-818

Craig H (1953) The geochemistry of the stable carbon isotopes. Geochimica et Cosmochimica Acta 3:53-92

Currin CA, Newell SY, Paerl H (1995) The role of standing dead Spartina alterniflora and benthic microalgae in salt marsh food webs: considerations based on multiple stable isotope analysis. Mar Ecol Prog Ser 121:99-116

Dahdouh-Guebas F, Jayatissa LP, Di Nitto D, Bosire JO, Lo Seen D, Koedam N (2005) How effective were mangroves as a defence against the recent tsunami? Curr Biol 15: R443-R447

Demopoulos AW, Fry B, Smith CR (2007) Food web structure in exotic and native mangroves: a Hawaii–Puerto Rico comparison. Oecol 153:675-686

Docherty G, Jones V, Evershed RP (2001) Practical and theoretical considerations in the gas chromatography/combustion/isotope ratio mass spectrometry $\delta^{13}C$ analysis of small polyfunctional compounds. Rapid Commun Mass Spectrom 15:730-738

Dore JE, Brum JR, Tupas LM, Karl DM (2002) Seasonal and interannual variability in sources of nitrogen supporting export in the oligotrophic subtropical North Pacific Ocean. Limnol Oceanogr 47:1595-1607

Duke NC, Kovacs JM, Griffiths AD, Preece L, Hill DJE, van Oosterzee P, Mackenzie J, Morning HS, Burrows D (2017) Large-scale dieback of mangroves in Australia's Gulf of Carpentaria: a severe ecosystem response, coincidental with an unusually extreme weather event. Mar Freshwater Res 68: 1816-1829

Farquhar GD, Ehleringer JR, Hubick KT (1989) Carbon isotope discrimination and photosynthesis. Annu Rev Plant Biol 40:503-537

Fogel M, Wooller M, Cheeseman J, Smallwood B, Roberts Q, Romero I, Meyers MJJBD (2008) Unusually negative nitrogen isotopic compositions ($\delta^{15}N$) of mangroves and lichens in an oligotrophic, microbially-influenced ecosystem. Biogeosci 5:937-969

Fry B (2006) Stable Isotope Ecology. Springer-Verlag New York

Fry B, Bern AL, Ross MS, Meeder JF (2000) $\delta^{15}N$ studies of nitrogen use by the red mangrove, Rhizophora mangle L. in South Florida. Estuar Coast Shelf Sci 50:291-296

Fry B, Cormier N (2011) Chemical ecology of red mangroves, Rhizophora mangle, in the Hawaiian Islands1. Pac Sci 65:219-235

Fry B, Gest H, Hayes JM (1984) Isotope effects associated with the anaerobic oxidation of sulfide by the purple photosynthetic bacterium, Chromatium vinosum. FEMS Microbiol Lett 22:283-287

Fry B, Ruf W, Gest H, Hayes JM (1988) Sulfur isotope effects associated with oxidation of sulfide by O2 in aqueous solution. Chem Geol: Isotope Geoscience section 73:205-210

Fry B, Scalan RS, Winters JK, Parker PL (1982) Sulphur uptake by salt grasses, mangroves, and seagrasses in anaerobic sediments. Geochim Cosmochim Acta 46:1121-1124

Fry B, Smith TJ (2002) Stable isotope studies of red mangroves and filter feeders from the Shark River estuary, Florida. Bull Mar Sci 70:871-890

Fry B, Wainright SC (1991) Diatom sources of ^{13}C-rich carbon in marine food webs. Mar Ecol Prog Ser 76:149-157

Harris RMB, Beaumont LJ, Vance TR, Tozer CR, Remenyi TA, Perkins-Kirkpatrick SE, Mitchell PJ, Nicotra AB, McGregor S, Andrew NR, Letnic M, Kearney MR, Wernberg T, Hutley LB, Chambers LE, Fletcher MS, Keatley MR, Woodward CA, Williamson G, Duke NC, Bowman DMJS (2018) Biological responses to the press and pulse of climate trends and extreme events. Nat Clim Change 8:579-587

Hayes MA, Jesse A, Welti N, Tabet B, Lockington D, Lovelock CE (2019) Groundwater enhances above-ground growth in mangroves. J Ecol 107:1120-1128

Ishikawa NF, Chikaraishi Y, Takano Y, Sasaki Y, Takizawa Y, Tsuchiya M, Tayasu I, Nagata T, Ohkouchi N (2018) A new analytical method for determination of the nitrogen isotopic composition of methionine: Its application to aquatic ecosystems with mixed resources. Limnol Oceanogr Methods 16:607-620

Imbert D, Rousteau A, Scherrer P (2000) Ecology of mangrove growth and recovery in the Lesser Antilles: state of knowledge and basis for restoration projects. Restor Ecol 8:230-236

Kaplan I, Rittenberg S (1964) Microbiological fractionation of sulphur isotopes. Microbiology 34:195-212

Kelleway JJ, Mazumder D, Baldock JA, Saintilan N (2018) Carbon isotope fractionation in the mangrove Avicennia marina has implications for food web and blue carbon research. Estuar Coast Shelf Sci 205:68-74

Kling GW, Fry B, O'Brien WJ (1992) Stable Isotopes and Planktonic Trophic Structure in Arctic Lakes. Ecology 73:561-566

Larsen T, Bach LT, Salvatteci R, Wang YV, Andersen N, Ventura M, McCarthy MD (2015) Assessing the potential of amino acid ^{13}C patterns as a carbon source tracer in marine

sediments: effects of algal growth conditions and sedimentary diagenesis. Biogeosci 12:4979-4992
Larsen T, Taylor DL, Leigh MB, O'Brien DM (2009) Stable isotope fingerprinting: a novel method for identifying plant, fungal, or bacterial origins of amino acids. Ecology 90:3526-3535
Larsen T, Ventura M, Andersen N, O'Brien DM, Piatkowski U, McCarthy MD (2013) Tracing Carbon Sources through Aquatic and Terrestrial Food Webs Using Amino Acid Stable Isotope Fingerprinting. PLoS ONE 8:e73441
Larsen T, Wooller MJ, Fogel ML, O'Brien DM (2012) Can amino acid carbon isotope ratios distinguish primary producers in a mangrove ecosystem? Rapid Commun Mass Spectrom 26:1541-1548
Lee SY (2000) Carbon dynamics of Deep Bay, eastern Pearl River estuary, China. II: Trophic relationship based on carbon-and nitrogen-stable isotopes. Mar Ecol Prog Ser 205:1-10
Lin G, Sternberg LS (1992a) Differences in morphology, carbon isotope ratios, and photosynthesis between scrub and fringe mangroves in Florida, USA. Aquat Bot 42:303-313
Lin G, Sternberg LS (1992b) Effect of growth form, salinity, nutrient and sulfide on photosynthesis, carbon isotope discrimination and growth of red mangrove (Rhizophora mangle L.). Funct Plant Biol 19:509-517
Lovelock CE, Feller IC, Reef R, Hickey S, Ball MC (2017) Mangrove dieback during fluctuating sea levels. Sci Rep 7:1680
Maher DT, Call M, Santos IR, Sanders CJ (2018) Beyond burial: lateral exchange is a significant atmospheric carbon sink in mangrove forests. Biol Lett 14:20180200
Maher DT, Santos IR, Golsby-Smith L, Gleeson J, Eyre BD (2013a) Groundwater-derived dissolved inorganic and organic carbon exports from a mangrove tidal creek: The missing mangrove carbon sink? Limnol Oceanogr 58:475-488
Maher DT, Santos IR, Schulz KG, Call M, Jacobsen GE, Sanders CJ (2017) Blue carbon oxidation revealed by radiogenic and stable isotopes in a mangrove system. Geophys Res Lett 44:4889-4896
Maher DT, Santos IR, Leuven JRFW, Oakes JM, Erler DV, Carvalho MC, Eyre BD (2013b) Novel Use of Cavity Ring-down Spectroscopy to Investigate Aquatic Carbon Cycling from Microbial to Ecosystem Scales. Environ Sci Technol 47:12938-12945
Mbense S, Rajkaran A, Bolosha U, Adams J (2016) Rapid colonization of degraded mangrove habitat by succulent salt marsh. S Afr J Bot 107:129-136
McCutchan JH, Lewis Jr WM, Kendall C, McGrath CC (2003) Variation in trophic shift for stable isotope ratios of carbon, nitrogen, and sulfur. Oikos 102:378-390
McKee KL, Feller IC, Popp M, Wanek W (2002) Mangrove isotopic ($\delta^{15}N$ and $\delta^{13}C$) fractionation across a nitrogen vs. phosphorus limitation gradient. Ecology 83:1065-1075
McKee KL, Rooth JE, Feller IC (2007) Mangrove recruitment after forest disturbance is facilitated by herbaceous species in the Caribbean. Ecol Appl 17:1678-1693
McMahon KW, Fogel ML, Elsdon TS, Thorrold SR (2010) Carbon isotope fractionation of amino acids in fish muscle reflects biosynthesis and isotopic routing from dietary protein. J Anim Ecol 79:1132-1141
Milbrandt E, Greenawalt-Boswell J, Sokoloff P, Bortone S (2006) Impact and response of Southwest Florida mangroves to the 2004 hurricane season. Estuaries Coasts 29:979-984
Natelhoffer KJ, Fry B (1988) Controls on Natural Nitrogen-15 and Carbon-13 Abundances in Forest Soil Organic Matter. Soil Sci Soci Am J 52:1633-1640

Ohkouchi N, Chikaraishi Y, Close HG, Fry B, Larsen T, Madigan DJ, McCarthy MD, McMahon KW, Nagata T, Naito YI, Ogawa NO, Popp BN, Steffan S, Takano Y, Tayasu I, Wyatt ASJ, Yamaguchi YT, Yokoyama Y (2017) Advances in the application of amino acid nitrogen isotopic analysis in ecological and biogeochemical studies. Org Geochem 113:150-174

Okada N, Sasaki A (1995) Characteristics of Sulfur Uptake by Mangroves: an Isotopic Study. Tropics 4:201-210

Okada N, Sasaki A (1998) Sulfur isotopic composition of mangroves. Isot Environ Heal S 34:61-65

Otero XL, Méndez A, Nóbrega GN, Ferreira TO, Santiso-Taboada MJ, Meléndez W, Macías F (2017) High fragility of the soil organic C pools in mangrove forests. Mar Poll Bull 119:460-464

Peterson BJ, Fry B (1987) Stable isotopes in ecosystem studies. Annu Rev Ecol Syst 18:293-320

Rashid S, Biswas SR, Böcker R, Kruse M (2009) Mangrove community recovery potential after catastrophic disturbances in Bangladesh. For Ecol and Manag 257:923-930

Raven MR, Fike DA, Gomes ML, Webb SM (2019) Chemical and isotopic evidence for organic matter sulfurization in redox gradients around mangrove roots. Front Earth Sci 7:98

Riekenberg PM, Carney RS, Fry B (2016) Trophic plasticity of the methanotrophic mussel Bathymodiolus childressi in the Gulf of Mexico. Mar Ecol Prog Ser 547:91-106

Santini NS, Reef R, Lockington DA, Lovelock CE (2015) The use of fresh and saline water sources by the mangrove Avicennia marina. Hydrobiologia 745:59-68

Sherman RE, Fahey TJ, Martinez P (2001) Hurricane Impacts on a Mangrove Forest in the Dominican Republic: Damage Patterns and Early Recovery 1. Biotropica 33:393-408

Sippo JZ, Lovelock CE, Santos IR, Sanders CJ, Maher DT (2018) Mangrove mortality in a changing climate: An overview. Estuar, Coast Shelf Sci 215:241-249

Sippo JZ, Maher DT, Schulz KG, Sanders CJ, McMahon A, Tucker J, Santos IR (2019) Carbon outwelling across the shelf following a massive mangrove dieback in Australia: Insights from radium isotopes. Geochim Cosmochim Acta 253:142-158

Sjöling S, Mohammed SM, Lyimo TJ, Kyaruzi JJ (2005) Benthic bacterial diversity and nutrient processes in mangroves: impact of deforestation. Estuar, Coast Shelf Sci 63:397-406

Smallwood BJ, Wooller MJ, Jacobson ME, Fogel MLJGT (2003) Isotopic and molecular distributions of biochemicals from fresh and buried Rhizophora mangle leaves. Geochem trans 4:38

Smith TJ, Robblee MB, Wanless HR, Doyle TW (1994) Mangroves, hurricanes, and lightning strikes: assessment of Hurricane Andrew suggests an interaction across two differing scales of disturbance. BioScience 44:256-262

Sweetman A, Middelburg J, Berle A, Bernardino A, Schander C, Demopoulos A, Smith C (2010) Impacts of exotic mangrove forests and mangrove deforestation on carbon remineralization and ecosystem functioning in marine sediments. Biogeosci 7:2129-2145

Tomlinson PB (2016) The botany of mangroves. Cambridge University Press

Trust B, Fry B (1992) Stable sulphur isotopes in plants: a review. Plant, Cell Environ 15:1105-1110

Vander Zanden MJ, Rasmussen JB (2001) Variation in $\delta^{15}N$ and $\delta^{13}C$ trophic fractionation: Implications for aquatic food web studies. Limnol Oceanogr 46:2061-2066

Wada E, Mizutani H, Minagawa M (1991) The use of stable isotopes for food web analysis. Crit Rev Food Sci Nutr 30:361-371

Walsh RG, He S, Yarnes CT (2014) Compound‐specific $\delta^{13}C$ and $\delta^{15}N$ analysis of amino acids: a rapid, chloroformate‐based method for ecological studies. Rapid Commun Mass Spectrom 28:96-108
Werth M, Mehltreter K, Briones O, Kazda M (2015) Stable carbon and nitrogen isotope compositions change with leaf age in two mangrove ferns. Flora 210:80-86

Chapter 4

Combined analysis of bulk stable CNS isotopes and compound-specific stable CN isotopes of amino acids in analysing mangrove food webs.

This chapter is an unpublished paper. The bibliographical details of the co-authored paper, including all authors are:

Harada Y, Fry B, Connolly RM, Lee SY (in preparation) Combined analysis of bulk stable CNS isotopes and compound-specific stable CN isotopes of amino acids in analysing mangrove food webs.

Author Contributions
The study was conceptualized by all authors. Writing was led by YH and contributed to by all. Field sampling was executed by YH. Data compilation and analysis was coordinated by YH and contributed to by all.

(Signed) _____

Corresponding (1st) author: Yota Harada

(Countersigned) _____

Supervisor (and co-author): Rod M. Connolly

Abstract

Analyses of bulk stable CNS isotopes and compound-specific stable CN isotopes of amino acids were compared to test which isotope tracers are more conservative and suited for tracing mangrove organic matter in a food web in the subtropical east coast of Australia. Substantial bulk stable CNS isotope differences between the red mangrove *Rhizophora stylosa* (-28.2 ± 0.4‰ $\delta^{13}C$, 5.9 ± 1.9‰ $\delta^{15}N$, -14.8 ± 2.3‰ $\delta^{34}S$) and the associated leaf-eating crab *Neosarmatium trispinosum* (-23.3 ± 0.4‰ $\delta^{13}C$, 5.3 ± 0.7‰ $\delta^{15}N$, -6.7 ± 0.7‰ $\delta^{34}S$) suggest that bulk stable isotopic compositions of mangrove organic matter reset during multiple steps of degradation, digestion and assimilation. The fingerprint pattern analysis as per Larsen et al. (2009) of $\delta^{13}C$ variation among essential amino acids (EAAs), particularly phenylalanine (Phe), isoleucine (Ile) and leucine (Leu), was informative for distinguishing the mangroves from the microphytobenthos (MPB). $\delta^{15}N$ values of Phe also distinguished the mangrove (15.2 ± 3.0‰) from the MPB (3.2 ± 0.1‰). Similarly, bulk $\delta^{34}S$ values also distinguished the mangrove (-14.8 ± 2.3‰) vs MPB (10.2 ± 0.1‰). Overall, direct use of mangrove-derived nutrients was largely under-detected for the consumers in the mangrove food web using bulk tissue analysis, and more nutritious MPB were expressed in their tissues. $\delta^{15}N$ of Phe and bulk $\delta^{34}S$, which similarly separated the mangrove from MPB, were relatively more conservative tracers of mangrove organic matter and gave similar dietary estimates. This is probably because of lower trophic fractionations during uptake of Phe and sulfur-containing amino acids. This approach using multiple stable isotope analytical methods rather than single/dual-isotope tracers of bulk tissue analysis helped to resolve the complex dynamics of mangrove food webs.

Introduction

Stable isotopes with their ability to track changes and processes over time provide ecologists with a natural way to directly trace details of element and/or organic matter cycling in the environment (Fry 2006). Stable isotopic compositions such as $^{13}C/^{12}C$, $^{15}N/^{14}N$ and $^{34}S/^{32}S$ of organic matter change in predictable ways (Peterson & Fry 1987, Wada et al. 1991) and can help to evaluate functional aspects of element and/or organic matter cycling and the health of ecosystems, e.g. integrity of the food web. Stable isotope analyses of total organic matter (''bulk'') have become widespread due to the relative ease and low cost of sample preparation and analysis (Fry 2006). Compound-specific isotope analysis is now increasingly employed as a complementary tool to help measure details of organic matter cycling (Potapov et al. 2019). For instance, patterns of C isotopic compositions in individual amino acids ("fingerprint") help to discriminate resource uses (Larsen et al. 2009, Larsen et al. 2013) and N isotopic compositions in amino acids such as phenylalanine and glutamic acid can be used to estimate trophic levels of organisms in food web analyses (Chikaraishi et al. 2009, Ohkouchi et al. 2017, Ishikawa et al. 2018).

Mangrove forests are highly productive and support the livelihoods of millions of people, protect coastal communities and underpin global fisheries (Lee et al. 2014). Investigating aquatic food webs with mixed resources, however, can be challenging. For example, the dynamics of mangrove food webs that have multiple inputs not only from vascular plants but also from aquatic food resources can be complex (Odum & Heald 1975). Stable isotopes have provided significant insight in this area (Fry & Ewel 2003, Bouillon et al. 2008). In most studies, bulk $\delta^{13}C$ and $\delta^{15}N$ measurements are used (Demopoulos et al. 2007, Bui & Lee 2014, Kristensen et al. 2017). In some cases, $\delta^{34}S$ measurements were also used for additional resolution (Fry & Smith 2002). However, compound-specific stable isotope methods of $\delta^{13}C$ measurements in individual amino acids, e.g. Larsen et al. (2009), as well as those of $\delta^{15}N$ measurements, e.g. Chikaraishi et al. (2009), have not been commonly used in mangrove food webs (Larsen et al. 2012, Bui & Lee 2015). While isotopic compositions in essential amino acids (EAAs) that cannot be synthesised by animals can be more conservative during trophic processes (Newsome et al. 2011), how they can help track organic matter cycling in mangrove food web analyses remain unclear. This is an important area to explore because in many cases, the more commonly used bulk stable C isotopic compositions are not conservative and can vary substantially in mangrove detritus food webs. For example, previous studies of typical mangrove leaf-eating crab species (Sesarmidae) consistently yield

large carbon isotope differences of about +5‰ vs mangroves (Skov & Hartnoll 2002, Mazumder & Saintilan 2010, Bui & Lee 2014, Kristensen et al. 2017).

In some cases, trophic fractionation at the basal level of marine benthic food webs can be large for carbon stable isotopes (Fry et al. 1983, Demopoulos et al. 2017), particularly detritus food chains that are relatively long, involving microbial and/or meiofaunal intermediates before reaching benthic macrofaunal consumers (McConnaughey & McRoy 1979). Similarly, many terrestrial detritivores are significantly enriched in ^{13}C compared to plant detritus (Potapov et al. 2013, Korobushkin et al. 2014). For instance, soil animals like earthworms can be enriched in ^{13}C by about +5‰ or more vs plant litter, reflecting the use of ^{13}C-enriched microbial biomass fractions of plant detritus (Potapov et al. 2018). Such large $\delta^{13}C$ shift may also reflect low growth efficiency on low quality diets (high C with low N) (Hobbie 2005, Lehmeier et al. 2016).

In this study, use of widely used bulk $\delta^{13}C$, $\delta^{15}N$, and $\delta^{34}S$ measurements and more specialised compound-specific $\delta^{13}C$ and $\delta^{15}N$ measurements of amino acids are compared to evaluate which isotope compositions are more conservative during trophic processes and can help discriminate mangrove organic matter in food web analyses. We tested hypotheses that stable C and N isotopic compositions in amino acids help discriminate mangrove organic matter in food web analyses, and that those in essential amino acids that cannot be synthesised by animals would be more conservative in food web links between mangrove organic matter and consumers. Three reference crab species from a subtropical mangrove forest in Australia were compared, a leaf-eating specialist *Neosarmatium trispinosum*, an algivore specialist *Uca vomeris* that consumes microphytobenthos (MPB), and a generalist-feeding crab *Parasesarma erythodactyla* that consumes mangrove leaves but also MPB.

Methods

Study location and samples

All samples were collected from a mangrove forest at Tallebudgera Creek, Queensland, Australia, during January to March 2017. The intertidal mangrove forest (28°06'25.5"S 153°26'49.5"E) is located approximately 2 km from of the river mouth (Fig. 4.1). The maximum tidal range is about 1.5 m. *Rhizophora stylosa* (red mangrove) and *Avicennia marina* (grey mangrove) are the dominant mangrove species. The samples (Table 4.1) were collected within 150 m of each other at the location (Fig. 4.1). Mangrove leaves (n=3) were

collected from two species (*A. marina* and *R. stylosa*). They were harvested directly from trees as yellow, i.e. senescent, leaves that most closely represents mangrove organic matter that enters mangrove detrital food webs. Three crab species with different foraging types were collected from three difference zones (Fig 4.1). A leaf-eating specialist crab (*N. trispinosum*, n=3) that predominantly feeds on red mangrove leaves under the stilt roots (Harada & Lee 2016) were collected from the dense red mangrove zone. A specialist algivore crab (*Uca vomeris* fiddler crab, n=3) that feeds on MPB were collected from the canopy gap zone. A generalist feeding crab (*Parasesarma erythodactyla*, n=3) that feeds on leaf litter of mangroves, particularly of *A. marina*, but also MPB (Bui & Lee 2014) were collected from the sparse red and grey mangrove zone. MPB (n=3) were collected from the soil surface (top 0.5 cm) from the forest of the canopy gap area (Fig. 4.1). All leaves and crabs were thoroughly washed in distilled water. All samples were kept on ice until they were transported to the laboratory at Griffith University, Gold Coast, QLD, Australia. Immediately after arriving at the laboratory, samples of MPB were further separated by density gradient centrifugation in Ludox colloidal silica (Sigma) following the method described in Bui and Lee (2014). The separated samples were examined under a microscope to ensure that they contained MPB (e.g. cyanobacteria and diatoms). The samples most likely also contained phytoplankton deposited on the forest floor. Muscle tissue samples of crabs were obtained from the claws. All the samples were freeze-dried and homogenised to a fine powder using a mortar and pestle.

Fig. 4.1. Study location and sampling. There are three sampling zones within a mangrove forest at Tallebudgera Creek (28°06'25.5"S 153°26'49.5"E). The dense red mangrove zone is associated with a leaf-eating specialist crab (*Neosarmatium trispinosum*) that predominantly feeds on red mangrove leaves under the stilt roots (Harada & Lee 2016). The canopy gap zone is dominated by a specialist algivore crab (*Uca vomeris* fiddler crab) that feeds on MPB. The sparse red and grey mangrove zone is dominated by a generalist feeding crab (*Parasesarma erythodactyla*) that feeds on leaf litter of mangroves, particularly of *A. marina*, but also MPB (Bui & Lee 2014).

Stable isotope analysis

Bulk $\delta^{13}C$, $\delta^{15}N$ and $\delta^{34}S$ values were measured with an elemental analyser, Europa EA-GSL coupled to an isotope ratio mass spectrometer, Sercon 20-22 SERCON at Griffith University, Nathan, QLD, Australia. For individual amino acid stable C and N isotope measurements, dry, homogenised sample materials were weighed into 8mg aliquots (animal tissues) or 30 mg aliquots (plant tissues) and transferred to borosilicate vials with heat and acid-resistant caps. The samples were flushed with N_2 gas, sealed and hydrolysed in 0.5 mL (animal tissues) or 2 mL (plant tissues) of 6M HCl at 150°C for 70 minutes. The samples were then dried in a heating block at 60°C under a stream of N_2 gas. The dried samples were derivatised by methoxycarbonylation (methoxycarbonyl amino acid methyl esters for $\delta^{13}C_{AA}$ measurements) or esterification-acetylation (N-acetyl amino acid isopropyl esters for $\delta^{15}N_{AA}$ measurements) as described elsewhere (Walsh et al. 2014, Yarnes & Herszage 2017). AA derivatives were separated by a Trace GC Ultra gas chromatograph (Thermo Scientific) using a DB-23 column (Agilent, 30m × 0.25mm, 0.25um film) for $\delta^{13}C_{AA}$ measurements, and using a DB-1301 (Agilent, 60m × 0.25mm, 1um film) for $\delta^{15}N_{AA}$ measurements at the Stable Isotope Facility at the University of California (Davis, CA, USA). The gas chromatograph was interfaced with a Delta V Plus isotope ratio mass spectrometer via a GC IsoLink (Thermo Scientific). For quality control and assurance, L-norleucine was used as an internal standard and used to calculate provisional values for each sample. Mixtures composed of pure amino acids with calibrated $\delta^{13}C$ and $\delta^{15}N$ were co-measured with samples. One mixture was used for final isotopic calibration of each amino acid, while the other served as the scale normalisation standard. Additionally, a third mixture served as the primary quality assurance standard (unused in corrections), while two well-described, natural materials were co-measured as secondary quality assurance materials. Exogenous carbon from the derivatization was accounted for using the procedure of Docherty et al. (2001). Using these methods, $\delta^{13}C$ and $\delta^{15}N$ values were determined for 10 AAs (Ala, alanine; Asp, aspartic acid; Glu, glutamic acid; Gly, glycine; Ile, isoleucine; Leu, leucine; Lys, lysine; Phe, phenylalanine; Pro, proline; and Val, valine). Three amino acids, Met, methionine; Thr, threonine; and Tyr, tyrosine; presented at or below the limit of quantitation (LOQ) for some samples and were omitted.

For this study, we were mainly interested in the $\delta^{13}C$ values of essential amino acids (EAAs) and hence present results for Ile, Leu, Lys, Phe and Val. Additionally, the $\delta^{13}C$ values of non-

essential amino acids (NEAAs) including Ala, Asp, Glu, Gly and Pro are also reported. The $\delta^{15}N$ values of Glu and Phe that are more commonly used in food web analyses, e.g. Chikaraishi et al. (2009), are also reported in this study. All stable isotope data are expressed in delta (δ) notation as $\delta = [(R_{sample}/R_{standard}) - 1] \times 1000$ ‰, where R is the ratio of the heavy to the light isotope; and the standard is Vienna Pee Dee Belemnite (VPDB) for C, atmospheric air (AIR) for N, and Canyon Diablo Troilite (VCDT) for S.

Data analysis

To explore patterns of $\delta^{13}C$ among EAAs and NEAAs, $\delta^{13}C_{EAA}$ and $\delta^{13}C_{NEAA}$ values were normalised to the respective sample means following the procedure of Larsen et al. (2009) as follows: $Norm(\delta_{EAA}) = \delta_{EAA} - \mu$, where μ represents the mean value of all five EAAs (Ile, Leu, Lys, Phe and Val) in the sample and $Norm(\delta_{NEAA}) = \delta_{NEAA} - \mu$, where μ represents the mean value of all five NEAAs (Gly, Asp, Pro, Glu and Ala) in the sample. ANOVA was performed to explore the differences between group means. Before performing ANOVA, the assumptions of homogeneity of variance and normality in distribution were checked by performing Levene's test and Shapiro-Wilk's test, respectively. PERMANOVA was performed to compare the pattern of $\delta^{13}C_{EAA}$ between samples and also the pattern of $\delta^{13}C_{NEAA}$ between the samples. In this analysis, the normalized $\delta^{13}C_{EAA}$ and $\delta^{13}C_{NEAA}$ datasets were used and Euclidean distance was used as the distance metric. Permutation test of multivariate homogeneity of dispersions was performed to check whether dispersions around the centroids are similar between the samples. All statistical analyses were conducted in R version 3.4.3 with RStudio interface version 1.1.414, with α at 0.05.

Results

Bulk $\delta^{13}C$, $\delta^{15}N$ and $\delta^{34}S$ measurements

Bulk $\delta^{13}C$, $\delta^{15}N$ and $\delta^{34}S$ values generally separated the producers. The consumers also differed in their isotope values, but there were substantial mismatches between the producers and consumers (Table 4.1). $\delta^{13}C$ values of the producers including the red mangroves, the grey mangrove, and MPB ranged from -28.6 to -20.3‰ and were significantly different (ANOVA $F_{2, 6} = 218.3$, $p = < 0.001$). The red mangrove and grey mangrove did not differ ($p = 0.11$), but MPB was significantly higher. $\delta^{13}C$ values significantly differed between the consumers (ANOVA $F_{2, 6} = 319.7$, $p < 0.001$) and ranged from -23.7 to -14.8‰. $\delta^{15}N$ values did not differ significantly between either the producers (ANOVA $F_{2, 6} = 3.82$ $p = 0.09$) or the consumers (ANOVA $F_{2, 6} = 4.39$, $p = 0.06$). $\delta^{34}S$ values of the producers varied significantly

(ANOVA $F_{2, 6}$ = 336.6, p < 0.001) and ranged from -17.2 to 10.4‰. Red mangrove was significantly lower than grey mangrove and MPB (p < 0.001). $\delta^{34}S$ values significantly differed between the consumers (ANOVA $F_{2, 6}$ = 175.5, p < 0.001) and ranged from -7.3 to 12.4‰. $\delta^{34}S$ values of the leaf-eating specialist found in the red mangrove zone were significantly lower than the generalist and the specialist algivore (P < 0.001). There were substantial isotope mismatches between the producers and consumers. For examples, the leaf-eating specialist crab (-23.3 ± 0.4‰) and its associated red mangrove (-28.2 ± 0.4‰) demonstrate a substantial difference in their $\delta^{13}C$ values (Δ ~ 4.9‰).

Table 4.1. Summary of the samples included in this study from Tallebudgera Creek, Australia, showing results for bulk $\delta^{13}C$, $\delta^{15}N$ and $\delta^{34}S$ values, the mean values of $\delta^{13}C_{AA}$ across 10 amino acids and $\delta^{13}C_{EAA}$ across five essential amino, $\delta^{15}N_{Glu}$ and $\delta^{15}N_{Phe}$ values (mean, SD, ‰), n = 3 samples in each case.

Common name	Latin name	Category	Bulk $\delta^{13}C$	Bulk $\delta^{15}N$	Bulk $\delta^{34}S$	Mean $\delta^{13}C_{AA}$	Mean $\delta^{13}C_{EAA}$	$\delta^{15}N_{Glu}$	$\delta^{15}N_{Phe}$
Red mangrove	*Rhizophora stylosa*	Vascular plant producer	-28.2, 0.4	5.9, 1.9	-14.8, 2.3	-25.5, 0.3	-27.9, 0.2	4.8, 0.5	15.2, 3.0
Grey mangrove	*Avicennia marina*	Vascular plant producer	-27.1, 0.8	6.1, 0.8	9.7, 0.4	-25.1, 0.3	-28.5, 0.2	9.3, 0.8	20.4, 1.8
MPB	NA	Microalgae producer	-20.4, 0.1	3.6, 0.0	10.2, 0.1	-17.3, 0.1	-21.0, 0.2	6.7, 0.2	3.2, 0.1
NA crab	*Neosarmatium trispinosum*	Consumer, leaf-eating specialist	-23.3, 0.4	5.3, 0.7	-6.7, 0.7	-23.7, 0.4	-28.9, 0.1	11.0, 1.3	11.6, 1.7
NA crab	*Parasesarma erythodactyla*	Consumer, generalist-feeder	-20.6, 0.6	5.5, 0.4	9.7, 2.2	-20.4, 0.2	-24.9, 0.3	13.9, 0.8	5.6, 0.6
Fiddler crab	*Uca vomeris*	Consumer, Specialist algivore	-14.8, 0.2	4.4, 0.2	12.1, 0.4	-15.7, 0.3	-20.4, 0.1	9.8, 0.6	2.4, 0.1

$\delta^{13}C_{AA}$ measurements

The mean $\delta^{13}C_{AA}$ values of 10 AAs were related to those of bulk $\delta^{13}C$ values (Table 4.1). The patterns of $\delta^{13}C_{EAA}$ data that were normalised to the mean of five EAAs (Ile, Leu, Met, Phe, and Val) varied significantly between producers (PERMANOVA $F_{2, 6}$ = 64.07, p = 0.003) (Fig. 4.2A). While $\delta^{13}C_{EAA}$ patterns of red mangrove and grey mangrove were fairly similar, MPB substantially differed from the mangroves (Fig. 4.2A). Normalised Phe values varied significantly between the producers (ANOVA $F_{2, 6}$ = 244, p < 0.001) with MPB being significantly lower than the red mangrove and the grey mangrove. Normalized Leu values also differed significantly between the producers (ANOVA $F_{2, 6}$ = 207.3, p < 0.001), with MPB being higher than both mangrove species. The two mangroves did not differ in their normalized Leu values (p = 0.193). Normalized Val values also differed significantly (ANOVA $F_{2, 6}$ = 25.95, p= 0.001), with the red mangroves being significantly lower than the grey mangrove and the MPB. Normalized Lys values did not significantly distinguish

between red mangroves, grey mangrove and MPB (ANOVA $F_{2, 6} = 1.57$, $p = 0.281$). Normalized Ile values varied significantly (ANOVA $F_{2, 6} = 25.22$, $p = 0.001$) with MPB being lower than red mangrove and the grey mangrove.

The patterns of $\delta^{13}C_{EAA}$ also varied significantly between the three consumers (PERMANOVA $F_{2, 6} = 67.70$, $p = 0.01$) (Fig. 4.2A). While the generalist and specialist algivore were fairly similar, the leaf-eating specialist differed, particularly in their Phe Val, and Leu. Normalized Phe values significantly varied between the consumers (ANOVA $F_{2, 6} = 154.9$, $p < 0.001$), with the leaf-eating specialist being significantly higher than the generalist and specialist algivore. Normalized Val values also significantly varied between the consumers (ANOVA $F_{2, 6} = 32.21$, $p < 0.001$) with the leaf-eating specialist being significantly lower than the generalist and specialist algivore. Normalized Leu values also varied significantly (ANOVA $F_{2, 6} = 74.88$, $p < 0.001$), with the leaf-eating specialist being significantly lower than the generalist and specialist algivore. Normalized Ile values did not significantly distinguish between the three consumers (ANOVA $F_{2, 6} = 1.37$, $p = 0.323$). Normalized Lys values significantly differed between all consumers (ANOVA $F_{2, 6} = 20.35$, $p = 0.002$). Overall, Phe, Leu, Val were more informative EAAs that distinguished mangrove leaf from MPB, with the isotope patterns in Phe, Leu and Val also distinguishing the leaf-eating specialist from the generalist and specialist algivore (Fig. 4.2A). While $\delta^{13}C_{EAA}$ profiles varied between the three crabs, their $\delta^{13}C_{NEAA}$ profiles did not differ significantly (PERMANOVA $F_{2, 6} = 1.69$, $p = 0.153$) (Fig. 4.2B).

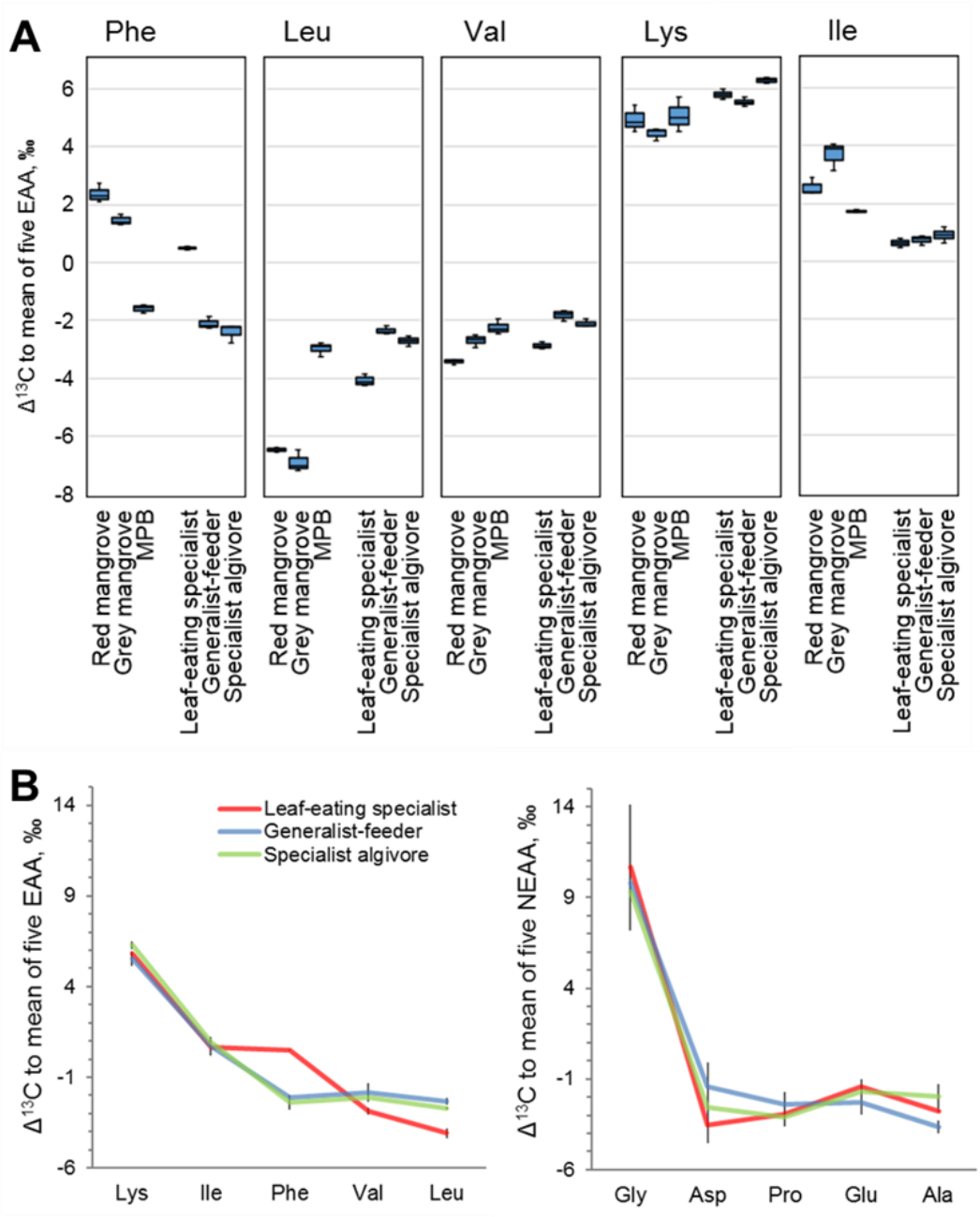

Fig. 4.2. Patterns of $\delta^{13}C_{EAA}$ in producers and three consumers, crabs with unique feeding modes in a mangrove ecosystem at Tallebudgera Creek, Australia (n = 3). (A) The box represents the interquartile range (IQR) with the line within the box indicating the median and the lower and upper end of whiskers represent the minimum and maximum values. (B) Patterns of $\delta^{13}C$ (mean, SD) in EAAs (left) and NEAAs (right) for three consumers

$\delta^{15}N_{Glu}$ and $\delta^{15}N_{Phe}$ measurements

$\delta^{15}N_{Phe}$ values of the producers differed significantly (ANOVA $F_{2, 6} = 58.8$, $p < 0.001$) and ranged from 3.1 to 21.1‰, with both mangroves having significantly higher values than MPB (Table 1 and Fig.3). Consumer $\delta^{15}N_{Phe}$ values also differed significantly (ANOVA $F_{2, 6} = 61.92$, $p < 0.001$) and ranged from 2.3 to 13.2‰, with the leaf-eating specialist being significantly higher than the generalist and specialist algivore. $\delta^{15}N_{Glu}$ values of all three food sources differed significantly (ANOVA $F_{2, 6} = 49.83$, $p < 0.001$) and ranged from 4.2 to 9.8‰. Consumer $\delta^{15}N_{Glu}$ values ranged from 9.1 to 14.5‰, being significantly different among the three consumers.

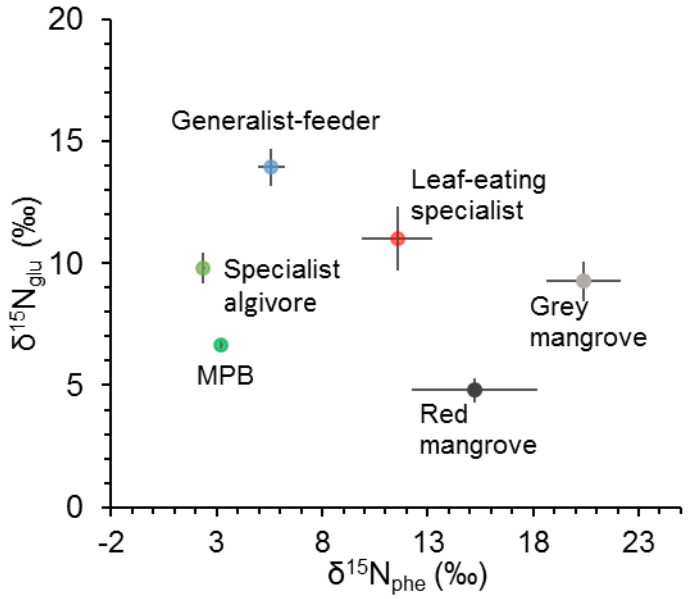

Fig. 4.3. $\delta^{15}N_{Glu}$ and $\delta^{15}N_{Phe}$ values (mean SD, n=3) of producers and three crabs with unique feeding modes in a mangrove ecosystem at Tallebudgera Creek, Australia.

Discussion

Bulk $\delta^{13}C$, $\delta^{15}N$ and $\delta^{34}S$

$\delta^{13}C$ values of mangrove macrofauna, mostly invertebrates such as crabs, gastropods and bivalves are generally ^{13}C-enriched relative to the mangrove $\delta^{13}C$ values (Lee 2000, Sheaves & Molony 2000, Bouillon et al. 2002). Higher consumer $\delta^{13}C$ values are usually attributed to dependence on the MPB. Trophic enrichment of about +1‰ typically occurs for $\delta^{13}C$ during each trophic step for small invertebrates (Vander Zanden & Rasmussen 2001, McCutchan et al. 2003). Leaf-eating sesarmid crabs that are observed to consume mangrove leaves typically show a lower $\delta^{13}C$ range closer to the mangroves (Sheaves & Molony 2000, Harada & Lee 2016), but usually show ^{13}C enrichment (+5‰) relative to the mangrove leaf values, likely

due to accumulative isotope effects during digestion and assimilation steps of this low-quality organic matter (Bui & Lee 2014). In many cases, $\delta^{13}C$ values can be largely non-conservative for tracing mangrove organic matter, consistent with observations on many other detrital food webs. For example, earthworms that ingest plant detritus can be enriched in ^{13}C by +5‰ or even more vs plant detritus, reflecting the use of ^{13}C enriched microbial biomass (Potapov et al. 2018, Potapov et al. 2019). Similarly, trophic ^{13}C fractionation at the basal level of marine benthic food webs can be large (Fry et al. 1983, Demopoulos et al. 2017), reflecting detritus food chains that are relatively long with multiple trophic steps, involving microbes and/or meiofauna intermediates (McConnaughey & McRoy 1979).

In the present case, $\delta^{13}C$ values of mangroves and MPB ranged from -28.6 to -20.3‰, whereas the consumer $\delta^{13}C$ values ranged from -23.7 to -14.8‰, suggesting that there are substantial isotope mismatches between the sampled end-members and consumers. Firstly, there was a large mismatch ($\Delta \sim 4.9$‰) between the leaf-eating specialist crab (-23.3 ± 0.4‰) and its associated red mangrove (-28.2 ± 0.4‰), which is possibly associated with microbial degradation of organic matter (Potapov et al. 2018, Potapov et al. 2019) as well as a low quality diet and low growth efficiency (Hobbie 2005, Lehmeier et al. 2016). There was also a large mismatch ($\Delta \sim 6.5$‰) between the generalist feeding crab (-20.6 ± 0.6‰) and its associated grey mangrove (-27.1 ± 0.8‰), similar to the leaf-eating specialist crab, but this crab matched more with MPB (-20.4 ± 0.1‰). The algivore specialist crab (-14.8 ± 0.2‰) was unlikely dependent on mangrove leaves. However, this crab differed significantly ($\Delta \sim 5.6$‰) from the MPB values. This mismatch probably suggests an under-sampling of MPB in the field where MPB may show patchiness. For example, there should be more ^{13}C-enriched diatoms and/or filamentous cyanobacteria fractions of MPB, with reported values of about -15 to -20‰ (Craig 1953, Fry & Wainright 1991) that may be preferentially assimilated by the algivore crabs. Overall, due to the number of uncertainties, including in large ^{13}C isotope fractionations and representativeness in sampling MPB, quantitative assessment of feeding dependencies using mixing models were not achieved with the bulk $\delta^{13}C$ dataset.

$\delta^{15}N$ values of mangroves and MPB ranged from 3.6 to 8.0‰. Mangroves had a higher range of 4.2 to 8.0‰ compared to MPB (3.6 ± 0.0‰). Lower $\delta^{15}N$ values are generally associated with N fixation inputs, which is ~ 0‰ (Fogel et al. 2008) or marine N inputs (Dore et al. 2002), whereas much higher $\delta^{15}N$ values of >10‰ typically indicate anthropogenic N inputs (Fry & Cormier 2011). Mean trophic enrichment of about +2.2‰ occurs for $\delta^{15}N$ during each

trophic step for small invertebrates (Vander Zanden & Rasmussen 2001, McCutchan et al. 2003). Overall, consumer $\delta^{15}N$ values ranged from 4.2 to 5.9‰. The leaf-eating specialist (5.3 ± 0.7‰) and generalist feeding (5.5 ± 0.4‰) crabs were similar. The algivore specialist had slightly lower values of 4.4 ± 0.2‰. Based on the mean trophic enrichment of +2.2‰, expected food values for those consumers should be around 2.0 to 3.7‰, but the measured end-member values of 3.6 to 8.0‰ largely disagreed with this expectation. Overall, the data generally suggested that use of mangrove-derived N (4.2 to 8.0‰) was probably limited, but MPB derived-N of about 3.6‰ played a more important role. The disagreements in $\delta^{15}N$ values between the consumers and sampled organic matter are probably because of uses of various N sources including dissolved inorganic N in soil and water by microbial intermediates.

Mangroves generally show high $\delta^{34}S$ variability with leaf $\delta^{34}S$ values, typically ranging between -20 to 20‰ (Fry et al. 1982, Okada & Sasaki 1995, 1998, Fry & Smith 2002). Our mangrove leaf $\delta^{34}S$ values ranged from -17.2 to 10.1‰ with the red mangrove (-14.8 ± 2.3‰) being lower than the grey mangrove (9.7 ± 0.4‰). This is likely associated with the difference in sedimentary environments, e.g. presence of pneumatophores in the grey mangrove that can oxygenate the sediment. Higher leaf $\delta^{34}S$ values of about 14 to 18‰ are typically associated with seawater sulfate (i.e. 21‰), with small fractionation during plant uptake (Okada & Sasaki 1995). Because of a large isotope effect (up to about 70‰) during sulfate reduction (Kaplan & Rittenberg 1964), sedimentary sulfide-S is typically ^{34}S depleted, e.g. -21‰ (Okada & Sasaki 1995), so that lower $\delta^{34}S$ values are typically associated with root incorporation of sulfide-S. Fixation of sulfate by phytoplankton occurs with a small isotope effect of about 1 to 2‰ (Fry 2006), so that phytoplankton $\delta^{34}S$ values from the coastal ocean are near the seawater sulfate-S (21‰) value. MPB generally have lower $\delta^{34}S$ values than the phytoplankton due to some use of sedimentary sulfide-S with our MPB $\delta^{34}S$ values averaging 10.2 ± 0.1‰. $\delta^{34}S$ values of organic matter in marine environments, for example, mangrove and saltmarsh detritus may gradually increase due to degradation by fungi and/or bacteria that incorporate seawater sulfate-S (Currin et al. 1995, Fry & Smith 2002). Trophic fractionation for $\delta^{34}S$ is typically small (about 0‰), due to little to no fractionation during assimilation of sulfur-containing amino acids (e.g. methionine) (McCutchan et al. 2003). Overall, mangrove and MPB $\delta^{34}S$ values ranged from -17.2 to 10.4‰ and consumer $\delta^{34}S$ values ranged from -7.3 to 12.4‰. The leaf-eating specialist (-6.7

± 0.7‰) was related to the red mangrove (-14.8 ± 2.3‰), but there was still a large difference (Δ ~8.1‰), probably suggesting degradation that involves fungal and bacteria intermediates in the gut microbiome, i.e. similar explanation for the above-mentioned $\delta^{13}C$ shift of Δ ~ 4.9‰. The generalist (9.7 ± 2.2‰) was similar to grey mangrove (9.7 ± 0.4‰) and MPB (10.2 ± 0.1‰). The specialist algivore (12.1 ± 0.4‰) was most probably associated with MPB (10.2 ± 0.1‰).

Overall, our bulk $\delta^{13}C$, $\delta^{15}N$ and $\delta^{34}S$ dataset provided an overall view of assessing feeding dependencies from the biogeochemical cycling of C, N and S elements. However, in a quantitative sense, $\delta^{13}C$ and $\delta^{15}N$ data did not show clear mixing dynamics. This is probably because bulk $\delta^{13}C$ and $\delta^{15}N$ values largely reset during digestion and assimilation steps and were not largely conservative in detrital food webs as well as the fact that characterization of end-members using bulk isotope values was weak. However, $\delta^{34}S$ appeared relatively more conservative and could distinguish red mangrove (-14.8 ± 2.3‰) from MPB (10.2 ± 0.1‰). Using these two end-members, a mixing model analysis of the leaf-eating specialist (-6.7 ± 0.7‰) estimated a mean dietary contribution of red mangrove (68%) and the remaining is MPB (trophic enrichment of +0‰ assumed for $\delta^{34}S$ mixing model analysis), but this estimate most likely includes some intermediate contributions that we could not characterise, but were indicated by the above-mentioned substantial isotope shift for $\delta^{13}C$ (Δ ~ 4.9‰) and $\delta^{34}S$ (Δ ~8.1‰). Therefore, it is more appropriate to consider the 68% as a maximum mangrove contribution.

$\delta^{13}C_{AA}$

Environmental resources such as vascular plants and microalgae have been reported to display distinctive $\delta^{13}C$ patterns ('fingerprint') in AAs due to different biosynthesis of AAs (Larsen et al. 2009, Larsen et al. 2012, Larsen et al. 2013). This was previously demonstrated in a mangrove ecosystem in Spanish Lookout Cays (SLC), Belize, where Larsen et al (2012) found different $\delta^{13}C_{AA}$ patterns between vascular plants and microbial mat, similar to our finding. It is also reported that $\delta^{13}C_{AA}$ patterns are largely unaffected by environmental conditions. For example, $\delta^{13}C_{AA}$ patterns of a marine diatom *Thalassiosira weissflogii* did not respond to different growth conditions such as light, salinity, temperature and pH, despite substantial changes in bulk $\delta^{13}C$ values (Larsen et al. 2015). Similar isotope patterns were reported for seagrass *Posidonia oceanica* and the giant kelp *Macrocystis pyrifera* that showed

consistent $\delta^{13}C_{AA}$ patterns regardless of growth conditions (Larsen et al. 2013). For these reasons, $\delta^{13}C_{AA}$ patterns should generally be consistent across various geographical regions. In our $\delta^{13}C_{AA}$ dataset, these basic expectations were generally met - the $\delta^{13}C_{AA}$ patterns of our mangroves and MPB were reasonably consistent with comparable samples collected in other geographical locations and ecosystem types (Fig. 4.4). Our two mangrove species (red mangrove and grey mangrove) were similar to mangroves from Spanish Lookout Cays, Belize (Larsen et al. 2012), red mangroves (*Rhizophora mangle*) from Twin Cays, Belize (Smallwood et al. 2003), as well as terrestrial vascular plants collected in a boreal forest ecosystem in interior Alaska (Larsen et al. 2009). Our MPB samples were similar to the microbial mat (i.e. MPB) from SLC and microalgae from laboratory cultures (Larsen et al. 2013). Overall, Phe and Leu and partially Val appeared as more informative EAAs for distinguishing mangroves from MPB, with fungi and bacteria isolated from a boreal forest in interior Alaska also showing distinctive patterns (Larsen et al. 2009) (Fig. 4.4). Overall, $\delta^{13}C_{AA}$ patterns of the consumers generally matched more with MPB, consistent with other mangrove systems across different geographical locations including Spanish Lookout Cays, Belize (Larsen et al. 2012) and the Gulf of Carpentaria, Australia (Harada et al. unpublished, chapter 3), with all the consumer clustered within the MPB/microalgae group (Fig. 4.5).

The variance in our $\delta^{13}C_{AA}$ dataset is primarily explicable by differences in bulk $\delta^{13}C$ values, which are reflected in the average of the $\delta^{13}C_{AA}$ values. However, normalization to the average of five essential amino acids (Phe, Leu, Val, Lys and Ile) as per Larsen et al. (2009) provided a more differentiated view of assessing feeding dependencies from the fingerprint pattern of normalized EAA data. The patterns of $\delta^{13}C$ in the three consumers varied relatively more in the EAAs than in the NEAAs. This is probably because more complex EAAs are originated from the diets (McMahon et al. 2010, Newsome et al. 2011) whereas NEAAs were synthesised using components drawn from the body biochemical pools (Webb et al. 2017), with these crabs probably also sharing similar NEAA synthesis pathways.

Overall, Phe, Leu, Val were relatively more informative EAAs for distinguishing mangroves from MPB, with the isotope patterns in Phe, Leu and Val also able to distinguish the leaf-eating specialist from the generalist and the algivore specialist. The generalist and the specialist algivore had similar Phe, Leu and Val profiles that were also similar to those of MPB, with the importance of mangrove Phe, Leu and Val being undetected for these two

crab species. However, the leaf-eating specialist had distinctive Phe Leu, and Val profiles, suggested likely contributions of mangrove-derived Phe, Leu and Val. For Phe, using the two end-members of red mangrove (2.4 ± 0.3‰) and MPB (-1.6 ± 0.1‰), a mixing model analysis of the leaf-eating specialist (0.5 ± 0.0‰) estimated mean dietary contributions of red mangrove (52.5%) and MPB (47.5%) (trophic enrichment of +0‰ assumed for the EAA mixing model analysis). For Leu, using the two end-members of red mangrove (-6.5 ± 0.1‰) and MPB (-3.0 ± 0.2‰), a mixing model analysis of the leaf-eating specialist (-4.0 ± 0.2‰) estimated mean dietary contributions of red mangrove (28.6%) and MPB (71.4%). For Val, using the same two end-members of red mangrove (-3.4 ± 0.1‰) and MPB (-2.3 ± 0.3‰), a mixing model analysis of the leaf-eating specialist (-2.9 ± 0.2‰) estimated mean dietary contributions of red mangrove (54.5%) and MPB (45.5%). Overall, the estimated mangrove contributions to the leaf-eating specialist ranged from 28.6 to 54.5%, with the remaining being MPB.

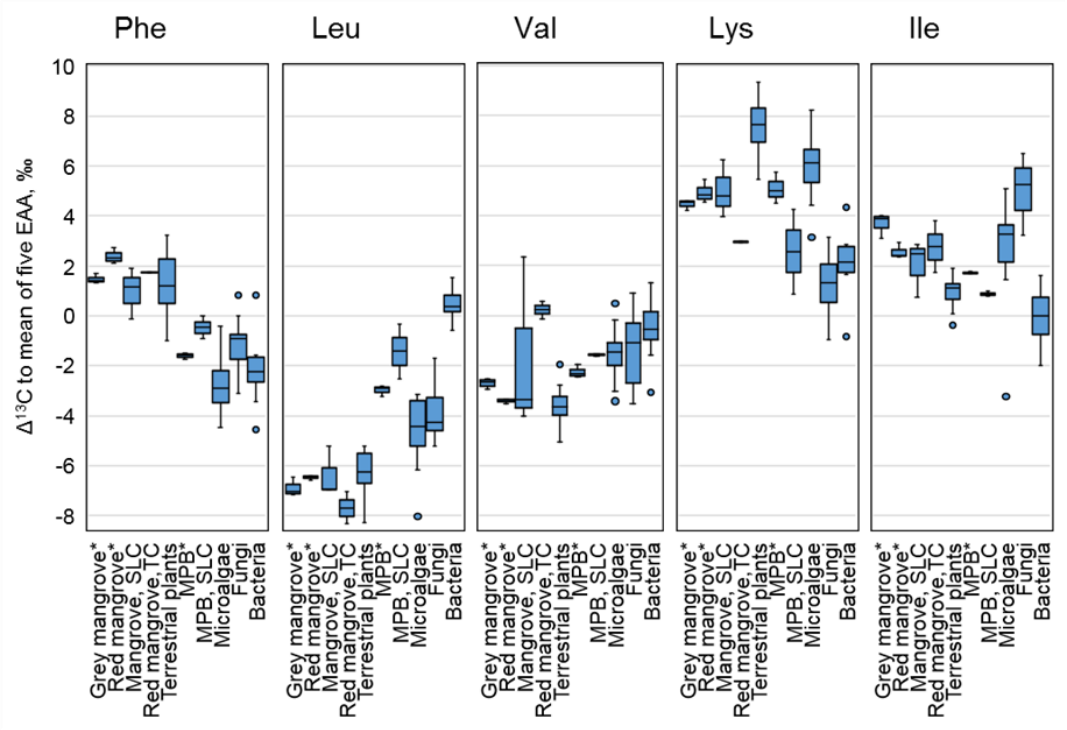

Fig. 4.4. Patterns of $\delta^{13}C_{EAA,}$ fingerprints in two mangrove species and MPB from Tallebudgera Creek (*) (n = 3), along with literature data reported elsewhere. $\Delta^{13}C$ values, normalized to the mean $\delta^{13}C$ value of five selected essential amino acids (Phe, Leu, Val, Lys and Ile) in the sample, are shown. Mangrove species (n = 3) and MPB (microbial mat samples, n = 2) from Spanish Lookout Cay (SLC), Belize (Larsen et al. 2012). Red mangroves (*Rhizophora mangle*, n = 2) from Twin Cays (TC), Belize (Smallwood et al. 2003). Terrestrial vascular plants (n = 10) from a boreal forest in Alaska (Larsen et al. 2009). Microalgae (n = 26) from laboratory cultures (Larsen et al. 2013). Fungi (n = 13) and Bacteria (n = 10) isolated from a boreal forest in Alaska (Larsen et al. 2009). The box represents the interquartile range (IQR), with the line within the box indicating the median and the lower and upper end of whiskers represent minimum and maximum values that are not outliers. Circles indicate outliers (i.e. outside 1.5 IQR range).

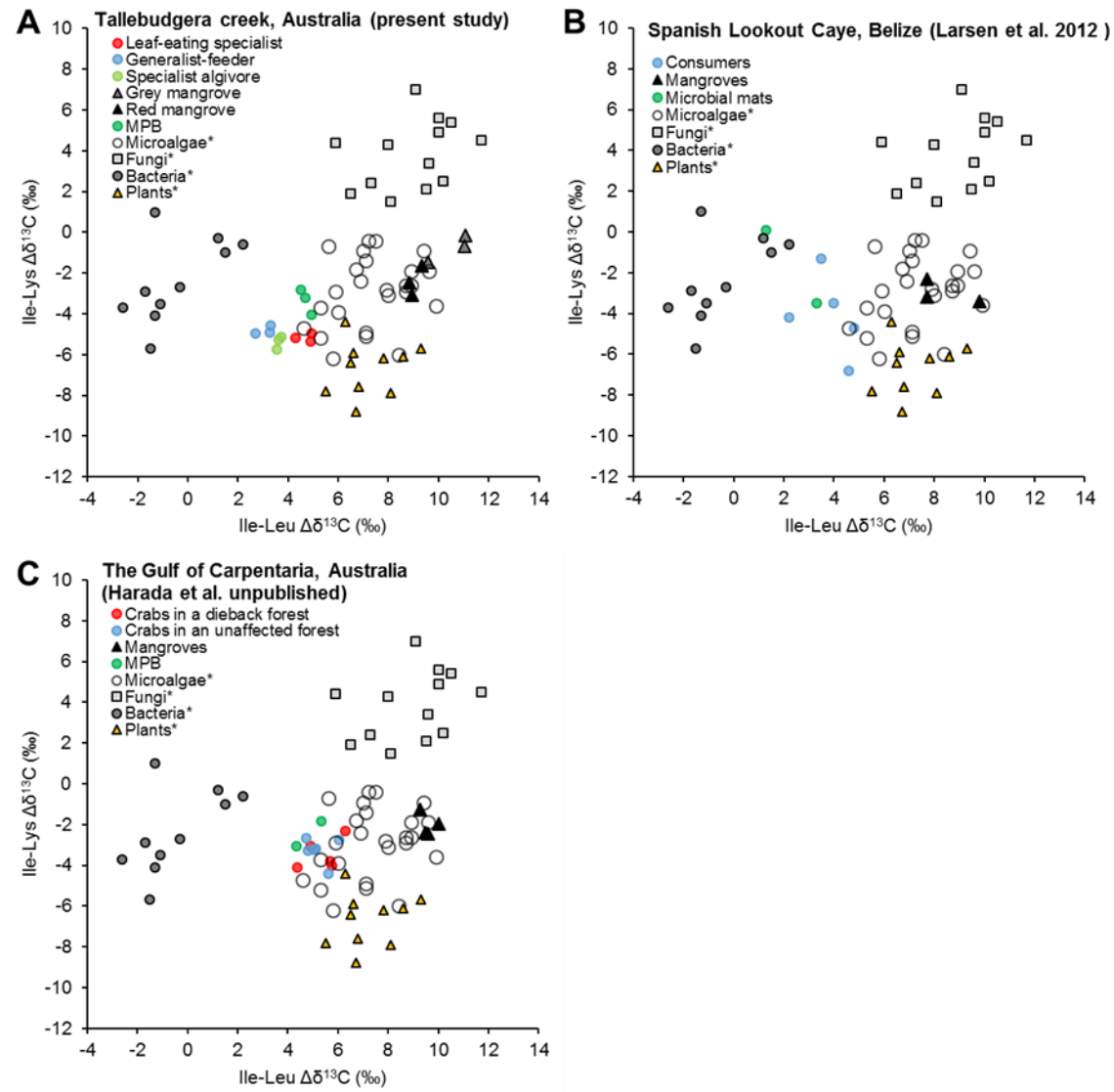

Fig. 4.5. Three informative EAAs (Ile, Leu and Lys) for distinguishing fungal, bacterial and plant-derived EAAs, as suggested by Larsen et al (2009) (see their Fig. 3). All the consumers show an importance of MPB/microalgae, but a minor importance of fungal, bacterial and plant-derived EAAs in the mangrove consumers across the three locations. (*) indicates $^{13}C_{AA}$ fingerprint data obtained from Larsen et al. (2009, 2013).

$\delta^{15}N_{phe}$ and $\delta^{15}N_{glu}$

Trophic amino acids (e.g. Ala, Asp, Glu, Ile, Leu, Pro, and Val) typically show larger trophic ^{15}N enrichment (+3-8‰) relative to diet during each trophic step, e.g. ~ +8‰ for Glu, whereas source amino acids (e.g. Met, Lys, and Phe) show relatively small trophic ^{15}N enrichment (+0-1‰), e.g. < 0.5‰ for Phe (Ohkouchi et al. 2017). $\delta^{15}N_{phe}$ values are therefore informative for estimating the basal $\delta^{15}N$ value of the food web. In most cases, vascular plant $\delta^{15}N_{phe}$ values are relatively higher compared to algae $\delta^{15}N_{phe}$ values, due to the deamination

of Phe for lignin biosynthesis, a process specific to vascular plants (Naito et al. 2016). Reported β values (isotope differences among $\delta^{15}N_{glu}$ and $\delta^{15}N_{phe}$ in primary producers) range from ~ +8.4‰ for vascular plants and ~ -3.4‰ for algae (Chikaraishi et al. 2009, Chikaraishi et al. 2010). In our $\delta^{15}N_{phe}$ and $\delta^{15}N_{glu}$ dataset, these basic expectations were generally met, in that $\delta^{15}N_{phe}$ values of red mangrove (15.2 ± 3.0‰) and grey mangrove (20.4 ± 1.8‰) were much higher than that of MPB (3.2 ± 0.1‰), with β values of 10.4‰, 11.2‰ and -3.5‰, respectively. These findings are consistent with other marine vascular plants including seagrasses (Vander Zanden et al. 2013, Choi et al. 2017). $\delta^{15}N_{phe}$ values distinguished the leaf-eating specialist (11.6 ± 1.7‰) from the generalist (5.6 ± 0.6‰) and specialist algivore (2.4 ± 0.1‰). Using the two end-members of red mangrove and MPB, a mixing model analysis of the leaf-eating specialist estimated mean dietary contributions of red mangrove (70%) and MPB (30%) (trophic enrichment of +0‰ assumed in this $\delta^{15}N_{phe}$ mixing analysis). $\delta^{15}N_{Glu}$ values of producers were generally lower than those of the consumers, likely due to the trophic ^{15}N enrichment of Glu.

Conclusions

Stable isotopic compositions of mangrove organic matter largely reset during multiple trophic steps including degradation, digestion and assimilation. Consequently, direct use of mangrove nutrients by detritivorous consumers has generally been under-detected. Conversely, more nutritious and easily assimilated MPB appear to be more expressed in their tissue isotopic compositions. Compound-specific isotope analysis of AAs, used as a supporting tool to the bulk analysis, helped to reveal details of organic matter flow in food web analysis in a multi-source system. For example, the fingerprint pattern analysis of $\delta^{13}C$ variation among EAAs, particularly Phe, Ile and Leu, distinguished mangrove organic matter from the MPB. $\delta^{15}N_{Phe}$ also distinguished the mangrove from the MPB, supporting the hypothesis that stable isotopic compositions in AAs help discriminate mangrove organic matter in food web analyses. $\delta^{34}S$ values also distinguished the mangrove from MPB. $\delta^{15}N_{Phe}$ and $\delta^{34}S$ values that gave similar dietary estimates from two source mixing models are relatively more conservative tracers of mangrove organic matter. For example, maximum dietary contributions of the red mangrove to the associated leaf-eating estimated using $\delta^{15}N_{Phe}$ and $\delta^{34}S$ were 70% and 68%, respectively. This consistency is probably because of the lower trophic fractionations during the uptake of Phe and sulfur-containing amino acids (e.g. methionine), supporting the hypothesis that stable isotopic compositions in essential amino acids that cannot be synthesised by animals would be more conservative in food web

links between mangrove organic matter and consumers. This is also supported by the finding that $\delta^{13}C$ pattern in EAAs differed between the consumers, but those of NEAAs were fairly consistent.

This study demonstrated that compound-specific isotope analysis of AAs complements bulk stable isotope analysis in multiple end-member mangrove food web analyses. However, various isotope compositions can change during complex trophic processes in mangrove food webs. For this reason, future studies of mangrove food webs may benefit from use of multiple stable isotope tracers. This study was limited by a narrow focus on mangrove-associated consumers that live within mangrove forests, but future applications of the same approach may benefit from including various estuarine consumers and larger-scale spatial comparisons that can help to elucidate how mangrove organic matter support estuary-wide food webs, e.g. Abrantes et al. (2015).

References

Abrantes KG, Johnston R, Connolly RM, Sheaves M (2015) Importance of Mangrove Carbon for Aquatic Food Webs in Wet–Dry Tropical Estuaries. Estuaries Coasts 38:383-399

Bouillon S, Koedam N, Raman A, Dehairs F (2002) Primary producers sustaining macro-invertebrate communities in intertidal mangrove forests. Oecol130:441-448

Bouillon S, Connolly RM, Lee SY (2008) Organic matter exchange and cycling in mangrove ecosystems: Recent insights from stable isotope studies. J Sea Res 59:44-58

Bui THH, Lee SY (2014) Does 'You Are What You Eat' Apply to Mangrove Grapsid Crabs? PLOS ONE 9:e89074

Bui THH, Lee SY (2015) Potential contributions of gut microbiota to the nutrition of the detritivorous sesarmid crab Parasesarma erythodactyla. Mar Biol 162:1969-1981

Chikaraishi Y, Ogawa NO, Kashiyama Y, Takano Y, Suga H, Tomitani A, Miyashita H, Kitazato H, Ohkouchi N (2009) Determination of aquatic food-web structure based on compound-specific nitrogen isotopic composition of amino acids. Limnol Oceanogr Methods 7:740-750

Chikaraishi Y, Ogawa NO, Ohkouchi N (2010) Further evaluation of the trophic level estimation based on nitrogen isotopic composition of amino acids. In: Ohkouchi N, Tayasu I, Koba K (eds) Earth, life, and isotopes. Kyoto University Press, Kyoto, pp 37-51

Choi B, Ha S-Y, Lee JS, Chikaraishi Y, Ohkouchi N, Shin K-H (2017) Trophic interaction among organisms in a seagrass meadow ecosystem as revealed by bulk $\delta^{13}C$ and amino acid $\delta^{15}N$ analyses. Limnol Oceanogr 62:1426-1435

Craig H (1953) The geochemistry of the stable carbon isotopes. Geochim Cosmochim Acta 3:53-92

Currin CA, Newell SY, Paerl H (1995) The role of standing dead Spartina alterniflora and benthic microalgae in salt marsh food webs: considerations based on multiple stable isotope analysis. Mar Ecol Prog Ser 121:99-116

Demopoulos AW, Fry B, Smith CR (2007) Food web structure in exotic and native mangroves: a Hawaii–Puerto Rico comparison. Oecol 153:675-686

Demopoulos AW, McClain-Counts J, Ross SW, Brooke S, Mienis F (2017) Food-web dynamics and isotopic niches in deep-sea communities residing in a submarine canyon and on the adjacent open slopes. Mar Ecol Prog Ser 578:19-33

Docherty G, Jones V, Evershed RP (2001) Practical and theoretical considerations in the gas chromatography/combustion/isotope ratio mass spectrometry $\delta^{13}C$ analysis of small polyfunctional compounds. Rapid Commun Mass Spectrom 15:730-738

Dore JE, Brum JR, Tupas LM, Karl DM (2002) Seasonal and interannual variability in sources of nitrogen supporting export in the oligotrophic subtropical North Pacific Ocean. Limnol Oceanogr 47:1595-1607

Fogel M, Wooller M, Cheeseman J, Smallwood B, Roberts Q, Romero I, Meyers MJ (2008) Unusually negative nitrogen isotopic compositions ($\delta^{15}N$) of mangroves and lichens in an oligotrophic, microbially-influenced ecosystem. Biogeosci 5:937-969

Fry B (2006) Stable Isotope Ecology. Springer-Verlag New York

Fry B, Cormier N (2011) Chemical Ecology of Red Mangroves, Rhizophora mangle, in the Hawaiian Islands1. Pac Sci 65:219-235

Fry B, Ewel K (2003) Using stable isotopes in mangrove fisheries research - a review and outlook. Isot Environ Healt S 39:191-196

Fry B, Scalan R, Parker P (1983) $^{13}C/^{12}C$ ratios in marine food webs of the Torres Strait, Queensland. Mar Freshwater Res 34:707-715

Fry B, Scalan RS, Winters JK, Parker PL (1982) Sulphur uptake by salt grasses, mangroves, and seagrasses in anaerobic sediments. Geochim Cosmochim Acta 46:1121-1124

Fry B, Smith TJ (2002) Stable isotope studies of red mangroves and filter feeders from the Shark River estuary, Florida. Bull Mar Sci 70:871-890
Fry B, Wainright SC (1991) Diatom sources of ^{13}C-rich carbon in marine food webs. Mar Ecol Prog Ser:149-157
Harada Y, Lee SY (2016) Foraging behavior of the mangrove sesarmid crab Neosarmatium trispinosum enhances food intake and nutrient retention in a low-quality food environment. Estuar Coast Shelf Sci 174:41-48
Hobbie EA (2005) Using isotopic tracers to follow carbon and nitrogen cycling of fungi. In: Dighton J, JF White, Oudemans P (eds) The fungal community: its organization and role in the ecosystem. Taylor & Francis, Boca Raton, FL, USA
Ishikawa NF, Chikaraishi Y, Takano Y, Sasaki Y, Takizawa Y, Tsuchiya M, Tayasu I, Nagata T, Ohkouchi N (2018) A new analytical method for determination of the nitrogen isotopic composition of methionine: Its application to aquatic ecosystems with mixed resources. Limnol Oceanogr Methods 16:607-620
Kaplan I, Rittenberg S (1964) Microbiological fractionation of sulphur isotopes. Microbiology 34:195-212
Korobushkin DI, Gongalsky KB, Tiunov AV (2014) Isotopic niche (δ^{13}C and δ^{15}N values) of soil macrofauna in temperate forests. Rapid communications in mass spectrometry 28:1303-1311
Kristensen E, Lee SY, Mangion P, Quintana CO, Valdemarsen T (2017) Trophic discrimination of stable isotopes and potential food source partitioning by leaf-eating crabs in mangrove environments. Limnol Oceanogr 62:2097-2112
Larsen T, Bach LT, Salvatteci R, Wang YV, Andersen N, Ventura M, McCarthy MD (2015) Assessing the potential of amino acid ^{13}C patterns as a carbon source tracer in marine sediments: effects of algal growth conditions and sedimentary diagenesis. Biogeosci 12:4979-4992
Larsen T, Taylor DL, Leigh MB, O'Brien DM (2009) Stable isotope fingerprinting: a novel method for identifying plant, fungal, or bacterial origins of amino acids. Ecology 90:3526-3535
Larsen T, Ventura M, Andersen N, O'Brien DM, Piatkowski U, McCarthy MD (2013) Tracing Carbon Sources through Aquatic and Terrestrial Food Webs Using Amino Acid Stable Isotope Fingerprinting. PLoS ONE 8:e73441
Larsen T, Wooller MJ, Fogel ML, O'Brien DM (2012) Can amino acid carbon isotope ratios distinguish primary producers in a mangrove ecosystem? Rapid Commun Mass Spectrom 26:1541-1548
Lee SY (2000) Carbon dynamics of Deep Bay, eastern Pearl River estuary, China. II: Trophic relationship based on carbon-and nitrogen-stable isotopes. Mar Ecol Prog Ser 205:1-10
Lee SY, Primavera JH, Dahdouh-Guebas F, McKee K, Bosire JO, Cannicci S, Diele K, Fromard F, Koedam N, Marchand C, Mendelssohn I, Mukherjee N, Record S (2014) Ecological role and services of tropical mangrove ecosystems: a reassessment. Glob Ecol Biogeogr 23:726-743
Lehmeier CA, Ballantyne IV F, Min K, Billings SA (2016) Temperature-mediated changes in microbial carbon use efficiency and ^{13}C discrimination. Biogeosci 13:3319-3329
Mazumder D, Saintilan N (2010) Mangrove Leaves are Not an Important Source of Dietary Carbon and Nitrogen for Crabs in Temperate Australian Mangroves. Wetlands 30:375-380
McConnaughey T, McRoy C (1979) Food-web structure and the fractionation of carbon isotopes in the Bering Sea. Mar Biol 53:257-262

McCutchan JH, Lewis Jr WM, Kendall C, McGrath CC (2003) Variation in trophic shift for stable isotope ratios of carbon, nitrogen, and sulfur. Oikos 102:378-390
McMahon KW, Fogel ML, Elsdon TS, Thorrold SR (2010) Carbon isotope fractionation of amino acids in fish muscle reflects biosynthesis and isotopic routing from dietary protein. J Anim Ecol 79:1132-1141
Naito YI, Bocherens H, Chikaraishi Y, Drucker DG, Wissing C, Yoneda M, Ohkouchi N (2016) An overview of methods used for the detection of aquatic resource consumption by humans: Compound-specific delta N-15 analysis of amino acids in archaeological materials. J. Archaeol. Sci 6:720-732
Newsome SD, Fogel ML, Kelly L, del Rio CM (2011) Contributions of direct incorporation from diet and microbial amino acids to protein synthesis in Nile tilapia. Funct Ecol 25:1051-1062
Odum WE, Heald EJ (1975) The detritus-band food web on an estuarine mangrove community. In: Cromin LE (ed), Estuarine Research, Academic Press, New York, pp 265–286
Ohkouchi N, Chikaraishi Y, Close HG, Fry B, Larsen T, Madigan DJ, McCarthy MD, McMahon KW, Nagata T, Naito YI, Ogawa NO, Popp BN, Steffan S, Takano Y, Tayasu I, Wyatt ASJ, Yamaguchi YT, Yokoyama Y (2017) Advances in the application of amino acid nitrogen isotopic analysis in ecological and biogeochemical studies. Orgc Geochem 113:150-174
Okada N, Sasaki A (1995) Characteristics of Sulfur Uptake by Mangroves: an Isotopic Study. Tropics 4:201-210
Okada N, Sasaki A (1998) Sulfur isotopic composition of mangroves. Isot Environ Healt S 34:61-65
Peterson BJ, Fry B (1987) Stable Isotopes in Ecosystem Studies. Annu Rev Ecol Syst 18:293-320
Potapov AM, Semenina EE, Kurakov AV, Tiunov AV (2013) Large $^{13}C/^{12}C$ and small $^{15}N/^{14}N$ isotope fractionation in an experimental detrital foodweb (litter–fungi–collembolans). Ecol Res 28:1069-1079
Potapov AM, Tiunov AV, Scheu S (2018) Uncovering trophic positions and food resources of soil animals using bulk natural stable isotope composition. Biol Rev 94:37-59
Potapov AM, Tiunov AV, Scheu S, Larsen T, Pollierer MM (2019) Combining bulk and amino acid stable isotope analyses to quantify trophic level and basal resources of detritivores: a case study on earthworms. Oecol 189:447-460
Sheaves M, Molony B (2000) Short-circuit in the mangrove food chain. Mar Ecol Prog Ser 199:97-109
Skov MW, Hartnoll RG (2002) Paradoxical selective feeding on a low-nutrient diet: why do mangrove crabs eat leaves? Oecol 131:1-7
Smallwood BJ, Wooller MJ, Jacobson ME, Fogel ML (2003) Isotopic and molecular distributions of biochemicals from fresh and buried Rhizophora mangle leaves. Geochem Trans 4:38
Vander Zanden HB, Arthur KE, Bolten AB, Popp BN, Lagueux CJ, Harrison E, Campbell CL, Bjorndal KA (2013) Trophic ecology of a green turtle breeding population. Mar Ecol Prog Ser 476:237-249
Vander Zanden MJ, Rasmussen JB (2001) Variation in $\delta^{15}N$ and $\delta^{13}C$ trophic fractionation: Implications for aquatic food web studies. Limnol Oceanogr 46:2061-2066
Wada E, Mizutani H, Minagawa M (1991) The use of stable isotopes for food web analysis. Crit Rev Food Sci Nutr 30:361-371

Walsh RG, He S, Yarnes CT (2014) Compound-specific $\delta^{13}C$ and $\delta^{15}N$ analysis of amino acids: a rapid, chloroformate-based method for ecological studies. Rapid Commun Mass Spectrom 28:96-108

Webb EC, Lewis J, Shain A, Kastrisianaki-Guyton E, Honch NV, Stewart A, Miller B, Tarlton J, Evershed RP (2017) The influence of varying proportions of terrestrial and marine dietary protein on the stable carbon-isotope compositions of pig tissues from a controlled feeding experiment. STAR:Science & Technology of Archaeological Research 3:28-44

Yarnes CT, Herszage J (2017) The relative influence of derivatization and normalization procedures on the compound - specific stable isotope analysis of nitrogen in amino acids. Rapid Commun Mass Spectrom 31:693-704

Chapter 5 – General discussion

The globally high rates of loss of mangrove forests recorded towards the end of the 20th century have begun to slow, but mangroves nevertheless continue to be lost in some regions (Hamilton & Casey 2017). In addition to this, sudden but extensive losses of mangrove forests due to extreme climatic events are anticipated (Duke et al. 2017, Lovelock et al. 2017, Sippo et al. 2018, Asbridge et al. 2019). Human-induced climate change is likely to increase the intensity and frequency of such extreme events (Coumou & Rahmstorf 2012, Stott 2016). These on-going losses of mangroves will negatively affect the important services expected to be provided by mangrove ecosystems (IPCC 2018). While some increases in the area covered by mangroves were reported in some regions e.g. Southeast Asia due to the increased restoration effort, it is unclear whether the functionality and services of mangrove ecosystems are sustainable or protected from future climate change impacts (Lee et al. 2019). For these reasons, there is an increasing importance of measuring changes in areal extent of mangrove forests, but also the functionality of mangrove ecosystems.

Reporting rare, extreme biological events can be challenging because such events can be sudden. Often pre-event sampling is not possible and the interpretation of events can only rely on spatial comparisons, for example impacted vs unimpacted sites (Smith 2011, Bailey & van de Pol 2016, Altwegg et al. 2017). In the case of the recent die-back in northern Australia, there was no pre-event collection of data due to the actual date of the event occurring being unknown, in addition to the fact that the event occurring in a remote and difficult to access location in the Gulf of Carpentaria, Australia. For these reasons, I undertook a field campaign comparing an impacted ecosystem vs. an adjacent unimpacted reference ecosystem using traditional ecological survey techniques combined with more conventional and novel stable isotope tracers, including ^{13}C, ^{15}N, ^{34}S in total organic matter ("bulk") samples and ^{13}C and ^{15}N in individual amino acids. Stable isotope analysis, with the relative ease and low cost of sample preparation and analysis, provided a cost-effective method to measure not only the health and structure of the ecosystem, but also its functional aspects. Furthermore, stable isotope analysis, with the relative ease of handling, sampling and preservation of analytical samples in the field, was highly practical and suited for this field-based investigation carried out in remote Gulf of Carpentaria where fieldwork is restricted to daytime, low tide and the dry season, not to mention also the occurrence of hazardous animals such as crocodiles.

The field investigation was carried out over a period of 18 months from August, 2016 to August 2018, approximately six to 30 months after the mortality event. The impacted forest had different faunal assemblages compared to the unimpacted forest and contained significantly fewer crabs that rely on mangrove litter (family Sesarmidae), but more crabs that rely on the microphytobenthos (MPB; *Uca* spp.). These findings support my first hypothesis that changes in benthic faunal assemblages would be evident due to mangrove mortality (Table 5.1). However, the total infaunal biomass including burrowing crabs, bivalves and worms was largely unaffected by the tree mortality. This is most likely because MPB, an important food source, was largely unaffected by tree mortality, which consequently buffered the food-web responses from the loss of mangrove litter food source (chapter 2). Furthermore, the $\delta^{13}C_{EAA}$ patterns of mangrove consumers did not differ between the impacted and unimpacted forests, suggesting that the feeding dependencies were largely unaffected (chapter 3). The $^{13}C_{EAA}$ patterns of mangrove consumers that consistently showed a dietary importance of MPB was consistent across other mangrove ecosystems from different geographical locations including Tallebudgera Creek, in subtropical Australia and Spanish Lookout Cay, in tropical Belize, suggesting that in general, MPB is an important food source to many of the mangrove consumers, but that the direct nutritional importance of mangrove leaf litter is fairly limited (chapter 4). These findings suggest that the observed changes in mangrove faunal community were most likely driven more by changes to the physical habitat structure, for example canopy loss. However, presence vs absence of mangrove litter as a food source may not have played a direct role in shifting mangrove faunal assemblages, since the mangrove fauna remained abundant regardless of the mangrove loss (chapter 2, 3 and 4). These findings did not strongly support the hypothesis that food web structure would be impacted by changes to available food resources. This is probably because in general, mangroves play an important role in providing habitat structure, but play a less important role in directly providing a food source since mangrove litter is comparatively low in nutrients (Lee et al. 2014). Hence, the loss of mangroves due to tree mortality is more likely to impact animals such as smaller juvenile fish that rely more on mangroves for habitat structure via reduced physical habitat complexity.

Table 5.1. Summary of hypotheses tested and findings of each chapter

Chapter	Key hypotheses tested	Key findings
2	• Changes in benthic faunal assemblages would be evident due to mangrove mortality. • Food web structure would be impacted by the tree mortality and changes to available food resources.	• The impacted forest had significantly fewer crabs that feed on mangrove litter (Sesarmidae), but more MPB feeding crabs (*Uca* spp.). • The total infaunal biomass including burrowing crabs was largely unaffected by the effect of mangrove mortality.
3	• Changes in C, N and S cycling would be evident due to mangrove mortality and be reflected in $\delta^{13}C$, $\delta^{15}N$ and $\delta^{34}S$ values of mangrove ecosystem components. • These isotopic compositions change over time with the recovery of mangrove vegetation.	• The impacted forest had different C, N and S cycling that were reflected in $\delta^{13}C$, $\delta^{15}N$, and $\delta^{34}S$ values of the ecosystem components. • The mangrove seedling and sapling densities substantially increased from 18 to 30 months after the mortality event, but the C, N and S cycling did not show recovery.
4	• C and N isotopic compositions in amino acids help discriminate mangrove organic matter in food web analyses • Stable isotopic compositions in EAAs that cannot be synthesised by animals would be more conservative in food web links between consumers and mangrove organic matter.	• $\delta^{13}C$ patterns in EAAs, particularly Phe, Ile and Leu distinguished mangroves from MPB. • $\delta^{15}N$ of Phe and $\delta^{34}S$ that also separated the mangrove vs MPB were more conservative tracers of mangrove organic matter due to lower trophic fractionations.

Mangrove mortality can occur due to natural causes including droughts (Duke et al. 2017), tsunami (Dahdouh-Guebas et al., 2005), and cyclones (Sherman et al. 2001). Recovery of mangrove vegetation after tree mortality events depends on whether the environmental conditions allow regrowth and recruitment of seedlings (Smith et al. 1994). Such natural disturbances may lead to altered environmental conditions that may affect recovery of mangroves. For example, drought events may lead to long-term hyper-saline conditions and sudden surges such as tsunami and cyclones may lead to more physical disturbances such as erosion. In the present case which was associated with drought conditions, mangrove seedling and sapling densities in the impacted forests increased substantially during the study period of 18 to 30 months after the mortality event, suggesting recovery of the mangrove vegetation (chapter 3). However, mangrove leaves collected from the impacted site in 2018 showed relatively higher $\delta^{13}C$ values that are likely associated with water stress. $\delta^{13}C$, $\delta^{15}N$, and $\delta^{34}S$ values of ecosystem components including mangroves, soil and invertebrates from the impacted site suggested lower mangrove C fixation/respiration, lower N fixation and lower sulfate reduction following the tree mortality event. While the vegetation recovered substantially, recovery of CNS cycling was not largely evident during the two-year period.

These findings support the hypothesis that changes in elemental cycling occur due to the mangrove mortality, but these findings did not support the secondary hypothesis that the elemental cycling change over time with the recovery of mangrove vegetation. Overall this suggested that there is a long-lasting impact of the mangrove dieback on the cycling of C, N and S elements (chapter 3).

While mangroves recover from perturbations, the ecosystem may display cryptic ecological degradation and consequently the degraded ecosystem may not function properly and not provide full ecosystem services. For example, cryptically degraded mangrove sites that are dominated by mangrove associates or minor mangrove species may experience a high destructive impact from perturbations such as tsunami (Dahdouh-Guebas et al., 2005). Perturbations such as sewage exposure may reduce and alter ecosystem engineering activities of crabs including burrowing and foraging that are beneficial for mangrove growth and ecosystem functioning (Bartolini et al., 2011). Our case, which shows fast recovery of mangrove vegetation and no recovery of CNS cycling may represent a possible example of cryptic ecological degradation in mangrove ecosystems. The study also suggest recovery of CNS may take much longer than 32 months and is likely associated with other key processes such as canopy development. For example, full recovery of mangrove soil C and N stock was associated with development of canopy that took over 10 years (Adame et al. 2018).

The use of bulk stable C, N and S isotope analyses provided an overall view of assessing organic matter cycling and/or food web dynamics based on the biogeochemical cycling of C, N and S elements. I then used compound-specific isotope analysis of amino acids as a complementary tool to help resolve details of organic matter cycling and feeding dependency (chapter 3). The fingerprint pattern analysis of $\delta^{13}C$ variation among essential amino acids, (EAAs; Larsen et al. 2009) provided a more differentiated view of assessing feeding dependencies with the pattern of normalized EAA, particularly Phe, Ile and Leu distinguishing mangrove organic matter from the microphytobenthos (MPB) (chapter 4). The use of bulk stable CNS isotopes and compound-specific stable CN isotopes of amino acids were compared (chapter 4). Overall, isotopic compositions of mangrove organic matter largely reset during digestion and assimilation. Consequently, the direct use of mangrove-derived nutrients was generally under-detected for consumers in the mangrove food web, and more nutritious MPB were apparently expressed in their tissues.

$\delta^{15}N$ of Phe and $\delta^{34}S$ that also distinguished mangrove organic matter from MPB were relatively more conservative tracers of mangrove organic matter with little changes in isotopic composition during trophic processes. This is likely because of lower trophic fractionation during uptake of EAAs including Phe (Ohkouchi et al. 2017) and methionine, a sulfur-containing amino acid (McCutchan et al. 2003). The findings support the hypothesis that stable isotopic compositions in EAAs that cannot be synthesised by animals would be more conservative in food web links between consumers and mangrove organic matter. The advantage of combining use of various isotope tracers including bulk measurements and amino acid stable isotope measurements to disentangle complex dynamics of food webs was highlighted recently (Potapov et al. 2019). Examples of such approaches include $\delta^{15}N$ measurements in glutamic acid, phenylalanine and methionine to estimate the trophic position of organisms (Ishikawa et al. 2018) and ^{13}C fingerprint pattern analysis of amino acids to assess resource use (Larsen et al. 2013). My study (chapter 4) highlights the benefits of using such multiple isotope tracer approaches to evaluate the dynamics of complex food webs.

This study demonstrates significant biological responses to extreme climatic events. Examples of such extreme biological responses include mass bleaching of coral reefs (Hughes et al. 2017), marine heatwaves inducing mass mortality of kelp forests (Wernberg et al. 2016) and seagrass meadows (Thomson et al. 2015) as well as saltmarsh die-off associated with drought conditions (Silliman et al. 2005). This research also offers a framework for combining the use of stable isotopes and traditional ecological survey techniques in reporting difficult to measure biological responses associated with extreme climatic events. While past conservation and/or management of mangrove forests generally focused more on the areal extent of mangrove forests, the approach I used throughout my research focussed on the functional aspects of mangrove ecosystems, providing a practical, efficient and cost-effective method of measuring mangrove ecosystem health and functionality.

The results of this research may also be used to help manage coastal wetlands for future impacts of climatic extreme events, and support wetlands conservation and restoration efforts. My results may also help develop a novel index for evaluating mangrove forest condition and health. For example, building a new index that can define, measure and model the health of mangrove ecosystems is fairy achievable from the stable isotope dataset. In my dataset, mangrove ecosystems with healthy food webs may be identified using isotope

indicators that show strong mangrove contributions, moderate to high N fixation and sulfate reduction inputs, while disturbed systems would show significantly different isotopic patterns (chapters 2 and 3). Such patterns are fairly consistent with findings from mangrove ecosystems that experienced other disturbances, e.g. deforestation in Malaysia (Adame et al. 2018) and Brazil (Bernardino et al. 2018).

In order to enhance the use of stable isotopes as indicators for evaluating mangrove ecosystem condition and health, future research may involve several key steps. Firstly, it is important to review existing indicators and know which stable isotopes are more suitable as indicators for measuring health or/and condition of mangrove ecosystems. Use of these stable isotope indicators should be compared and evaluated in various trial locations. This step may also involve reviewing data availability at trial locations. The second step may involve development of ecosystem assessments and protocols using stable isotopes. This step may focus on including the use of stable isotope indicators in the existing ecosystem assessments and monitoring programs. This addition may improve the cost-effectiveness of the existing ecosystem assessment framework, as stable isotopes are relatively inexpensive and powerful when they are combined with other traditional methods and indicators (Fry 2006). The final step focuses on the evaluation and refinement of the index, and extension and application of the index at the global scale, which may require participants from various geographical locations. For example, the ecosystem assessment and stable isotope sampling protocol developed here could be undertaken by participants from various geographical locations to help define a global isotopic pattern of mangrove ecosystem function.

The final product of this future work should not only be toward scientific contributions but also be used as a tool that can be easily accessed and applied by field ecologists and land managers. For this reason, the use of isotopes should be user-friendly, simple and easy to understand as well as cost-effective, with a focus on increasing end-user utilization of stable isotope techniques. This popularisation process may occur parallel to the development and/or application of new stable isotope techniques such as position-specific isotope analysis (Fry et al. 2018) and identifying new isotope patterns in specific compounds such as amino acids (Larsen et al. 2013, Ishikawa et al. 2018). Stable isotope data obtained from various geographical locations may also be used as a tool for predicting impacts and recovery of extreme events that are expected to become more “common”, such as the Gulf of

Carpentaria mangrove dieback (Duke et al. 2017) and mangrove dieback events in other locations (Lovelock et al. 2017, Asbridge et al. 2019).

References

Adame M, Zakaria R, Fry B, Chong V, Then Y, Brown C, Lee S (2018) Loss and recovery of carbon and nitrogen after mangrove clearing. Ocean Coast Manag 161:117-126

Altwegg R, Visser V, Bailey LD, Erni B (2017) Learning from single extreme events. Philos. Trans. Royal Soc. B 372:20160141

Asbridge EF, Bartolo R, Finlayson CM, Lucas RM, Rogers K, Woodroffe CD (2019) Assessing the distribution and drivers of mangrove dieback in Kakadu National Park, northern Australia. Estuar, Coast Shelf Sci 228:106353

Bailey LD, van de Pol M (2016) Tackling extremes: challenges for ecological and evolutionary research on extreme climatic events. J Anim Ecol 85:85-96

Bartolini F, Cimo F, Fusi M, Dahdouh-Guebas F, Lopes GP, Cannicci S (2011) The effect of sewage discharge on the ecosystem engineering activities of two East African fiddler crab species: Consequences for mangrove ecosystem functioning. Mar Environ Res 71:53-61

Bernardino AF, Gomes LEdO, Hadlich HL, Andrades R, Correa LB (2018) Mangrove clearing impacts on macrofaunal assemblages and benthic food webs in a tropical estuary. Mar Poll Bull 126:228-235

Coumou D, Rahmstorf S (2012) A decade of weather extremes. Nat Clim Change 2:491

Dahdouh-Guebas F, Jayatissa LP, Di Nitto D, Bosire JO, Lo Seen D, Koedam N (2005) How effective were mangroves as a defence against the recent tsunami? Curr Biol 15: R443-R447

Duke NC, Kovacs JM, Griffiths AD, Preece L, Hill DJE, van Oosterzee P, Mackenzie J, Morning HS, Burrows D (2017) Large-scale dieback of mangroves in Australia's Gulf of Carpentaria: a severe ecosystem response, coincidental with an unusually extreme weather event. Mar Freshwater Res 68:1816-1829

Fry B (2006) Stable Isotope Ecology. Springer-Verlag New York

Fry B, Carter JF, Yamada K, Yoshida N, Juchelka D (2018) Position-specific $^{13}C/^{12}C$ analysis of amino acid carboxyl groups – automated flow-injection analysis based on reaction with ninhydrin. Rapid Commun Mass Spectrom 32:992-1000

Hamilton SE, Casey D (2016) Creation of a high spatio-temporal resolution global database of continuous mangrove forest cover for the 21st century (CGMFC‐21). Glob Ecol Biogeogr 25:729-738

Hughes TP, Kerry JT, Álvarez-Noriega M, Álvarez-Romero JG, Anderson KD, Baird AH, Babcock RC, Beger M, Bellwood DR, Berkelmans R, Bridge TC, Butler IR, Byrne M, Cantin NE, Comeau S, Connolly SR, Cumming GS, Dalton SJ, Diaz-Pulido G, Eakin CM, Figueira WF, Gilmour JP, Harrison HB, Heron SF, Hoey AS, Hobbs J-PA, Hoogenboom MO, Kennedy EV, Kuo C, Lough JM, Lowe RJ, Liu G, McCulloch MT, Malcolm HA, McWilliam MJ, Pandolfi JM, Pears RJ, Pratchett MS, Schoepf V, Simpson T, Skirving WJ, Sommer B, Torda G, Wachenfeld DR, Willis BL, Wilson SK (2017) Global warming and recurrent mass bleaching of corals. Nature 543:373

IPCC (2018) Global warming of 1.5°C. An IPCC Special Report on the impacts of global warming of 1.5°C above pre-industrial levels and related global greenhouse gas emission pathways, in the context of strengthening the global response to the threat of climate change, sustainable development, and efforts to eradicate poverty. Geneva, Switzerland:World Meteorological Organization

Ishikawa NF, Chikaraishi Y, Takano Y, Sasaki Y, Takizawa Y, Tsuchiya M, Tayasu I, Nagata T, Ohkouchi N (2018) A new analytical method for determination of the nitrogen isotopic composition of methionine: Its application to aquatic ecosystems with mixed resources. Limnol Oceanogr Methods 16:607-620

Larsen T, Taylor DL, Leigh MB, O'Brien DM (2009) Stable isotope fingerprinting: a novel method for identifying plant, fungal, or bacterial origins of amino acids. Ecology 90:3526-3535
Larsen T, Ventura M, Andersen N, O'Brien DM, Piatkowski U, McCarthy MD (2013) Tracing Carbon Sources through Aquatic and Terrestrial Food Webs Using Amino Acid Stable Isotope Fingerprinting. PLoS ONE 8:e73441
Lee SY, Hamilton S, Barbier EB, Primavera J, Lewis RR (2019) Better restoration policies are needed to conserve mangrove ecosystems. Nat Ecol Evo 3:870
Lee SY, Primavera JH, Dahdouh-Guebas F, McKee K, Bosire JO, Cannicci S, Diele K, Fromard F, Koedam N, Marchand C, Mendelssohn I, Mukherjee N, Record S (2014) Ecological role and services of tropical mangrove ecosystems: a reassessment. Glob Ecol Biogeogr 23:726-743
Lovelock CE, Feller IC, Reef R, Hickey S, Ball MC (2017) Mangrove dieback during fluctuating sea levels. Sci Rep 7:1680
McCutchan JH, Lewis Jr WM, Kendall C, McGrath CC (2003) Variation in trophic shift for stable isotope ratios of carbon, nitrogen, and sulfur. Oikos 102:378-390
Ohkouchi N, Chikaraishi Y, Close HG, Fry B, Larsen T, Madigan DJ, McCarthy MD, McMahon KW, Nagata T, Naito YI, Ogawa NO, Popp BN, Steffan S, Takano Y, Tayasu I, Wyatt ASJ, Yamaguchi YT, Yokoyama Y (2017) Advances in the application of amino acid nitrogen isotopic analysis in ecological and biogeochemical studies. Org Geochem 113:150-174
Potapov AM, Tiunov AV, Scheu S, Larsen T, Pollierer MM (2019) Combining bulk and amino acid stable isotope analyses to quantify trophic level and basal resources of detritivores: a case study on earthworms. Oecol 189:447-460
Silliman BR, van de Koppel J, Bertness MD, Stanton LE, Mendelssohn IA (2005) Drought, Snails, and Large-Scale Die-Off of Southern U.S. Salt Marshes. Science 310:1803-1806
Sippo JZ, Lovelock CE, Santos IR, Sanders CJ, Maher DT (2018) Mangrove mortality in a changing climate: An overview. Estuar, Coast Shelf Sci 215:241-249
Smith MD (2011) An ecological perspective on extreme climatic events: a synthetic definition and framework to guide future research. J Ecol 99:656-663
Smith TJ, Robblee MB, Wanless HR, Doyle TW (1994) Mangroves, hurricanes, and lightning strikes: assessment of Hurricane Andrew suggests an interaction across two differing scales of disturbance. BioScience 44:256-262
Stott P (2016) How climate change affects extreme weather events. Science 352:1517-1518
Thomson JA, Burkholder DA, Heithaus MR, Fourqurean JW, Fraser MW, Statton J, Kendrick GA (2015) Extreme temperatures, foundation species, and abrupt ecosystem change: an example from an iconic seagrass ecosystem. Glob Change Biol 21:1463-1474
Wernberg T, Bennett S, Babcock RC, de Bettignies T, Cure K, Depczynski M, Dufois F, Fromont J, Fulton CJ, Hovey RK, Harvey ES, Holmes TH, Kendrick GA, Radford B, Santana-Garcon J, Saunders BJ, Smale DA, Thomsen MS, Tuckett CA, Tuya F, Vanderklift MA, Wilson S (2016) Climate-driven regime shift of a temperate marine ecosystem. Science 353:169-172

Appendix

Supplementary information chapter 2

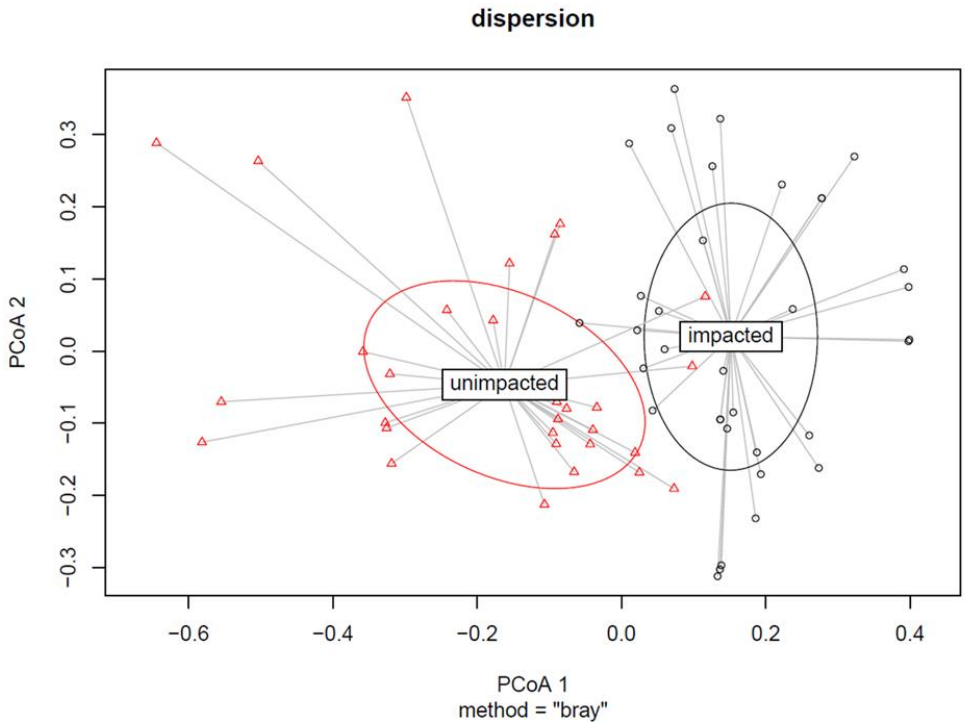

Fig. S2.1. Permutation test for homogeneity of multivariate dispersions. The ellipse represents the SD of distance to group centroid. While, the dispersions were not statistically different between the two groups (df = 1, F = 1.95, P = 0.15), the compositions between the two forests differed in spread or position in a multivariate space (PERMANOVA, df = 1, r^2 = 0.29, F = 27.22, p = 0.001) indicating that the forests differed in the assemblages of five epifaunal feeding groups.

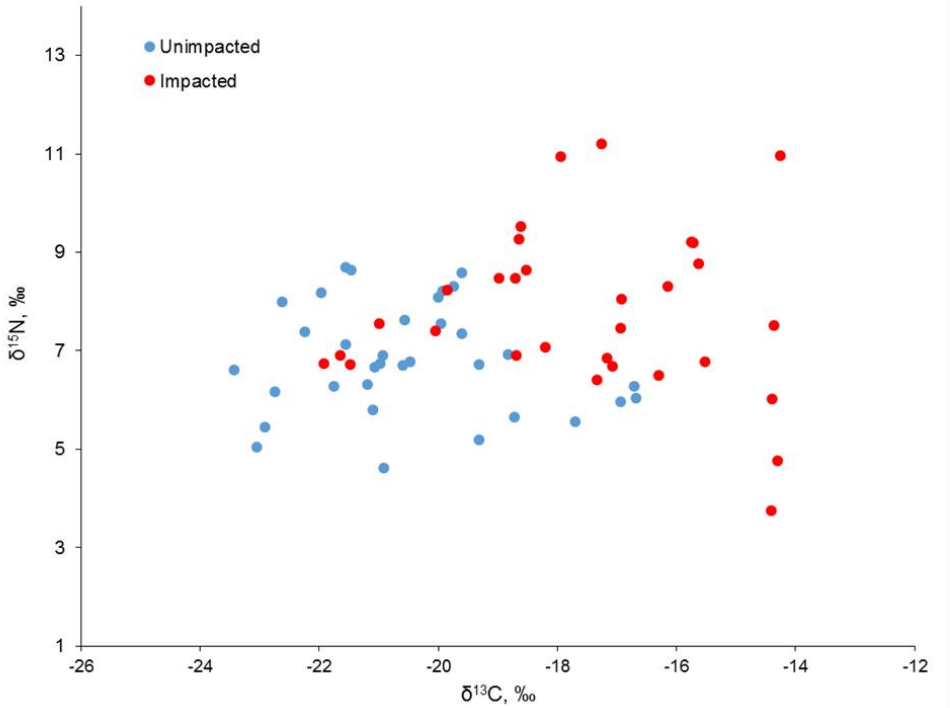

Fig. S2.2. Variability of epifaunal $\delta^{13}C$ and $\delta^{15}N$ values across the impacted and unimpacted mangrove forests.

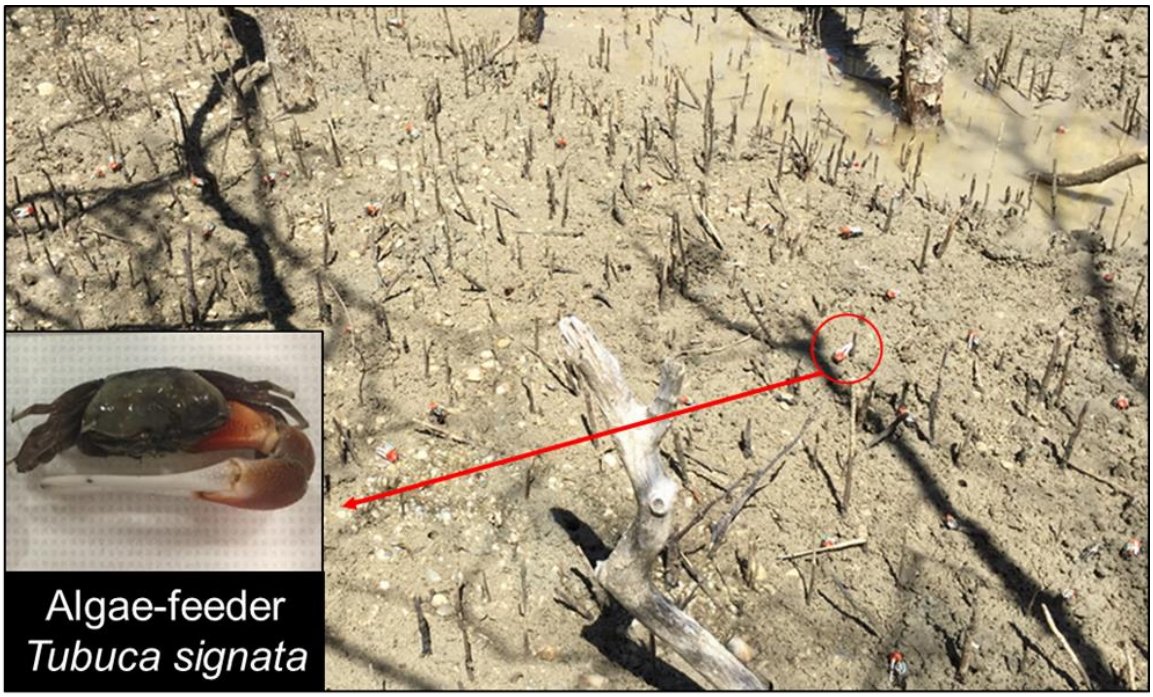

Fig. S2.3. Dominance of algae-feeder (*Tubuca signata*) in the impacted forest.

Supplementary information chapter 3

Table S3.1. Stable C, N and S isotopic compositions of animals

Forest	Year	Group	Taxa	$\delta^{13}C$	SE	$\delta^{15}N$	SE	$\delta^{34}S$	SE	n
Unimpacted	2016	algae feeder	*Tubuca signata*	-17.4	0.3	6.7	0.3	14.3	1.0	3
Unimpacted	2017	algae feeder	*Tubuca signata*	-17.1	0.8	6.0	0.2	14.2	0.2	3
Unimpacted	2018	algae feeder	*Tubuca signata*	-16.5	0.4	6.9	0.2	14.7	0.2	5
Unimpacted	2017	filter feeder	*Crassostrea* sp (oyster)	-19.3	0.2	7.8	0.1	13.5	0.4	3
Unimpacted	2018	filter feeder	*Crassostrea* sp (oyster)	-20.2	0.1	6.9	0.2	14.0	0.3	3
Unimpacted	2016	grazer	*Telescopium telescopium*	-20.3	0.1	7.1	0.0	10.9	1.0	2
Unimpacted	2017	grazer	*Telescopium telescopium*	-18.2	1.1	6.4	0.1	12.0	1.1	3
Unimpacted	2018	grazer	*Telescopium telescopium*	-18.4	0.8	7.3	0.2	11.3	0.9	6
Unimpacted	2016	leaf feeder	*Parasesarma or Episesarma*	-21.0	0.3	7.7	0.3	11.5	1.0	3
Unimpacted	2017	leaf feeder	*Parasesarma or Episesarma*	-21.1	0.8	8.1	0.4	12.9	2.0	4
Unimpacted	2018	leaf feeder	*Parasesarma or Episesarma*	-22.0	0.5	7.9	0.4	15.0	0.7	4
Impacted	2016	algae feeder	*Tubuca signata*	-15.7	0.7	7.5	0.2	17.0	0.2	3
Impacted	2017	algae feeder	*Tubuca signata*	-15.4	0.8	8.4	0.4	15.5	0.3	3
Impacted	2018	algae feeder	*Tubuca signata*	-15.1	0.2	7.3	0.4	16.7	0.2	6
Impacted	2017	filter feeder	*Crassostrea* sp oyster	-19.0	0.5	7.9	0.1	14.5	0.4	3
Impacted	2018	filter feeder	*Crassostrea* sp oyster	-20.0	0.0	7.5	0.1	15.2	0.2	3
Impacted	2016	grazer	*Telescopium telescopium*	-16.2	0.1	7.5	0.0	14.1	0.7	2
Impacted	2017	grazer	*Telescopium telescopium*	-16.7	0.8	7.2	0.1	14.7	0.4	3
Impacted	2018	grazer	*Telescopium telescopium*	-16.0	0.5	7.8	0.2	14.5	0.2	6
Impacted	2016	leaf feeder	*Parasesarma or Episesarma*	-18.6	0.0	9.0	0.4	15.7	0.1	2
Impacted	2017	leaf feeder	*Parasesarma or Episesarma*	-18.3	0.1	9.0	0.3	16.0	0.5	3
Impacted	2018	leaf feeder	*Parasesarma or Episesarma*	-18.0	0.7	7.7	0.9	19.4	1.2	3

Supplementary information chapter 4

Table S4.1. $\delta^{13}C$ values of 10 amino acids for samples included in this study from Tallebudgera Creek, Australia (mean, SD, n=3).

Samples	EAAs					NEAAs				
	Lys	Ile	Phe	Val	Leu	Gly	Asp	Pro	Glu	Ala
Rhizophora stylosa	-22.9	-25.3	-25.5	-31.3	-34.3	-16.6	-23.6	-22.3	-26.4	-26.3
SD	0.5	0.5	0.2	0.3	0.2	1	0.7	0.8	1.4	0.2
Avicennia marina	-24	-24.8	-27	-31.2	-35.3	-15.6	-19.8	-22.3	-25.1	-26.3
SD	0.4	0.4	0.4	0.2	0.5	0.8	1.5	1.2	0.7	0.3
MPB	-15.9	-19.3	-22.6	-23.2	-24	-7.8	-11.4	-15.1	-17.7	-16
SD	0.8	0.2	0.1	0.1	0.2	1.4	0.5	0.2	0.8	0
Neosarmatium trispinosum	-23.1	-28.3	-28.4	-31.8	-33	-7.8	-22	-21.4	-19.9	-21.2
SD	0.1	0.1	0	0.2	0.3	3.5	1	0.2	0.4	0
Parasesarma erythodactyla	-19.4	-24.2	-27	-26.8	-27.3	-6.2	-17.4	-18.3	-18.3	-19.6
SD	0.4	0.5	0.1	0.5	0.2	0.8	1.3	0.7	0.7	0.4
Uca vomeris	-14.1	-19.5	-22.8	-22.5	-23.1	-1.7	-13.5	-14	-12.6	-12.9
SD	0.2	0.2	0.4	0.3	0.1	1.2	0.8	0.5	0.6	0.7